AD-A169 009 AN ANALYSIS OF EXPLOSION-INDUCED BENDING DAMAGE IN SUBMERGED SHELL TARGETS(U) NAVAL SURFACE WEAPONS CENTER DAHLGREN VA M MOUSSOUROS DEC 84 NSWC/TR-84-300 1/1

UNCLASSIFIED F/G 19/4 NL

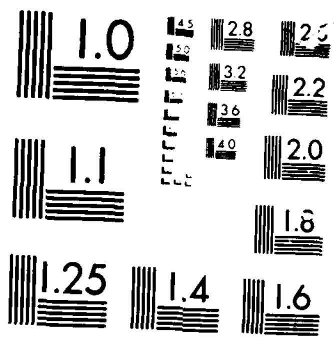
1.0
1.1
1.25
1.4
1.6
1.8
2.0
2.2
2.8
3.2
3.6
4.0
4.5
5.0

NSWC TR 84–380

(12)

AN ANALYSIS OF EXPLOSION-INDUCED BENDING DAMAGE IN SUBMERGED SHELL TARGETS

AD–A169 009

BY MINOS MOUSSOUROS

RESEARCH AND TECHNOLOGY DEPARTMENT

DECEMBER 1984

NAVAL SURFACE WEAPONS CENTER

Dahlgren, Virginia 22448 • Silver Spring, Maryland 20910

86 7

UNCLASSIFIED

SECURITY CLASSIFICATION OF THIS PAGE (When Data Entered)

REPORT DOCUMENTATION PAGE		READ INSTRUCTIONS BEFORE COMPLETING FORM
1. REPORT NUMBER NSWC TR 84-380	2. GOVT ACCESSION NO. A169009	3. RECIPIENT'S CATALOG NUMBER
4. TITLE (and Subtitle) AN ANALYSIS OF EXPLOSION-INDUCED BENDING DAMAGE IN SUBMERGED SHELL TARGETS		5. TYPE OF REPORT & PERIOD COVERED 6. PERFORMING ORG. REPORT NUMBER
7. AUTHOR(s) MINOS MOUSSOUROS		8. CONTRACT OR GRANT NUMBER(s)
9. PERFORMING ORGANIZATION NAME AND ADDRESS Naval Surface Weapons Center (Code R14) 10901 New Hampshire Avenue Silver Spring, MD 20903-5000		10. PROGRAM ELEMENT, PROJECT, TASK AREA & WORK UNIT NUMBERS 62633N; F33327; SF33327; R19BA
11. CONTROLLING OFFICE NAME AND ADDRESS		12. REPORT DATE December 1984 13. NUMBER OF PAGES 73
14. MONITORING AGENCY NAME & ADDRESS (if different from Controlling Office)		15. SECURITY CLASS. (of this report) UNCLASSIFIED 15a. DECLASSIFICATION/DOWNGRADING SCHEDULE

16. DISTRIBUTION STATEMENT (of this Report)

Approved for public release; distribution unlimited.

17. DISTRIBUTION STATEMENT (of the abstract entered in Block 20, if different from Report)

18. SUPPLEMENTARY NOTES

19. KEY WORDS (Continue on reverse side if necessary and identify by block number)

Finite element
Bend-buckling
Cylindrical
Explosion analysis

20. ABSTRACT (Continue on reverse side if necessary and identify by block number)

An underwater explosion gives rise to a violently oscillating bubble containing detonation gases. The oscillations cause pulses to impinge on a nearby submerged structure which, under some conditions, produce low frequency bending motion. The amplitude of the bending motion frequently is large enough to correspond to severe plastic deformation and bend-buckling. An analysis for this problem can be performed by treating the structure as a cylindrical shell subjected to two end couples set up by longitudinal membrane stresses.

20. (Cont.)

Such stresses are known to induce axial buckling and/or ovalization or plastification of the cross-section. As a first approximation, and in view of the low frequency response, inertia is neglected in this analysis.

Bending moment and work done on the structure are determined as a function of mean curvature. Computational results are presented for several shell geometries and published experimental data for these models compare favorably with the computations.

FOREWORD

This study represents the initial effort aimed at addressing the bend buckling of circular cylindrical shells subject to two self-equilibrating end moments and zero net axial loading. Such conditions may arise in the flexural response of a submerged cylinder excited by an underwater explosion bubble. The inertia forces are neglected here in view of the low frequency nature of the response. Both material and geometrical nonlinearities are included.

This analysis uses the nonlinear finite element program ABAQUS. Analytical predictions from ABAQUS are validated by comparison of results to experimental data available in the open literature.

Approved by:

Kurt F. Mueller

KURT F. MUELLER, Head
Energetic Materials Division

CONTENTS

ILLUSTRATIONS

ILLUSTRATIONS (Cont.)

TABLES

INTRODUCTION

The problem of the deformation of a straight or curved shell, subject to end bending moments and possibly internal pressure, has been addressed in numerous articles.[1-151]

This report addresses numerically the problem of a straight circular tube subject to external end bending moments without internal pressure, allowing for geometric and material nonlinearities. The nonlinear finite element program ABAQUS[152] is used. Experimental results from the open literature[93] are compared with the numerical results in order to validate ABAQUS for problems of this category.

References 3, 4, 30, and 36 are essentially concerned with the linear bending of tubes subject to end bending moments. In modern terminology, they are referred to as "geometrically linear" analyses. The first "geometrically nonlinear" analyses are due to Brazier,[7] Chwalla,[11,15] Wood,[51] Reissner,[55,60] Reissner and Weinitschke,[65] and Weinitschke,[90] to mention a few.

Ades,[48] assuming that the cross-sections of a long cylinder remain elliptical after deformation, accounted for geometric and material nonlinearities. Afendik[84,89] presented an approximate analysis incorporating plasticity. References 131 and 140 allowed for geometrical and material nonlinearities, while Reference 135 extended an earlier analysis[114] to elastoplastic behavior of imperfect cylinders. References 100, 108, 115, and 152 are the only numerical papers (as applied to straight cylindrical shells) by the finite element method of which the author is aware.

Interest in this problem stems from the fact that during an underwater explosion, external vertical forces are set up on a submerged structure and cause it to bend, as if subjected to end couples. An analysis could be of potential use to ship designers when questions of quantifying ultimate longitudinal strength arise (see Caldwell[72]). Another potential problem is related to curved pipes between fixed supports.[4,8,9,19,27,28,30,34,35,36,37,46] When a temperature increase occurs, the curved part is subjected to terminal couples, which reduce the radius of curvature.

METHOD

As mentioned previously, the dynamic problem will be approximated by a static equivalent in view of the low frequency of the motions. The complexity of the problem necessitates the use of a numerical procedure. The nonlinear finite element program ABAQUS[152] is used in this work.

First, we establish a global right-handed coordinate (x,y,z) system (Figures 1 and 2) with z the longitudinal axis of the cylindrical shell, x the vertical, and y the transverse direction. Next, we discretize the structure by modeling only one-half the length and one-half the periphery, i.e., we employ a quarter model. It is assumed that the cylinder is perfectly circular (without imperfections due to fabrication and residual strains) and the end loads are symmetrical with respect to the x-z plane, with the bending couples lying on the global y-axis. The cylindrical surface is replaced by ABAQUS S8R shell elements with 3 integration points across the thickness. Geometric and material nonlinearities are allowed. Perfect plasticity, von Mises isotropic yield, and an associated normal flow rule are used by ABAQUS. The employed mesh, including midside nodes, was 25 x 25 excluding an auxiliary node. Figure 18 displays a 13 x 13 mesh which excludes all midnodes.

BOUNDARY CONDITIONS

All boundary conditions are given in the global Cartesian frame of reference. Along both generators, AA' ($\theta = 0°$) and CC' ($\theta = 180°$), owing to symmetry, we have

$$v = \varphi_x = \varphi_z = 0$$

Along the half-circle ABC, symmetry implies that (half length analyzed only)

$$w = \varphi_x = \varphi_y = 0$$

Note that up to this point, the vertical rigid body motion has not yet been removed, and it must be constrained prior to solution. This will be done in co.junction with the method of exerting the external loading.

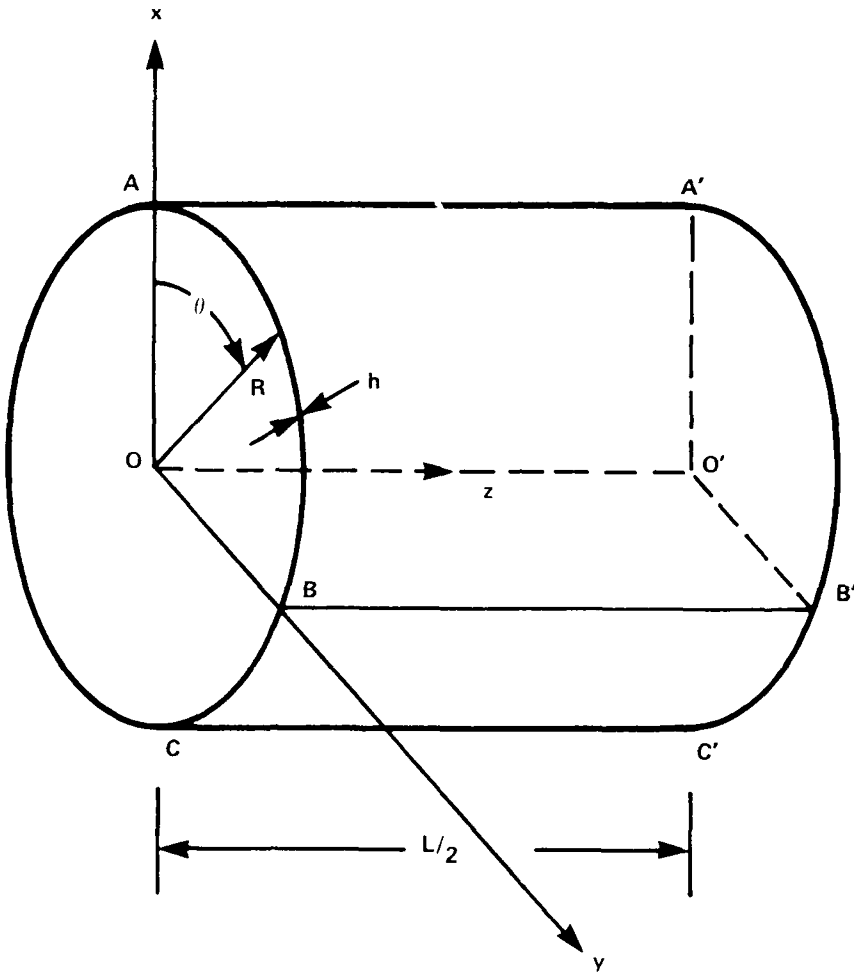

FIGURE 1. STRAIGHT CYLINDRICAL SHELL OF HALF LENGTH $L/_2$, MEAN RADIUS R, THICKNESS h, AND ASSOCIATED GLOBAL CARTESIAN COORDINATE SYSTEM (x, y, z)

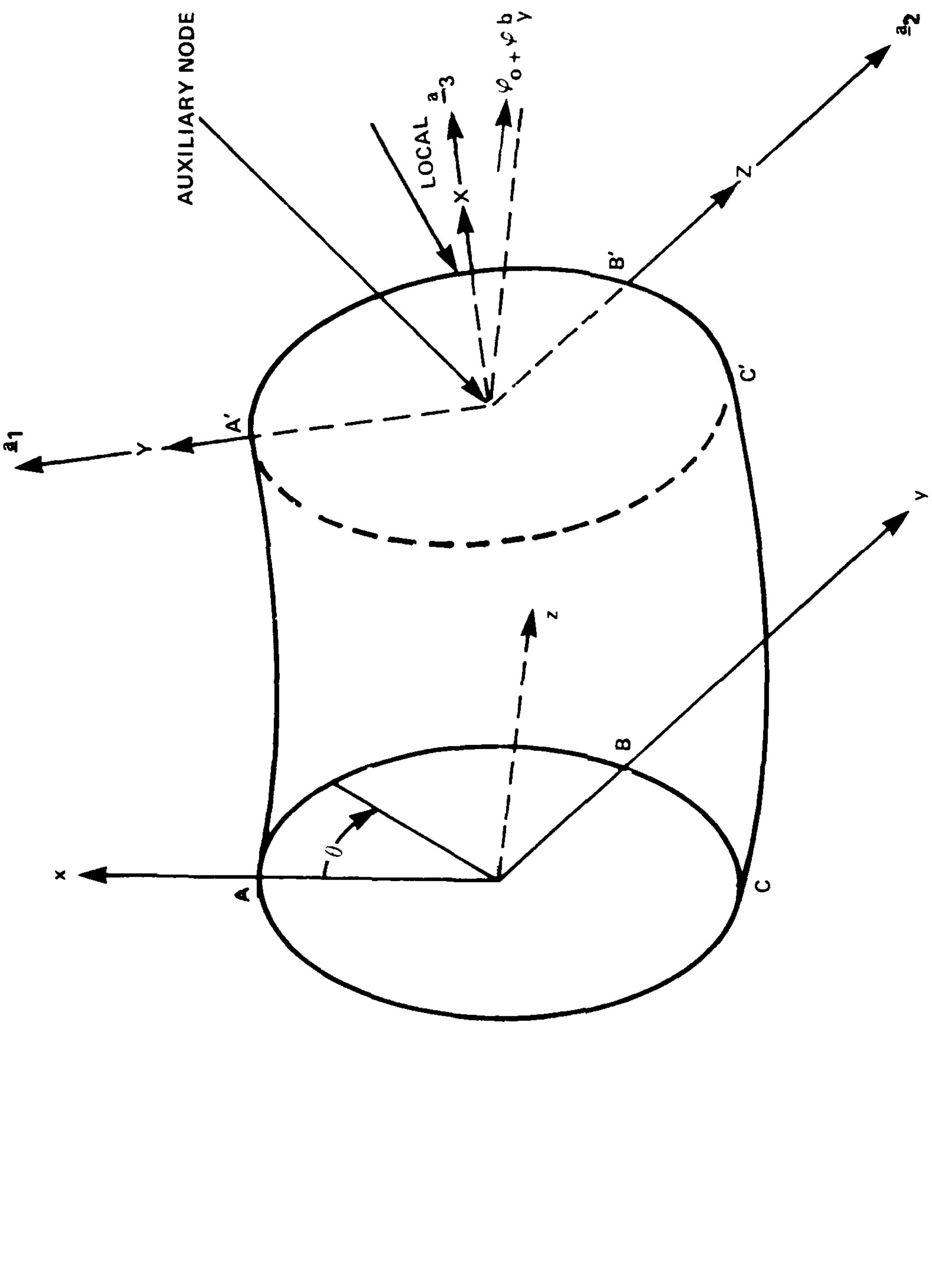

FIGURE 2. CYLINDRICAL SHELL WITH ASSOCIATED END SECTION A' B' C' AND AUXILIARY NODE AFTER DEFORMATION (LOCAL FRAME OF REFERENCE (X, Y, Z))

APPLIED LOADING

ABAQUS has a particularly attractive feature: a nonlinear multiple constraint capability (MPC).* The loading on the structure from the underwater explosion is approximated through an overall bending moment set up by the action of longitudinal membrane stresses. This will be modeled through a prescribed end rotation about the Y-axis applied incrementally. For small deformations, the vertical coordinate of the neutral axis from the center of the circular cross-section is extremely small. Consequently, the shift is approximately zero. However, for larger deformations this shift is substantial, necessitating an iteration if we are to assume that initially a linear distribution of forces produces a net applied moment. To avoid the above, the following method is used.

There are three conditions that must be fulfilled in this approach and are summarized here for clarity:

1. Plane sections remain plane at A'B'C' arc (Figure 2) (at the end where the external loading would have been applied).

2. There will be no rotation of A'B'C' plane (Figure 2) about the local Y-axis.

3. An end rotation about the global y (or local Z) is incrementally applied.

Condition 3 gives rise to a distribution of external longitudinal inplane forces along the local X-axis, which causes a bending moment.

An auxiliary node is set up to coincide with the center of the original undeformed plane. The terminal couple is applied at this section. After deformation, it is assumed that plane sections remain plane. By St. Venant's Principle of "elastic equivalence of statically equipollent systems of load,"[153,154] we conclude that for lengths larger than the cylinder diameter, the stress distribution away from the load, due to a zero net axial force and a terminal bending moment, does not depend on the traction distribution, except perhaps locally in the neighborhood of the point of application of the load. This condition can be fulfilled if vector $\underline{a}_3$ (Figure 2) of the local frame of reference, located on the deformed plane, is orthogonal to any vector on that plane.

The position vectors before deformation of nodes on the periphery of the shell, where the end couple is applied, are $\underline{r}_0$, and $\underline{r}_0^b$ for the auxiliary node. After displacements $\underline{u}$ of the peripheral nodes and $\underline{u}^b$ of the auxiliary node, we obtain

$$\underline{r} = \underline{r}_o + \underline{u} \tag{1}$$

$$\underline{r}^b = \underline{r}_o^b + \underline{u}^b \tag{2}$$

*MPC = Multiple Point Constraints

$$\underline{r} - \underline{r}^b = [\underline{r}_o - \underline{r}_o{}^b] + [\underline{u} - \underline{u}^b] \tag{3}$$

Therefore,

$$[\underline{r} - \underline{r}^b] \cdot \underline{a}_3 = 0 \tag{4}$$

where, in component notation,

$$\underline{r} - \underline{r}^b = [(x - x_b), (y - y_b), (z - z_b)] \tag{5}$$

and all quantitites are given with respect to the global undeformed frame. Now, if the original local x-axis (along vector $\underline{a}_3$) had an initial inclination φ_o with respect to the global y-axis, after deformation the angle would be $\varphi_o + \varphi_y{}^b$. Therefore, after deformation the direction cosines of the local vectors $\underline{a}_1$, $\underline{a}_2$, and $\underline{a}_3$ with respect to the global system would be

$$\underline{a}_1 = [\cos(\varphi_o + \varphi_y{}^b), \quad 0, \quad -\sin(\varphi_o + \varphi_y{}^b)] \tag{6}$$

$$\underline{a}_2 = [0, \quad 1, \quad 0] \tag{7}$$

$$\underline{a}_3 = [\sin(\varphi_o + \varphi_y{}^b), \quad 0, \quad \cos(\varphi_o + \varphi_y{}^b)] \tag{8}$$

Therefore,

$$\begin{aligned}(\underline{r} - \underline{r}^b) \cdot \underline{a}_3 &= (x - x_b)\sin(\varphi_o + \varphi_y{}^b) \\ &\quad + (z - z_b)\cos(\varphi_o + \varphi_y{}^b) = 0\end{aligned} \tag{9}$$

This can be further expanded by means of the trigonometric identities

$$\cos(\varphi_o + \varphi_y{}^b) = \cos\varphi_o \cos\varphi_y{}^b - \sin\varphi_o \sin\varphi_y{}^b \tag{10}$$

$$\sin(\varphi_o + \varphi_y{}^b) = \sin\varphi_o \cos\varphi_y{}^b + \cos\varphi_o \sin\varphi_y{}^b \tag{11}$$

Since our solution process is incremental and our constraints are nonlinear, our boundary conditions must be cast in incremental form. Consequently, we note that φ_o is a constant angle (which for straight tubes is zero). The incremental form of the left-hand side of Equation (3) can be obtained from the difference of the incremental forms of Equations (1) and (2), since

$$\underline{r} + \Delta\underline{r} = \underline{r}_o + \underline{u} + \Delta\underline{u} \tag{12}$$

$$\underline{r}^b + \Delta\underline{r}^b = \underline{r}_o{}^b + \underline{u}^b + \Delta\underline{u}^b \tag{13}$$

$$(\underline{r} + \Delta\underline{r}) - (\underline{r}^b + \Delta\underline{r}^b) = (\underline{r}_o - \underline{r}_o{}^b) + (\underline{u} - \underline{u}^b)$$

$$+ (\Delta\underline{u} - \Delta\underline{u}^b) \tag{14}$$

In view of Equation (3),

$$\Delta\underline{r} - \Delta\underline{r}^b = \Delta\underline{u} - \Delta\underline{u}^b \tag{15}$$

The incremental form of the righthand side of Equation (9) with respect to increments of the displacements u_z, u_x, $\varphi_y{}^b$, $u_z{}^b$, and $u_x{}^b$, by means of Equation (15) becomes

$$\begin{aligned}
&(\Delta u_z - \Delta u_z{}^b)[\cos\varphi_o \cos\varphi_y{}^b - \sin\varphi_0 \sin\varphi_y{}^b] \\
&+ (\Delta u_x - \Delta u_x{}^b)[\sin\varphi_o \cos\varphi_y{}^b + \cos\varphi_o \sin\varphi_y{}^b] \\
&+ (z - z_b)[-\cos\varphi_o \sin\varphi_y{}^b - \sin\varphi_o \cos\varphi_y{}^b]\Delta\varphi_y{}^b \\
&+ (x - x_b)\,[-\sin\varphi_o \sin\varphi_y{}^b + \cos\varphi_o \cos\varphi_y{}^b]\Delta\varphi_y{}^b = 0
\end{aligned} \tag{16}$$

or

$$(\Delta u_z - \Delta u_z{}^b)\cos(\varphi_o + \varphi_y{}^b) + (\Delta u_x - \Delta u_x{}^b)\sin(\varphi_o + \varphi_y{}^b)$$

$$+ \Delta\varphi_y^b \left\{(z - z_b)\sin(\varphi_o + \varphi_y^b) + (x - x_b)\cos(\varphi_o + \varphi_y^b)\right\} = 0 \qquad (17)$$

Next, we note the end plane does not rotate about the local Y-axis, i.e., there will be no component of rotation about vector $\underline{a}_1$. A small rotation about the local Y-axis can be obtained by a rotation vector with respect to the global system

$$\underline{\Omega} = (\varphi_x, \varphi_y, \varphi_z) \qquad (18)$$

If this vector is normal to vector $\underline{a}_1$, then it has no rotational component about $\underline{a}_1$, i.e.,

$$\underline{\Omega} \cdot \underline{a}_1 = [\varphi_x, \varphi_y, \varphi_z] \cdot [\cos(\varphi_y + \varphi_y{}^b), \quad 0,$$

$$-\sin(\varphi_o + \varphi_y{}^b)] = 0 \qquad (19)$$

or

$$\varphi_x\cos(\varphi_o + \varphi_y{}^b) - \varphi_z\sin(\varphi_o + \varphi_y{}^b) = 0 \qquad (20)$$

The incremental form of Equation (20) becomes

$$\Delta\varphi_x\cos(\varphi_o + \varphi_y{}^b) - \Delta\varphi_z\sin(\varphi_o + \varphi_y{}^b)$$

$$- \Delta\varphi_y{}^b\left\{\varphi_x\sin(\varphi_o + \varphi_y{}^b) + \varphi_z\cos(\varphi_o + \varphi_y{}^b)\right\} = 0 \qquad (21)$$

Finally, the essential boundary condition is that the rotation φ_y of all nodes on the periphery must equal the rotation about the local Z-axis ($\underline{a}_2$ vector or global y-axis) of the auxiliary node, i.e.,

$$\varphi_y = \varphi_y^{\ b} \tag{22}$$

and in incremental form

$$\Delta\varphi_y = \Delta\varphi_y^{\ b} \tag{23}$$

The vertical (global x-axis) rigid body motion must be removed. This can be accomplished by coupling the average X-displacement of the shell nodes on the end section to the vertical displacement of the auxiliary node. This, in turn, is set to zero. For element i, S8R element displacements across an edge are quadratic, i.e. (with $0 \leq \xi \leq 1$) the vertical displacement $u(\xi)$ is given in terms of its nodal values (u_k, u_{k+1}, u_{k+2})

$$u(\xi) = [(2\xi - 1)(\xi - 1),\ 4\xi(1 - \xi),\ \xi(2\xi - 1)] \begin{bmatrix} u_k \\ u_{k+1} \\ u_{k+2} \end{bmatrix} \tag{24}$$

For uniform finite element grid, where s denotes arc length, s_i arc length of element i, and L total arc length,

$$\ell_i = \frac{L}{N} \tag{25}$$

$$ds_i = \ell_i d\xi = \frac{L}{N}\, d\xi \tag{26}$$

At the element level (element i), with nodal vertical displacements (u_k, u_{k+1}, u_{k+2})

$$\int_{s=0}^{s=s_i} u(\xi)ds_i = \int_{\xi=0}^{\xi=1} u(\xi)\ell_i d\xi = \ell_i \int_0^1 u(\xi)d\xi$$

$$= \frac{\ell_i}{6} [1, 4, 1] \begin{bmatrix} u_k \\ u_{k+1} \\ u_{k+2} \end{bmatrix} = \frac{L}{6N} [1, 4, 1] \begin{bmatrix} u_k \\ u_{k+1} \\ u_{k+2} \end{bmatrix} \tag{27}$$

Since there are N elements (with 2 corner and 1 midside nodes, i.e. 3 nodes total), there will be 2N+1 nodes and associated nodal values of vertical displacements. Therefore, by Equation (24)

$$\int_{s=0}^{s=L} u(s)ds = \sum_{i=1}^{i=N} \int_{\xi=0}^{\xi=1} u(\xi)\ell_i d\xi$$

$$= \underset{\{1x(2N+1)\}}{\frac{L}{6N} [1, 4, 2, 4, \ldots, 2, 4, 1]} \underset{\{(2N+1) \times 1\}}{\begin{bmatrix} u_s \\ u_{s+1} \\ \cdot \\ \cdot \\ u_{s+2N-1} \\ u_{s+2N} \end{bmatrix}} \tag{28}$$

Consequently, the boundary condition

$$\frac{1}{L} \int_{s=0}^{s=L} u(s)ds = u_x^{\,b} \tag{29}$$

can be recast, in view of Equation (28), to

$$\frac{1}{6N}\underset{\{1\times(2N+1)\}}{[1,4,2,4,\ldots,2,4,1]}\underset{\{(2N+1)\times 1\}}{\begin{bmatrix} u_s \\ u_{s+1} \\ \vdots \\ u_{s+2N-1} \\ u_{s+2N} \end{bmatrix}} = u_x^{\,b} \qquad (30)$$

for a uniform grid, where the nodal vector of Equation (30) denotes vertical displacements of shell nodes at the end plane. The above constraints can be incorporated through the nonlinear MPC capability of ABAQUS.[152] Furthermore, from Equations (3) and (9), Equation (9) can be rewritten as

$$\begin{aligned}&[x_o + u_x - x_o^{\,b} - u_x^{\,b}]\sin(\varphi_o + \varphi_y^{\,b}) \\ &\quad + [z_o + u_z - z_o^{\,b} - u_z^{\,b}]\cos(\varphi_o + \varphi_y^{\,b}) = 0\end{aligned} \qquad (31)$$

Following Reference 152, we eliminate u_z from Equation (31) first (i.e. at the shell node)

$$u_z = u_z^{\,b} + (z_o^{\,b} - z_o) - (x_o - x_o^{\,b} + u_x - u_x^{\,b})\tan(\varphi_o + \varphi_y^{\,b}) \qquad (32)$$

Solving for φ_x from Equation (20)

$$\varphi_x = \varphi_z \tan(\varphi_o + \varphi_y^{\,b}) \qquad (33)$$

and φ_y from Equation (22)

$$\varphi_y = \varphi_y^{\,b} \qquad (34)$$

Furthermore, we eliminate the vertical translation u_x. This follows from constraints involving the elimination of u_z. All previous steps are explained in Reference 152 or can be found in the FORTRAN listing for MPC constraints.

APPLICATIONS AND RESULTS

Four unstiffened circular cylinders[93] have been analyzed using the finite element program ABAQUS[152]: models 10A, 16A, 20A of Reference 93, and 20AI, which is an imperfect version of model 20A. Note that they are comparatively thick to avoid premature collapse and to exhibit plasticity effects as the applied external moment increases past the yield moment. The above models fall in the range of "long cylinders." Their perfect discrete analogues would fail by ovalization or the "Brazier effect," or by plastic deformation. The experimentally imperfect models failed by buckling "failure"[93] as displayed on the moment-curvature curves.

Table 1 gives the geometrical and material properties of these models and the stress-strain curves can be obtained from Reference 93. In Reference 93, the external loading was applied by the use of a so-called "shear span" prior to the test section "bending span." To create the external moment in our research, we employed an additional span beyond the bending span, equal to the "shear" span, and then applied a fixed angle of rotation. Table 2 contains some parameters used in reducing the stresses, moments, curvatures, and forces in nondimensional form, and they can be used to determine relative magnitude for critical quantities such as yield moment, etc.

Mean curvature k is defined as the ratio of the sum of the absolute values of direct longitudinal strains at 0° (top of cylinder, i.e. tension side) and 180° (bottom of cylinder, i.e. compression side) divided by the undeformed diameter of the shell. Figures 3 through 5 are the relevant M vs. k curves for models 10A, 16A, and 20A, together with the corresponding experimental results of Reference 93. Agreement between experimental (dots) and computed results is good for all three cylinders. Imperfection sensitivity and the analysis of medium and short cylinders, where short-wave length buckling may control the collapse mechanism, will be addressed elsewhere.

Figures 6 through 8 display the work done versus the moment parameter $\mu = M_{EXT}/M_0$, where $M_0 = 4R^2 h\sigma_y$, R = mean radius of cylinder, E = Young's Modulus, M_{EXT} = external bending moment, h = shell thickness, and σ_y = material yield stress.

We define two parameters, longitudinal stress/stress at bifurcation and hoop stress/stress at bifurcation, where stress at bifurcation is

$$\sigma_{CR} = \frac{E}{\sqrt{3\,(1-\nu^2)}}\ \frac{h}{R}$$

Figures 9 through 11 represent plots of the longitudinal inplane stress parameter versus angular position. Additional local bending stresses across the shell thickness are not addressed. Note, however, that the longitudinal membrane stress distribution in Figures 9 through 11 does not follow simple beam theory. The stress distribution from the 0° and 180° points (top and bottom of

TABLE 1. GEOMETRICAL AND MATERIAL PROPERTIES OF MODELS [93]

MODEL No.	RADIUS R (IN)	THICKNESS h (IN)	YOUNG'S MODULUS E (ksi)	POISSON'S RATIO ν	YIELD STRESS σ_y (ksi)	HALF LENGTH USED IN COMPUTATION L/2 (IN)	R/h	L/R
10A	5.258	0.233	28,947.0	0.3	50.000	108.0	22.566	41.08
16A	7.870	0.260	30,000.0	0.3	45.272	162.0	30.629	41.17
20A	9.873	0.255	28,947.0	0.3	50.000	162.0	38.717	32.82

TABLE 2. CHARACTERISTIC PARAMETERS OF MODELS

MODEL No.	(1) σ_{CR} (ksi)	(2) M_{CR} (k-in)	(3) K_{CR} (1/in)	(4) M_{BR} (k-in)	(5) M_o (k-in)	(6) F_o (k)	(7) I (in^4)
10A	776.35	15,711.0	0.510074×10^{-2}	8,552.0	1,288.33	384.88	106.40
16A	599.84	30,346.7	0.254063×10^{-2}	16,518.6	2,916.17	582.04	398.15
20A	452.49	35,334.7	0.158329×10^{-2}	19,233.8	4,971.28	790.93	770.97

NOTES:

(1) CRITICAL STRESS AT BIFURCATION $\sigma_{CR} = \frac{E}{\sqrt{3(1-\nu^2)}}\left(\frac{h}{R}\right)$

(2) CRITICAL MOMENT AT BIFURCATION $M_{CR} = \frac{\pi E}{\sqrt{3(1-\nu^2)}} Rh^2$

(3) CRITICAL CURVATURE AT BIFURCATION $k_{CR} = \frac{1}{\sqrt{3(1-\nu^2)}} \frac{h}{R^2}$

(4) CRITICAL BRAZIER MOMENT $M_{BR} = \frac{2\sqrt{2}}{9\sqrt{(1-\nu^2)}} \pi E Rh^2$

(5) PLASTIC MOMENT BASED ON YIELD STRESS $M_o = 4R^2h\sigma_y$

(6) AXIAL FORCE BASED IN YIELD STRESS $F_o = 2Rh\sigma_y$

(7) MOMENT OF INERTIA OF UNDEFORMED CROSS-SECTION $I = \pi R^3 h$

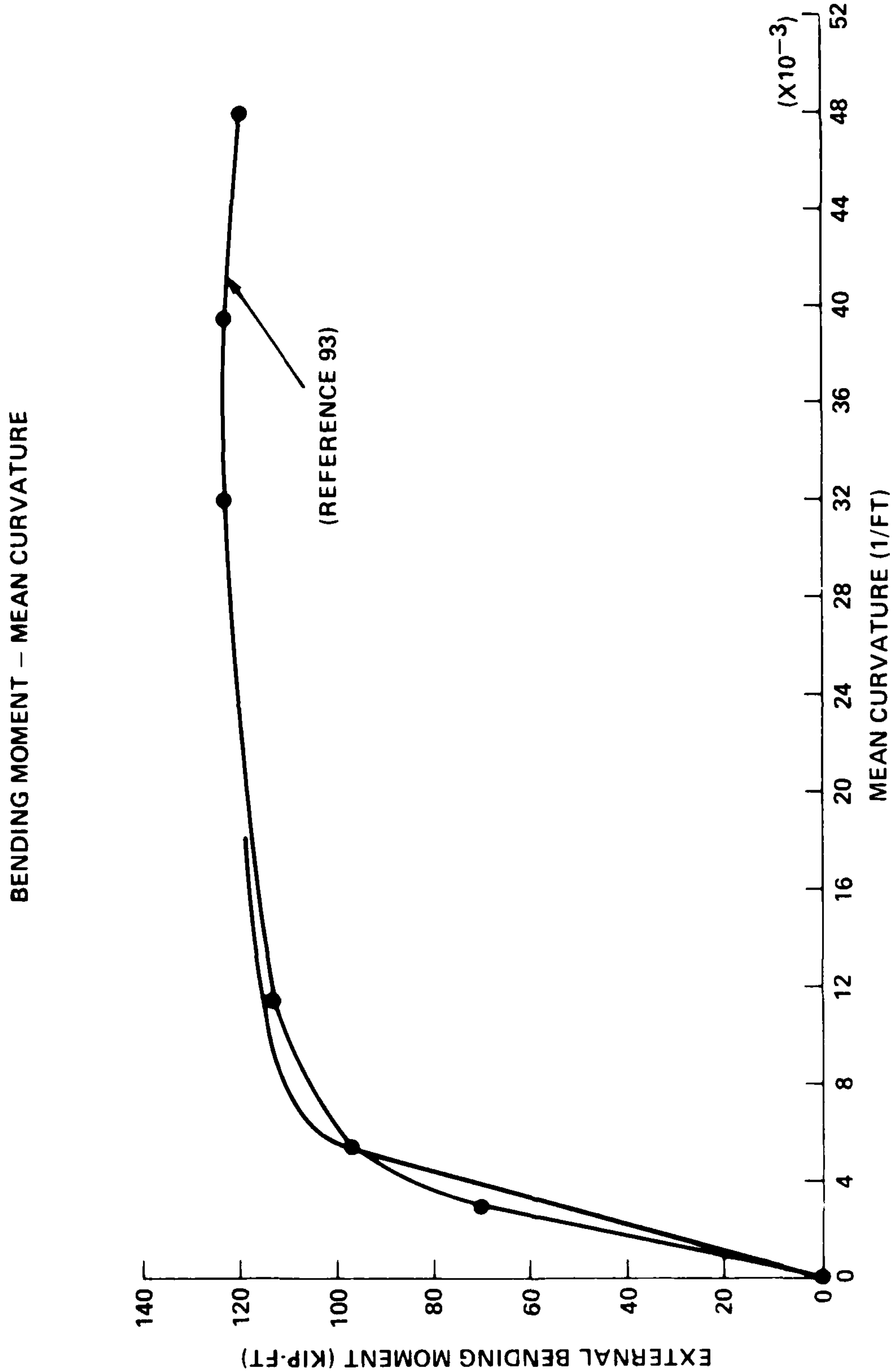

FIGURE 3. MOMENT – CURVATURE PLOTS FOR MODEL 10A

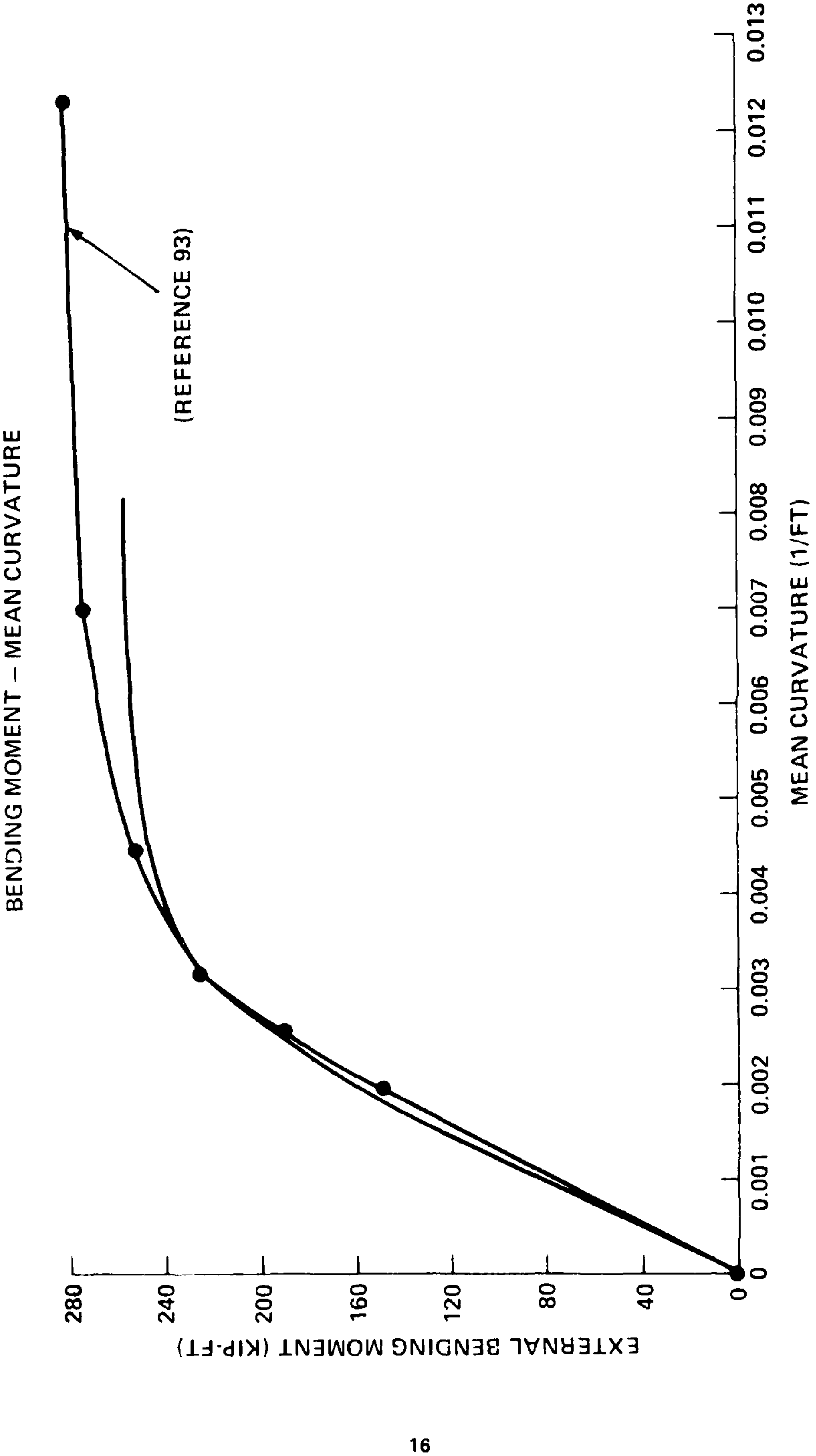

FIGURE 4. MOMENT – CURVATURE PLOTS FOR MODEL 16A

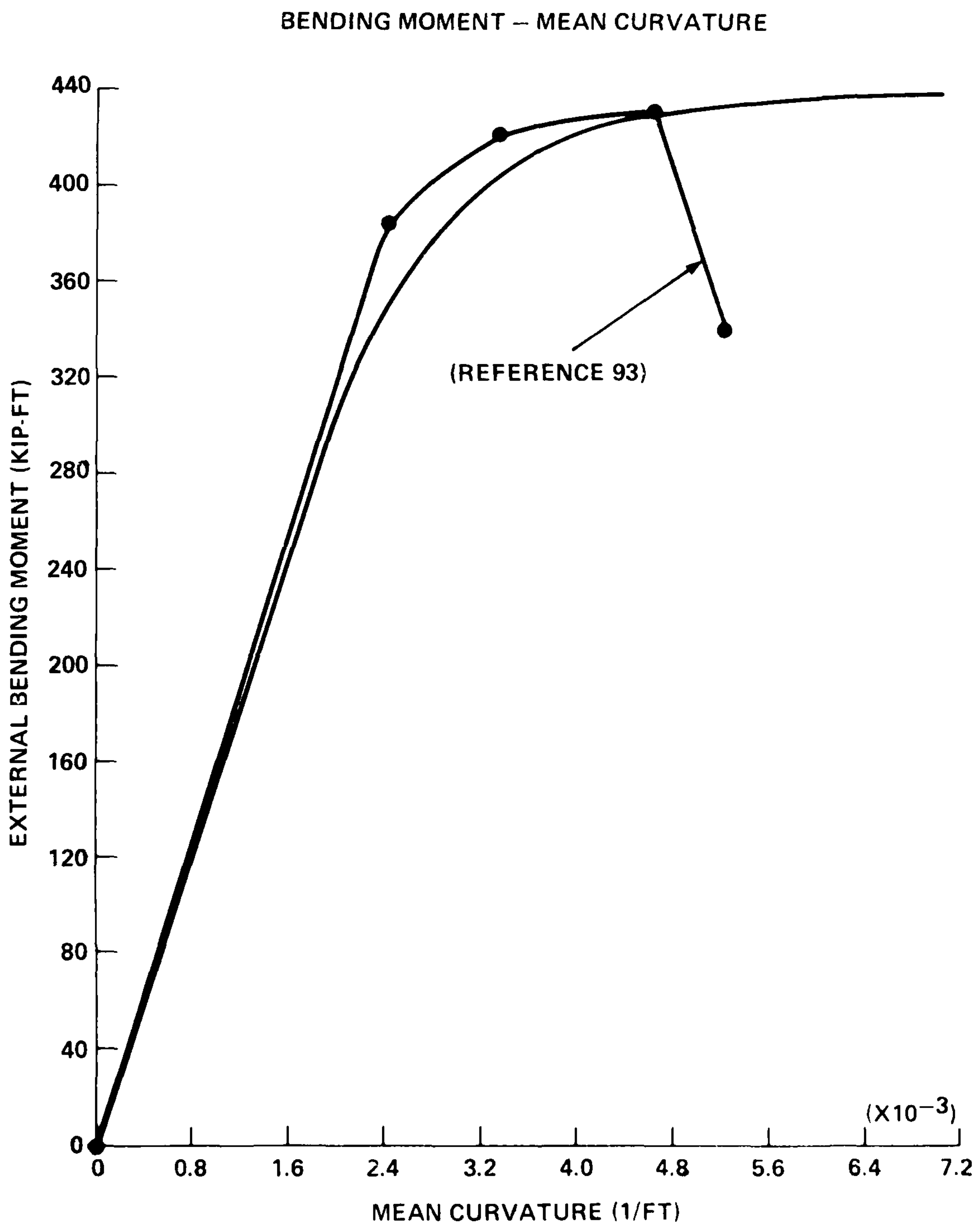

FIGURE 5. MOMENT – CURVATURE PLOTS FOR MODEL 20A

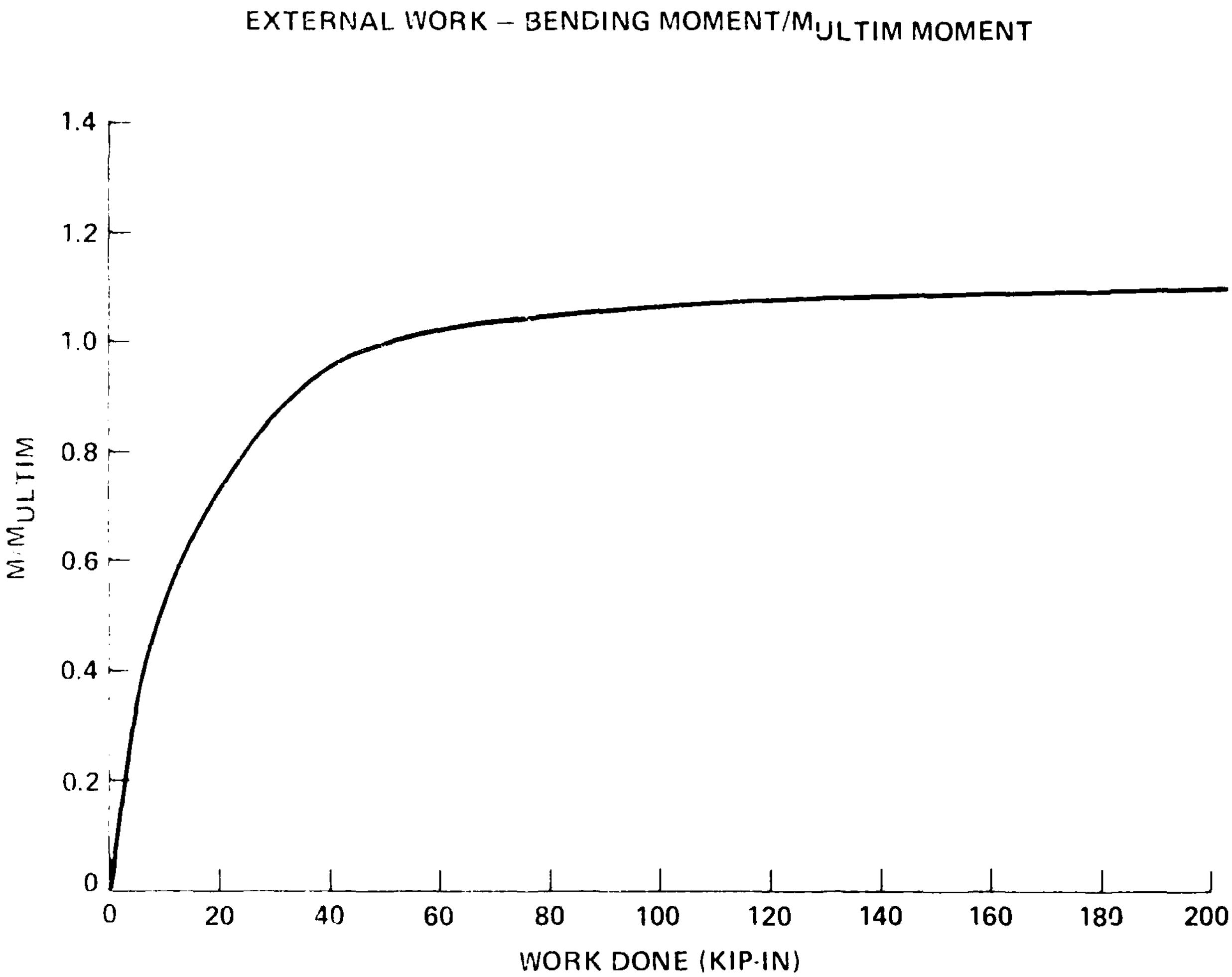

FIGURE 6. M/M_{ULTIM} WORK DONE (KIP-IN) FOR MODEL 10A

EXTERNAL WORK – BENDING MOMENT/M_{ULTIM} MOMENT

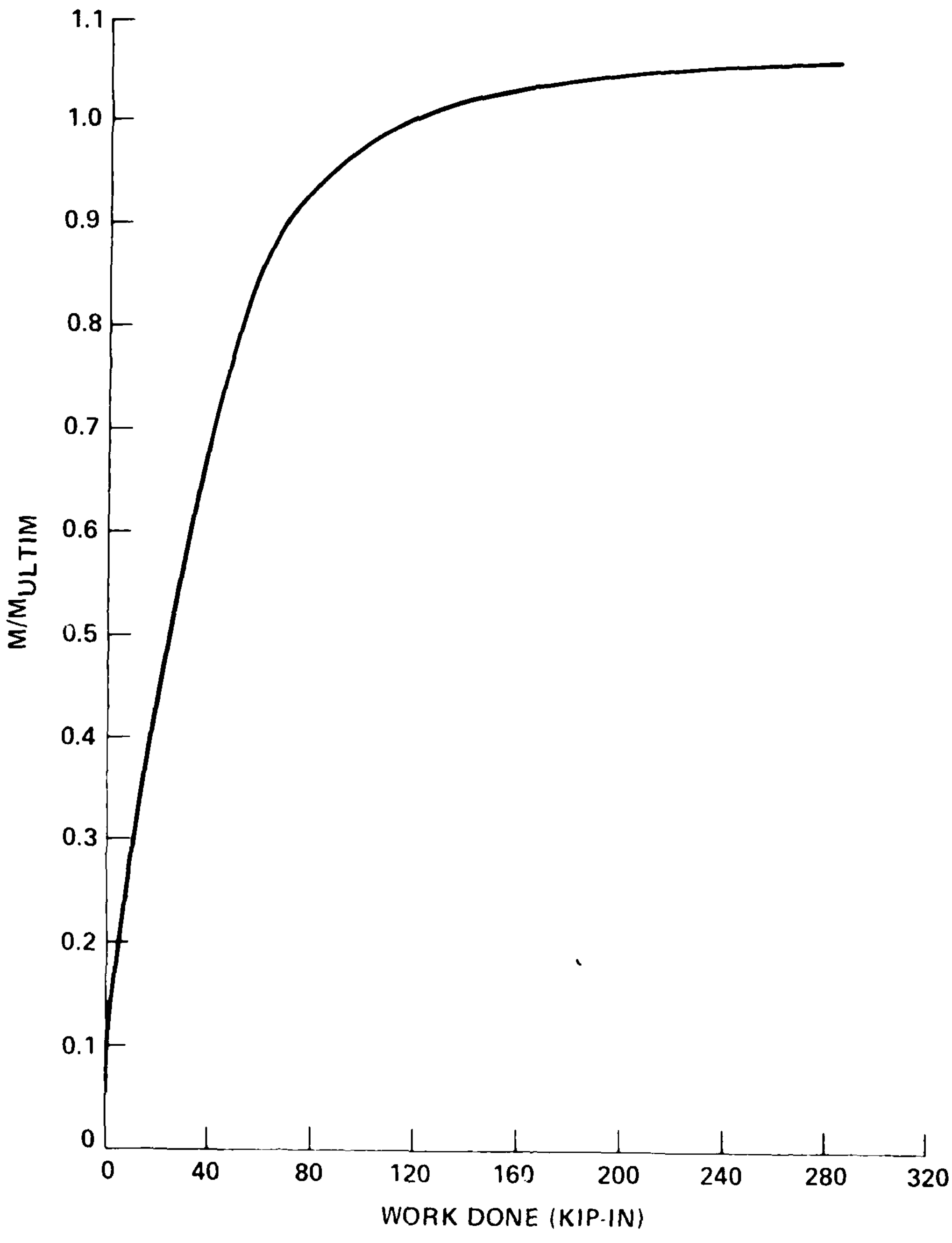

FIGURE 7. M/M_{ULTIM} WORK DONE (KIP-IN) FOR MODEL 16A

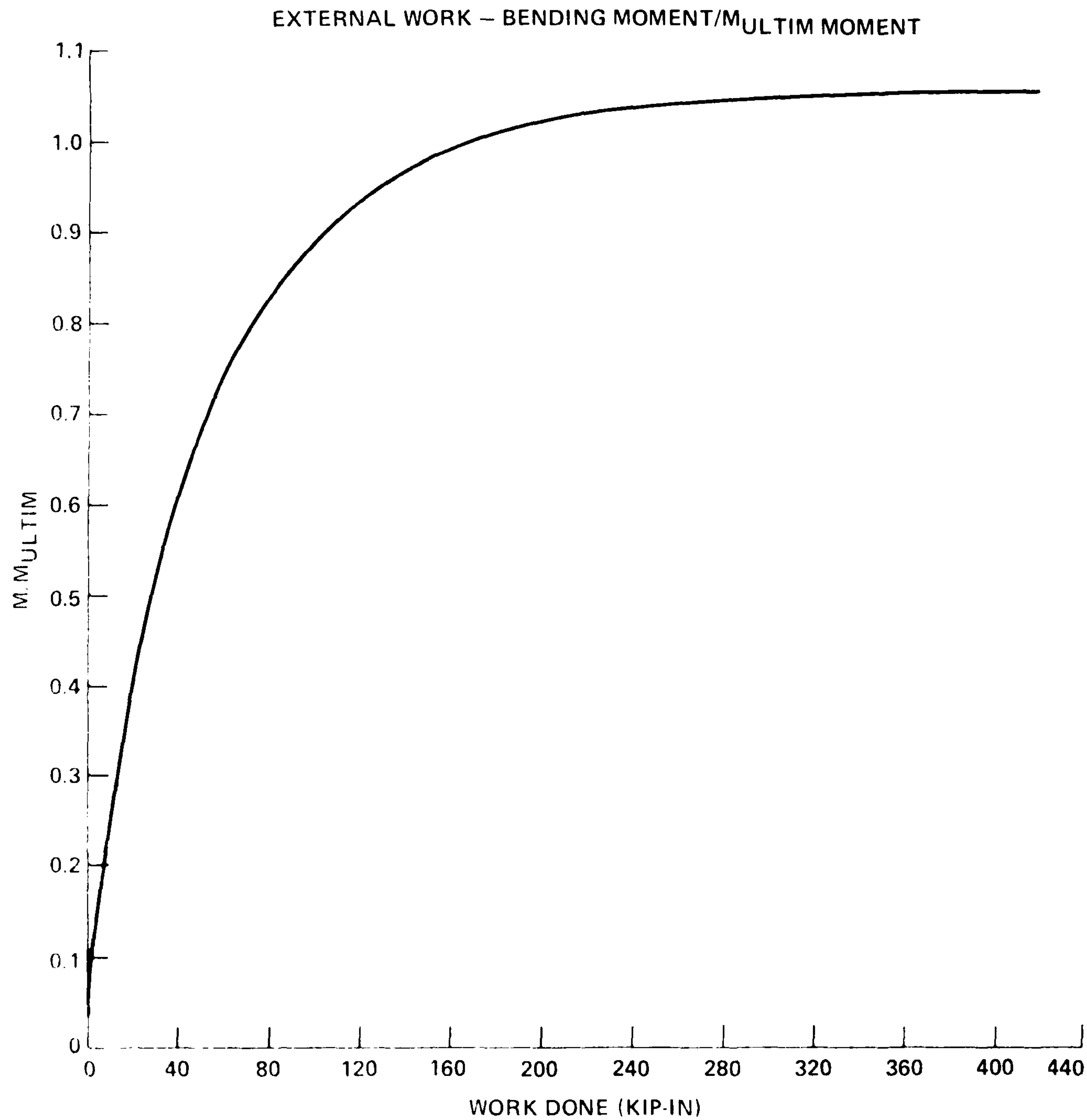

FIGURE 8. M/M_{ULTIM} WORK DONE (KIP-IN) FOR MODEL 20A

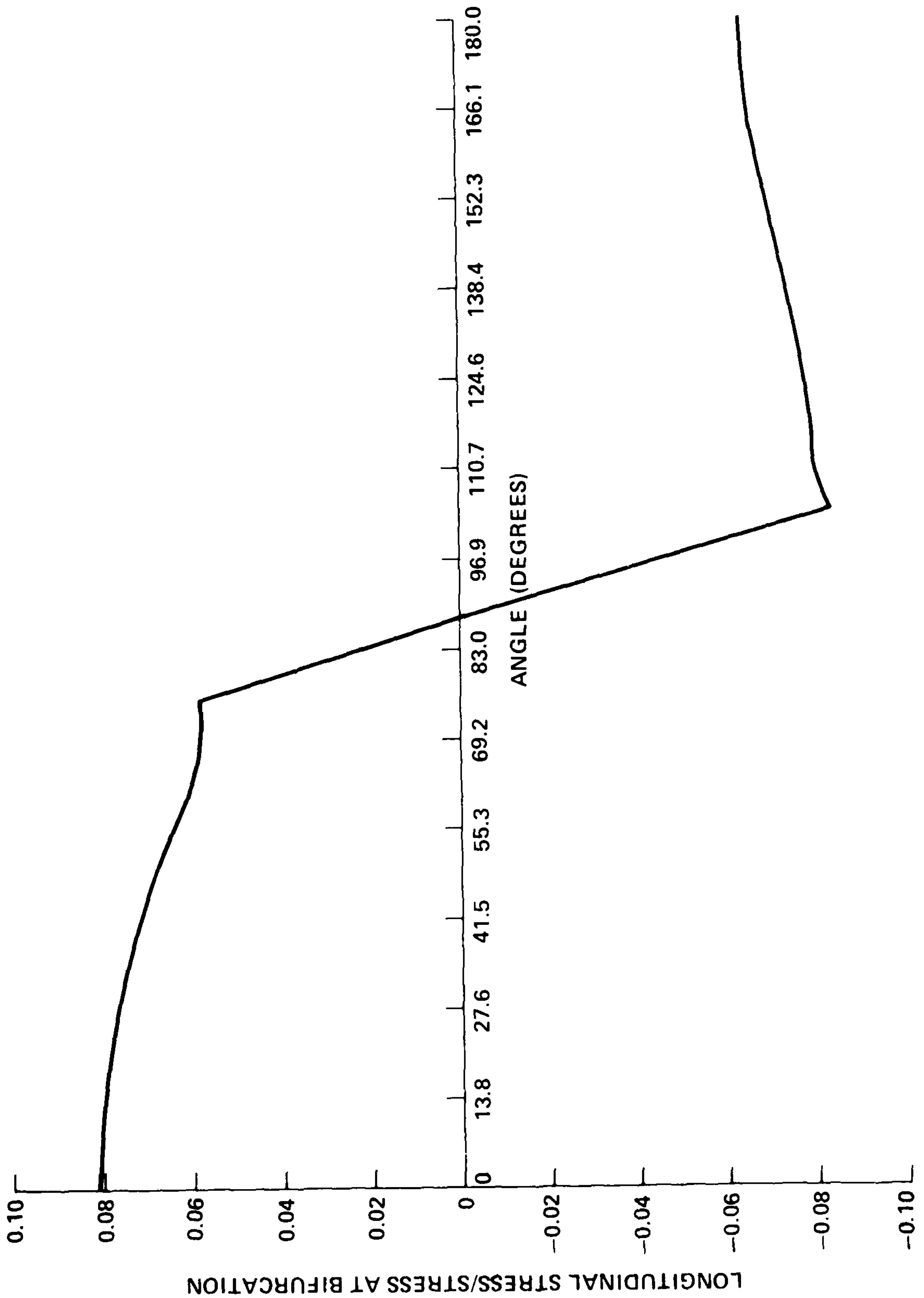

FIGURE 9. LONGITUDINAL STRESS (STEP 17) VERSUS ANGULAR POSITION FOR MODEL 10A

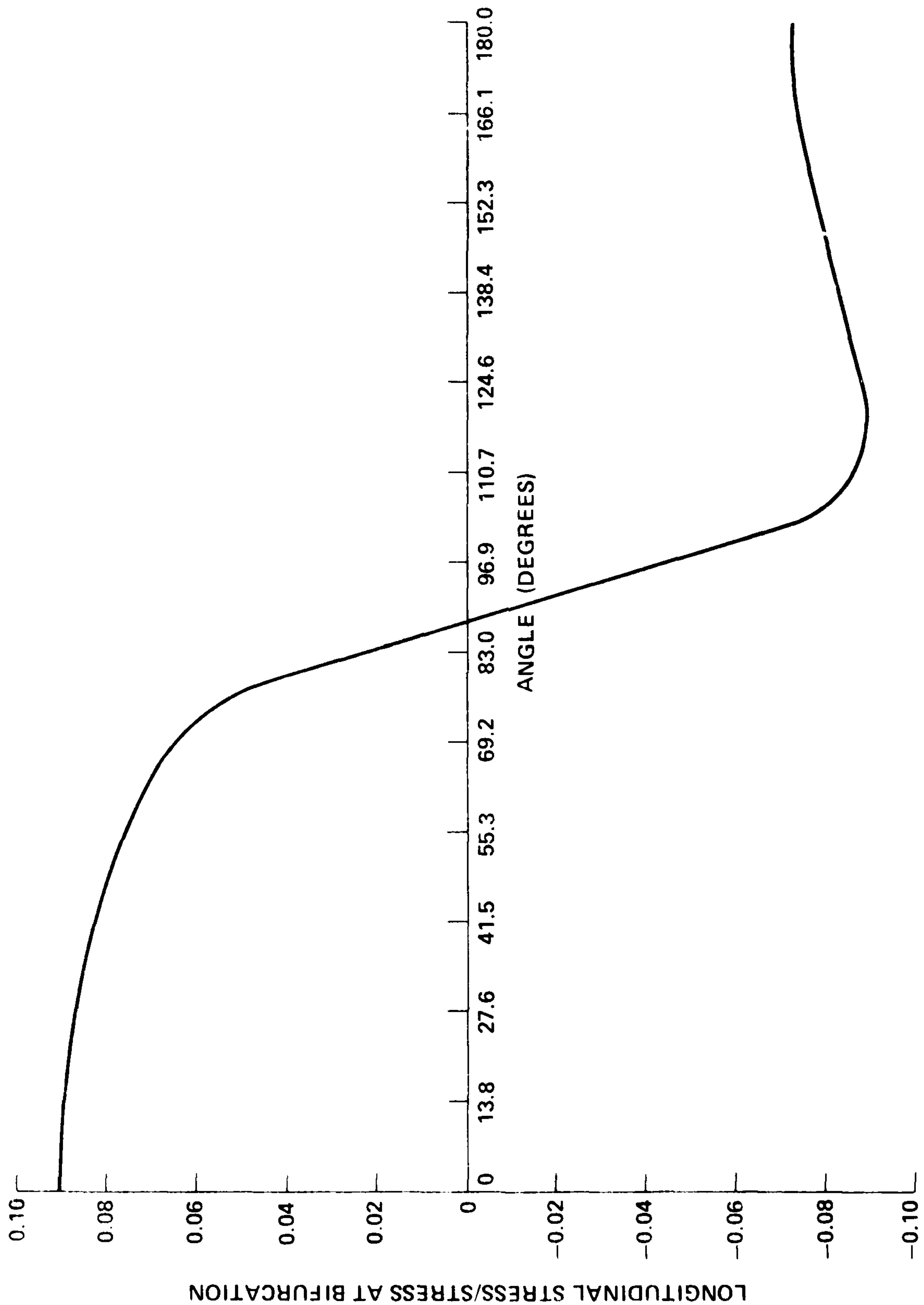

FIGURE 10. LONGITUDINAL STRESS (STEP 31) VERSUS ANGULAR POSITION FOR MODEL 16A

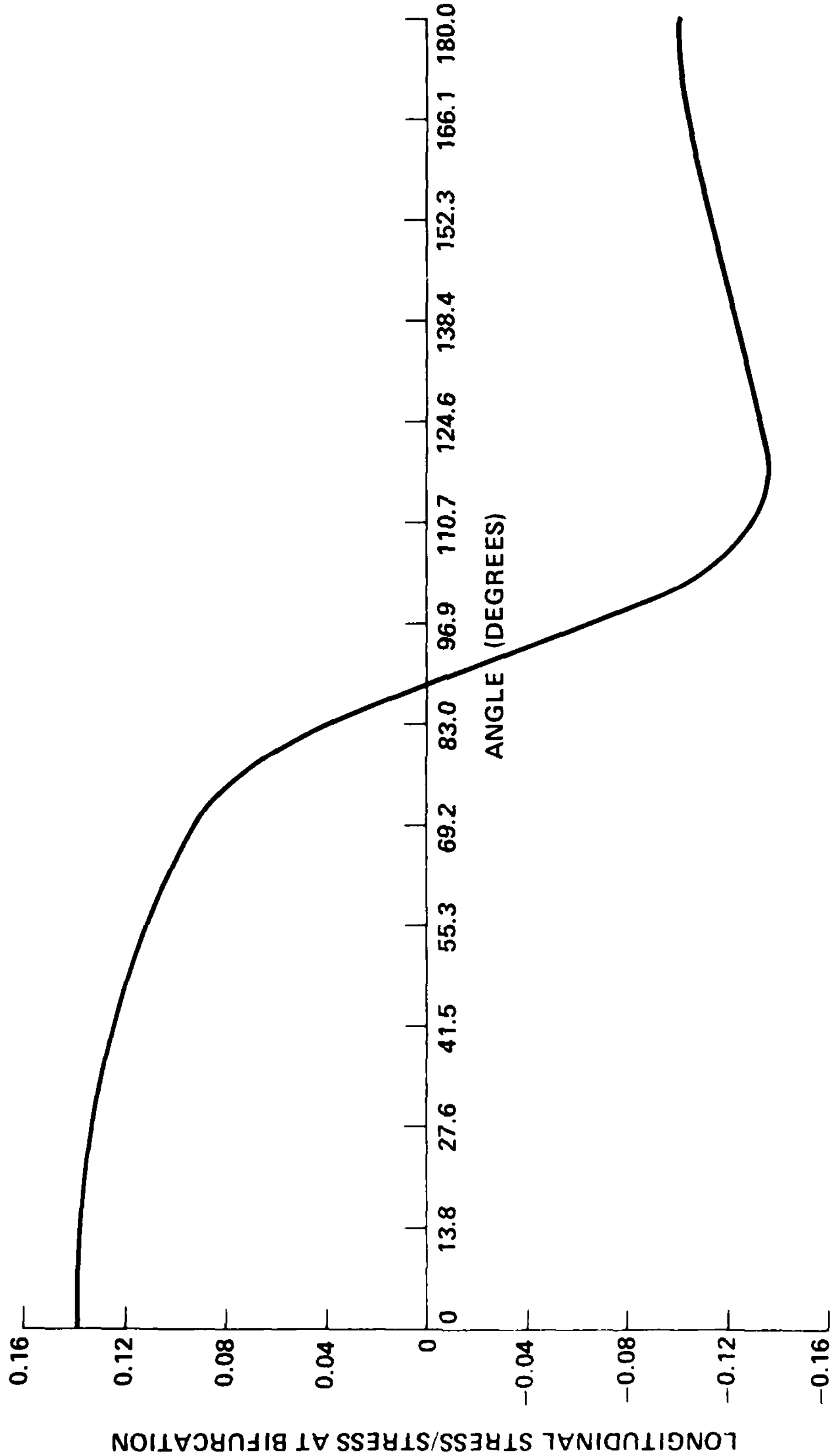

FIGURE 11. LONGITUDINAL STRESS (STEP 20) VERSUS ANGULAR POSITION FOR MODEL 20A

the half-section) is reduced (tension zone) or increased (compression zone) slightly before it assumes a linear form.

Figures 12 through 14 display the variation of the hoop stress parameter with angular location. The distribution of this stress over the half-section clearly indicates maximum compressive hoop stresses around the 90° location, with corresponding maximum tensile hoop stresses at 0° and 180°, respectively. These stresses, however, are smaller than the longitudinal membrane stresses by an order of magnitude. All stresses shown correspond to the final point of the moment-curvature plots.

Close examination of Figures 15 through 17 reveals that the M/M_{CR} vs. k/k_{CR} curves have a slope at the origin of approximately 1.0. This agrees fairly well with the initial slope predicted by Reissner's nonlinear theory[55] as well as Von Karman's linear analysis.[3] In the present notation, Reissner's relationship between M/M_{CR} and k/k_{CR} can be written as

$$M/M_{CR} = k/k_{CR}[1.0 - 0.5\,(k/k_{CR})^2 - (1/6)\,(k/k_{CR})^4 \; . \; . \; . \; . \;] \qquad (35)$$

with an obvious slope of 1.0 at the origin, maximum value of $M/M_{CR} = 0.5011$ at $k/k_{CR} = 0.71954$. The maximum value of 0.5011 is much higher than both experimental and numerical results, showing the effects of plasticity which Reissner's theory does not account for. Note that plots of $\mu = (M_{EXT}/M_0)$ versus work done (Figures 6 through 8) clearly display that ultimate moment is reached at $\mu \approx 1$ as predicted by beam plastic theory. Actually, it exceeds $\mu = 1$ by about 10 percent.

Figure 18 displays the deformed and undeformed profiles of cylindrical model 20A. Figure 19 represents the corresponding deformed and undeformed profiles of the imperfect version of model 20A, which from now on will be referred to as model 20AI. Figure 20 is an enlargement of the cross-sections at midlength before and after deformation of model 20AI. Figure 21 shows the moment-curvature plots of model 20AI compared with the experimental data (circled points). Similarly, Figures 22 through 25 show results for model 20AI of the following pairs of variables:

$\mu = M_{EXT}/M_0$ (or $M/M_{ULTIMATE}$) $\sim$ Work Done (kip-in.)

$\sigma^{LONG}_{INPLANE}/\sigma_{CR} \sim$ Angular Position

$\sigma^{HOOP}/\sigma_{CR} \sim$ Angular Position and $M/M_{CR} \sim k/k_{CR}$

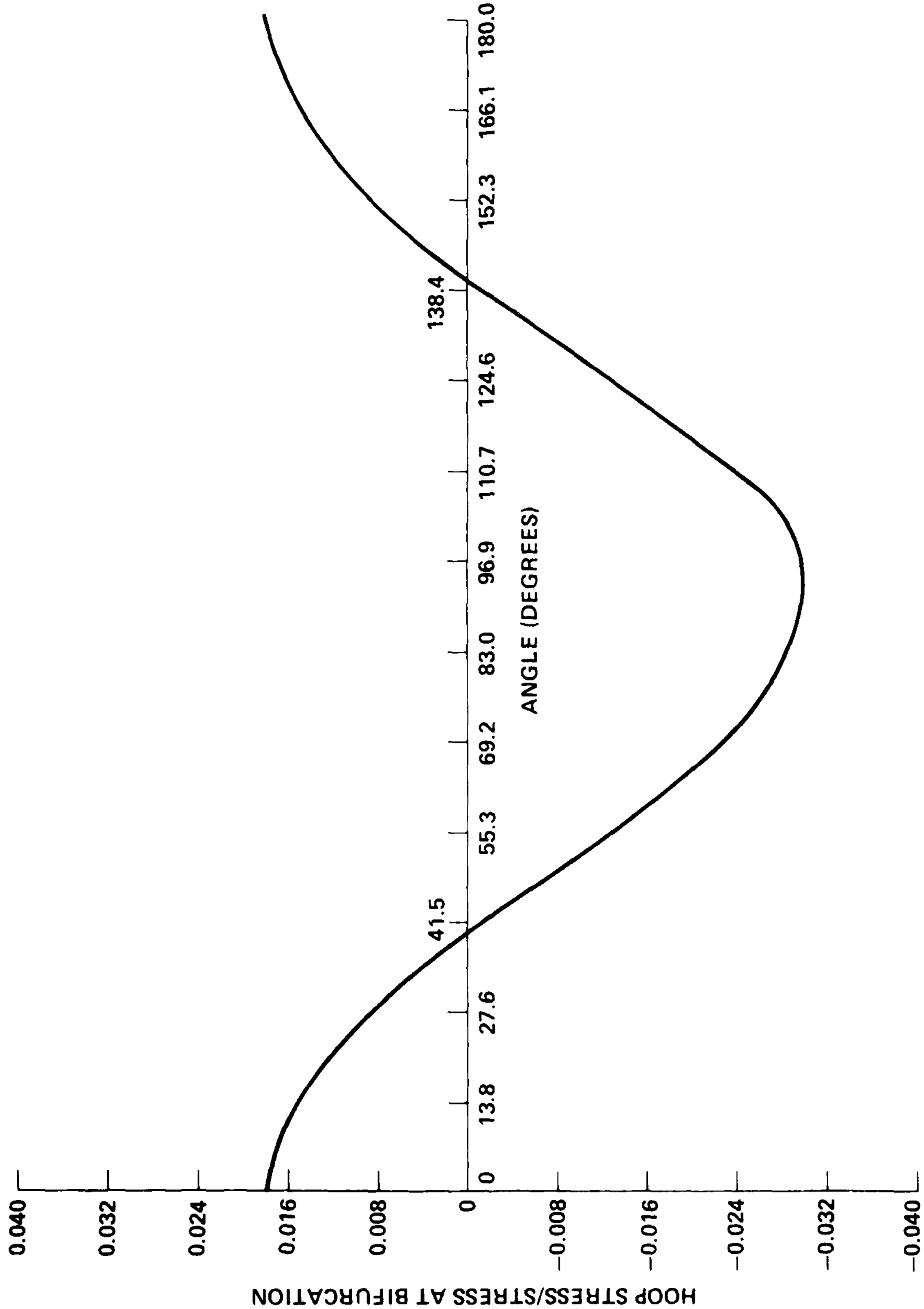

FIGURE 12. HOOP STRESS DISTRIBUTION (STEP 17) VERSUS ANGULAR POSITION FOR MODEL 10A

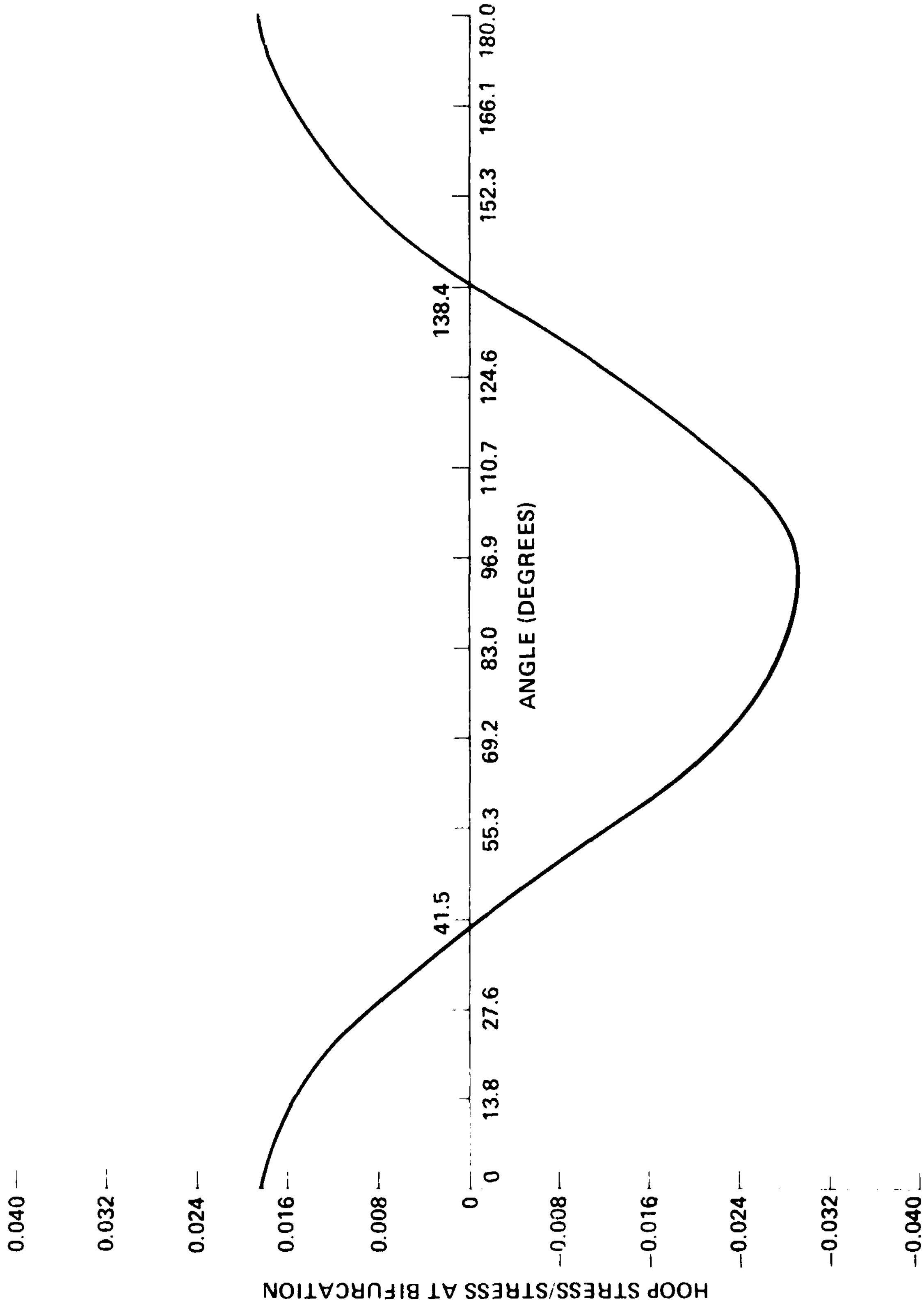

FIGURE 13. HOOP STRESS DISTRIBUTION (STEP 31) VERSUS ANGULAR POSITION FOR MODEL 16A

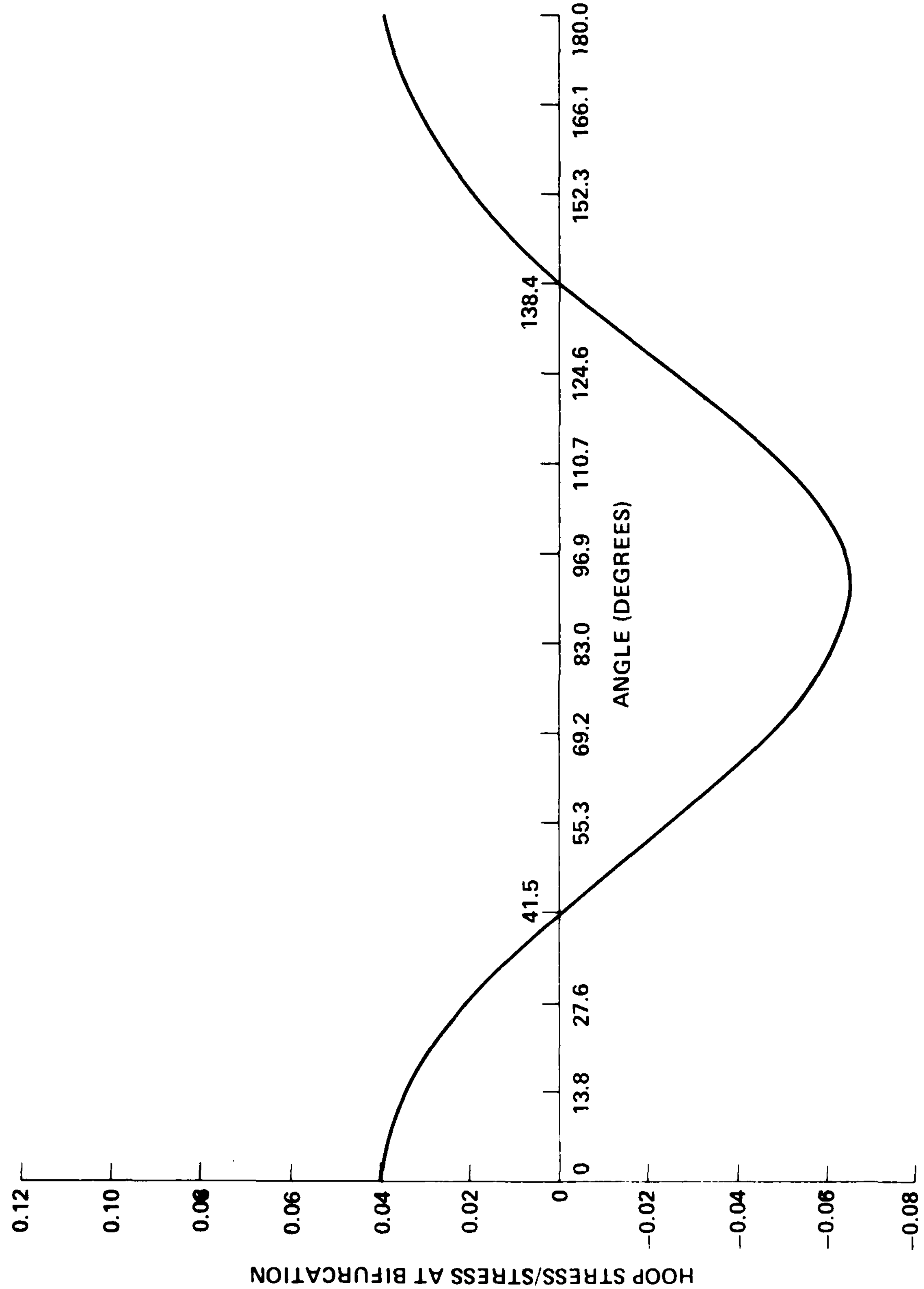

FIGURE 14. HOOP STRESS DISTRIBUTION (STEP 20) VERSUS ANGULAR POSITION FOR MODEL 20A

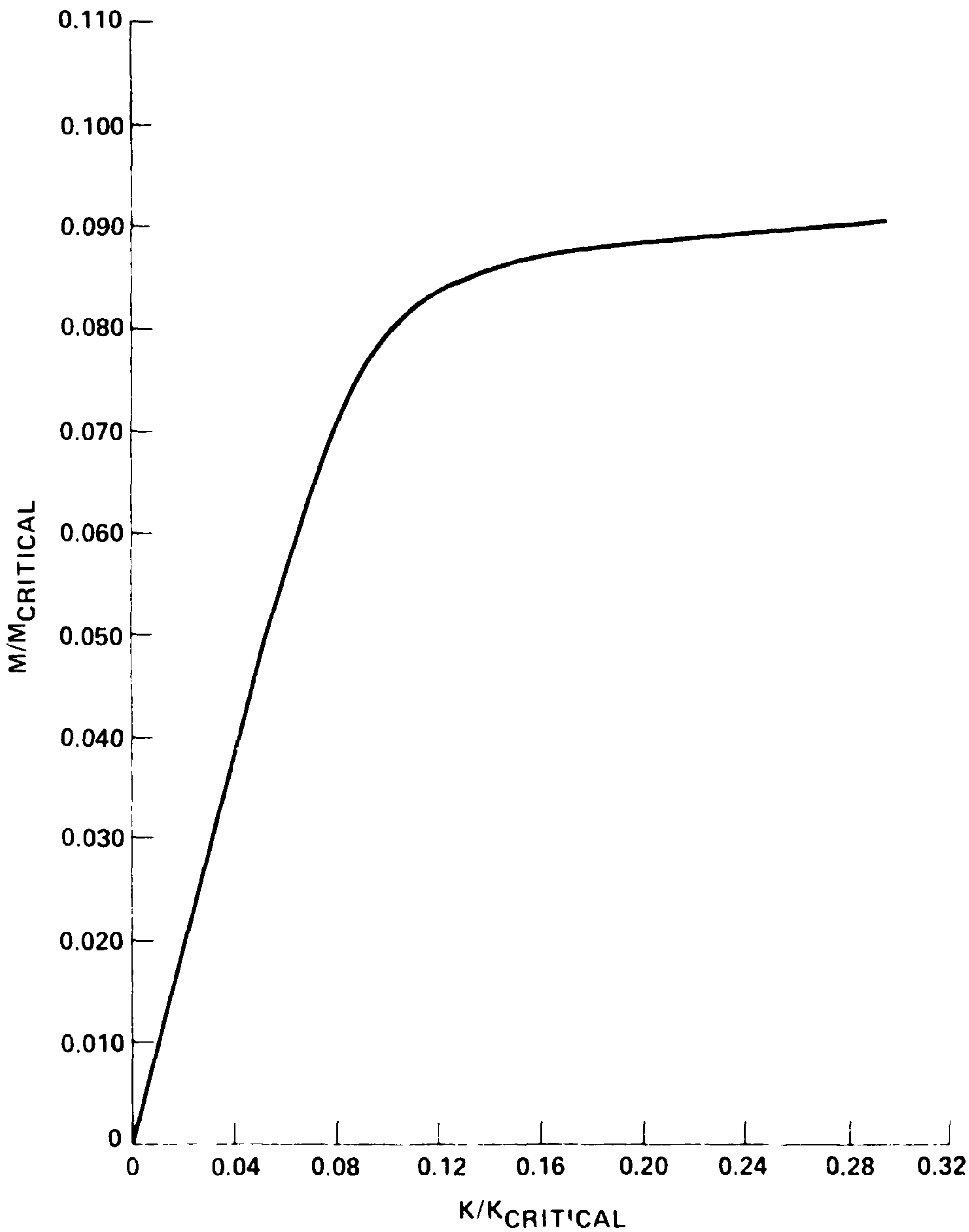

FIGURE 15. $M/M_{CRITICAL}$ VERSUS $K/K_{CRITICAL}$ FOR MODEL 10A

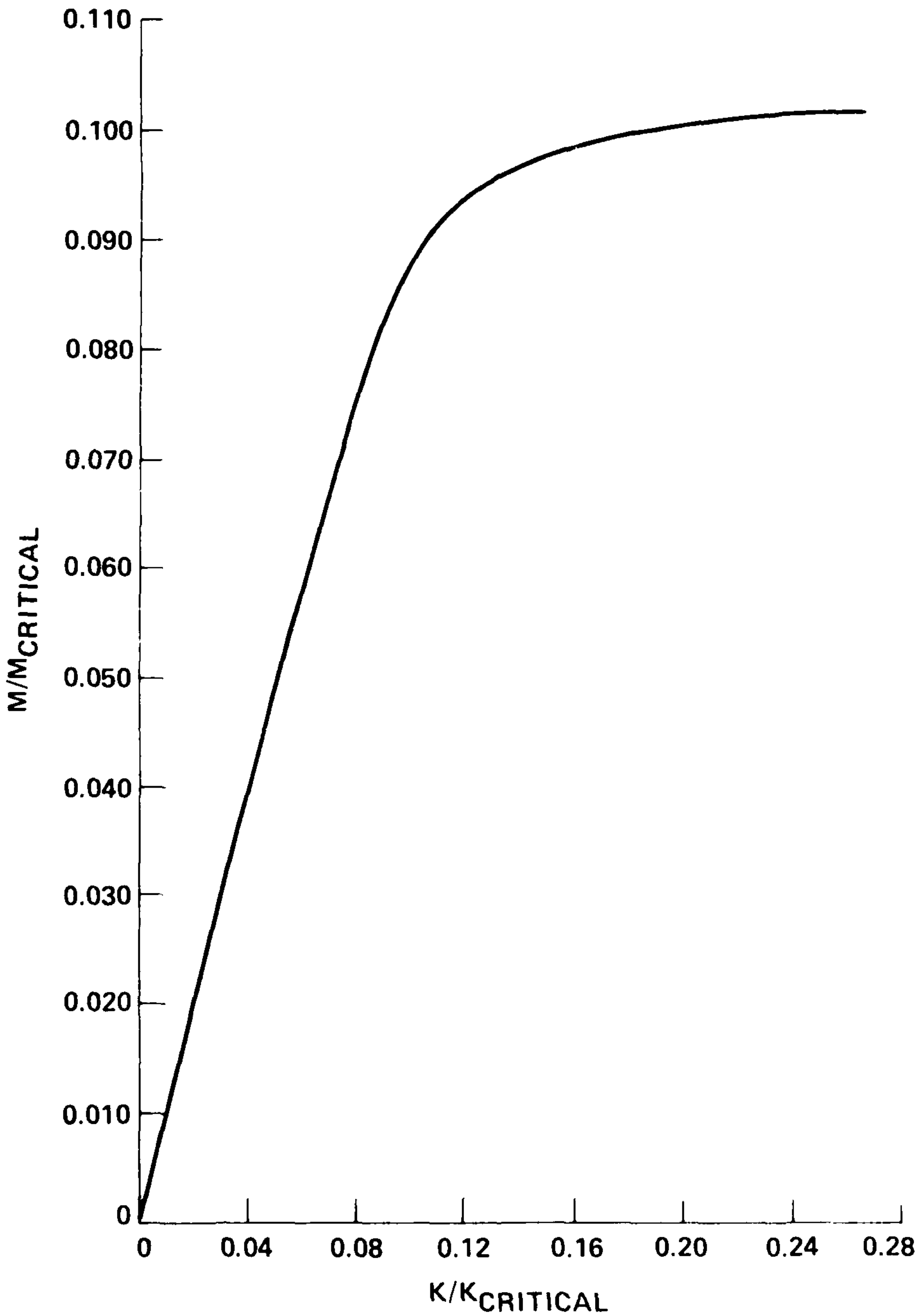

FIGURE 16. $M/M_{CRITICAL}$ VERSUS $K/K_{CRITICAL}$ FOR MODEL 16A

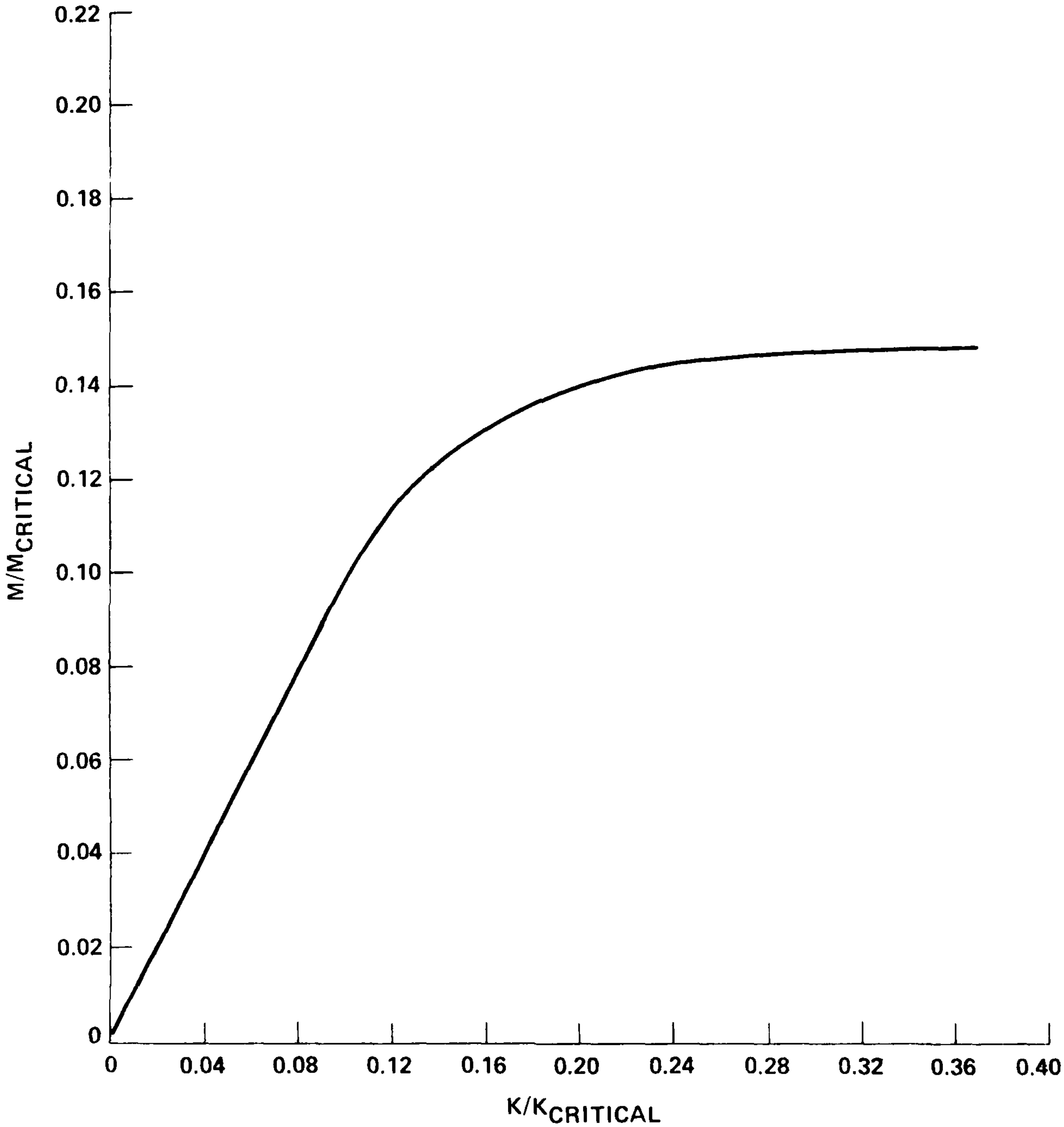

FIGURE 17. $M/M_{CRITICAL}$ VERSUS $K/K_{CRITICAL}$ FOR MODEL 20A

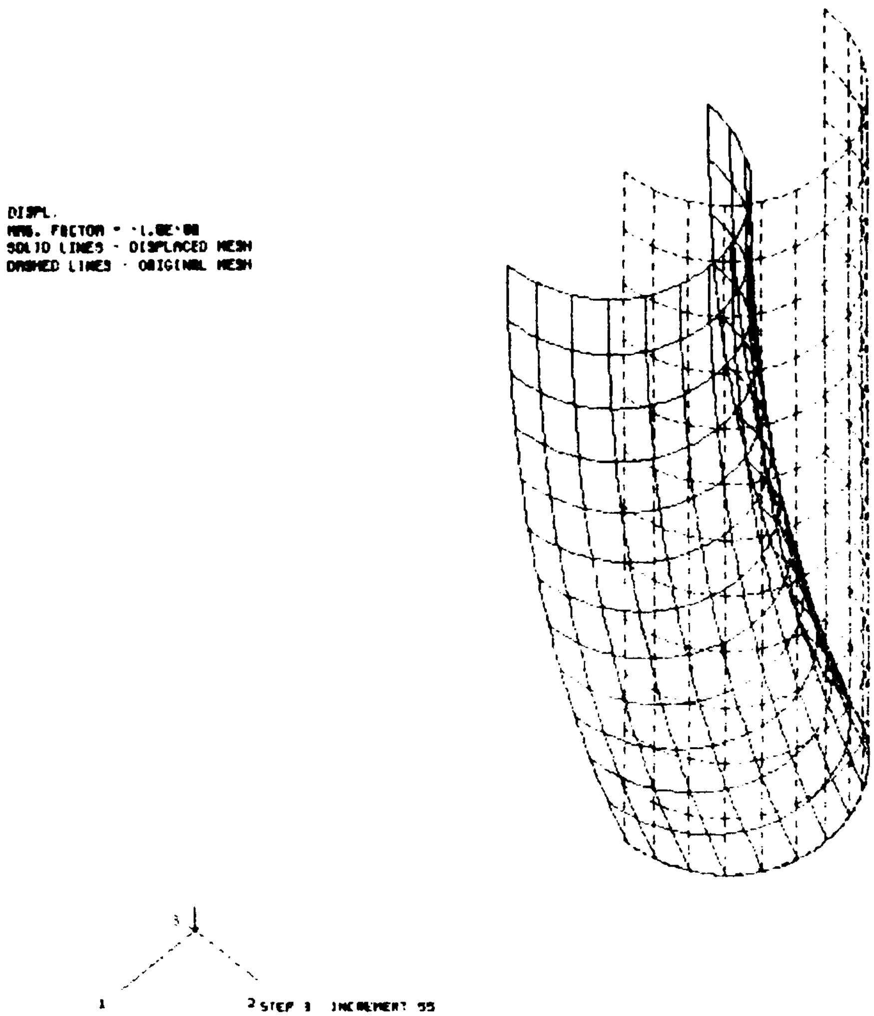

FIGURE 18. CYLINDRICAL SHELL (MODEL 20A) SUBJECT TO END BENDING MOMENT VIEWED FROM 100'',100'',500'' AT STEP 3, INCREMENT 55

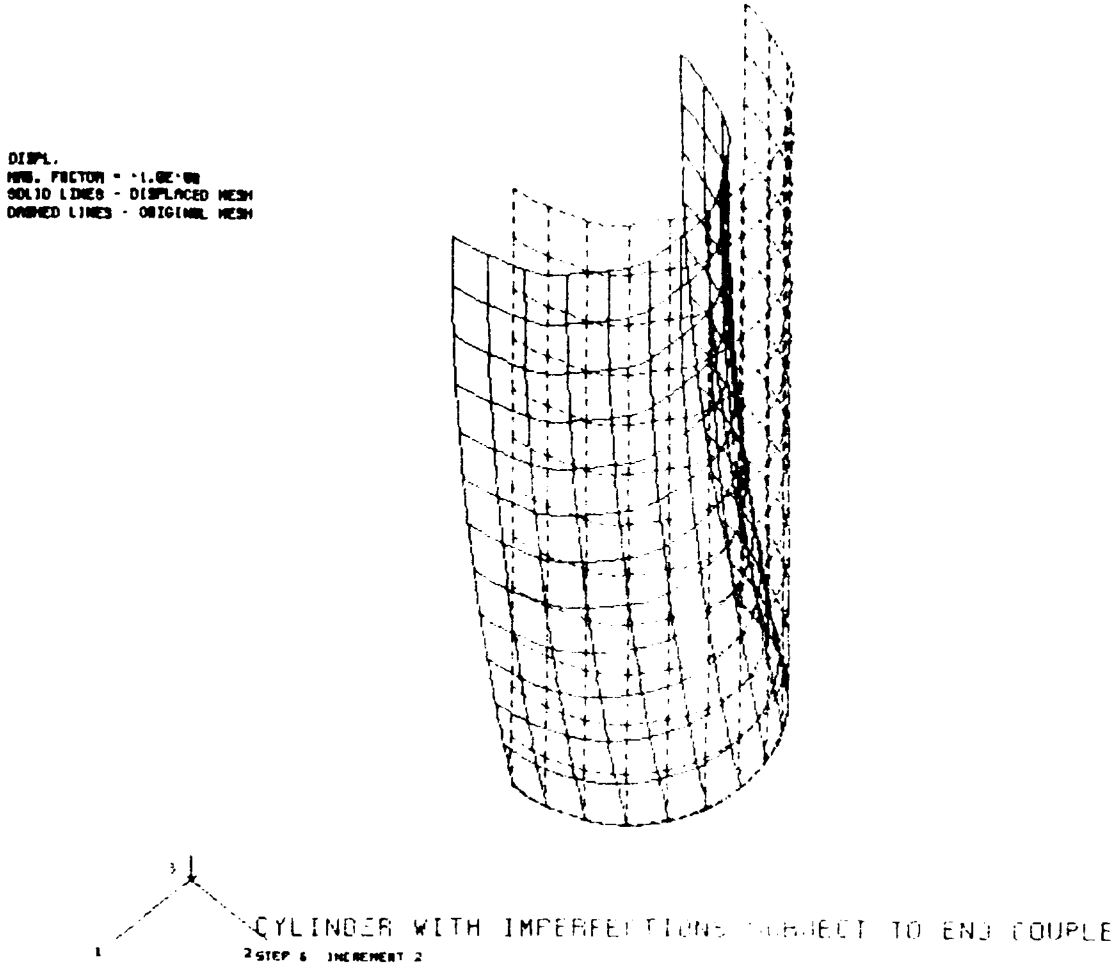

FIGURE 19. IMPERFECT CYLINDRICAL SHELL (VARIANT OF MODEL 20A) SUBJECT TO END BENDING MOMENT VIEWED FROM 100″,100″,500″ AT STEP 6, INCREMENT 2

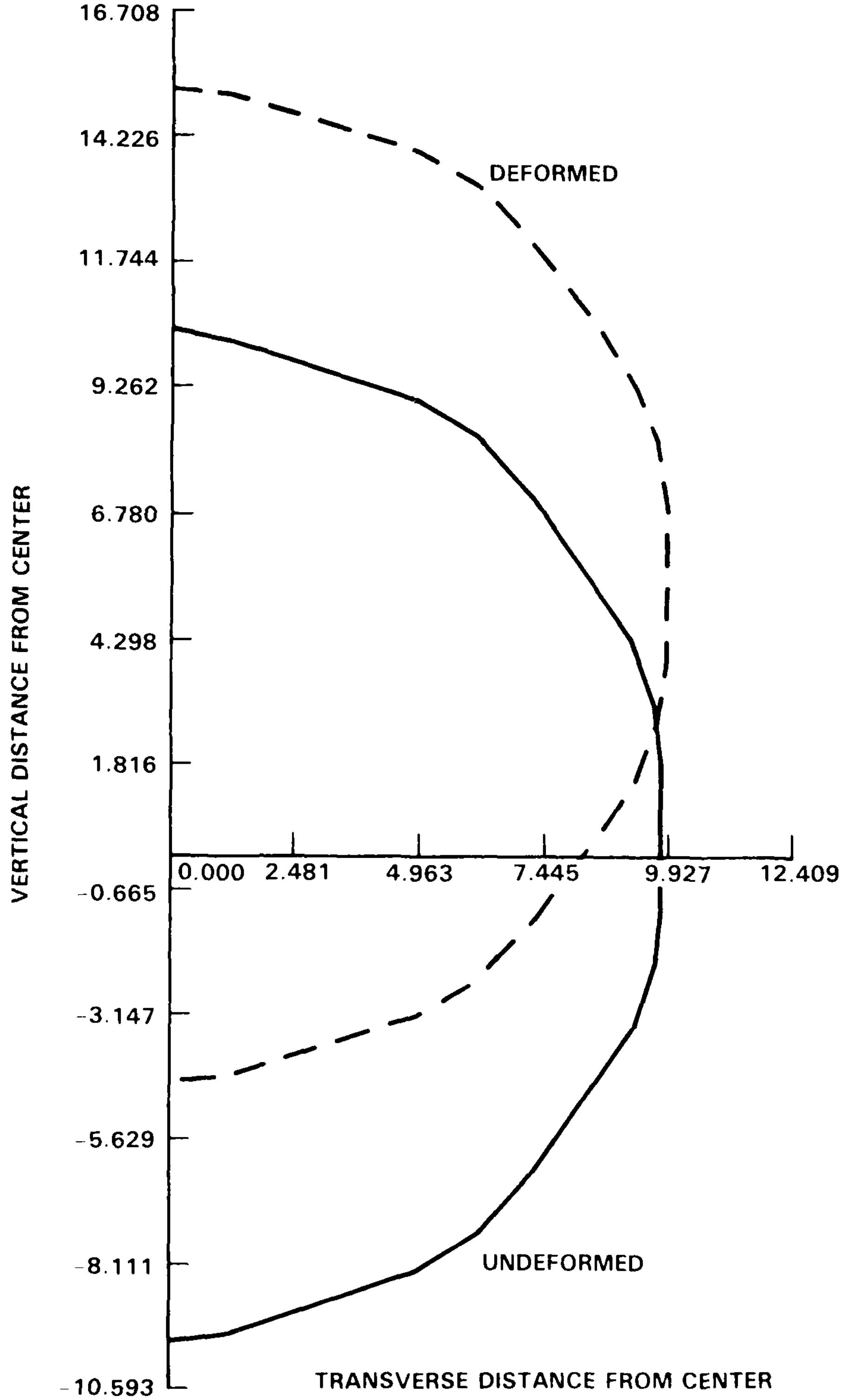

FIGURE 20. UNDEFORMED AND DEFORMED HALF-CROSS SECTION OF IMPERFECT VERSION OF MODEL 20A AT MIDLENGTH

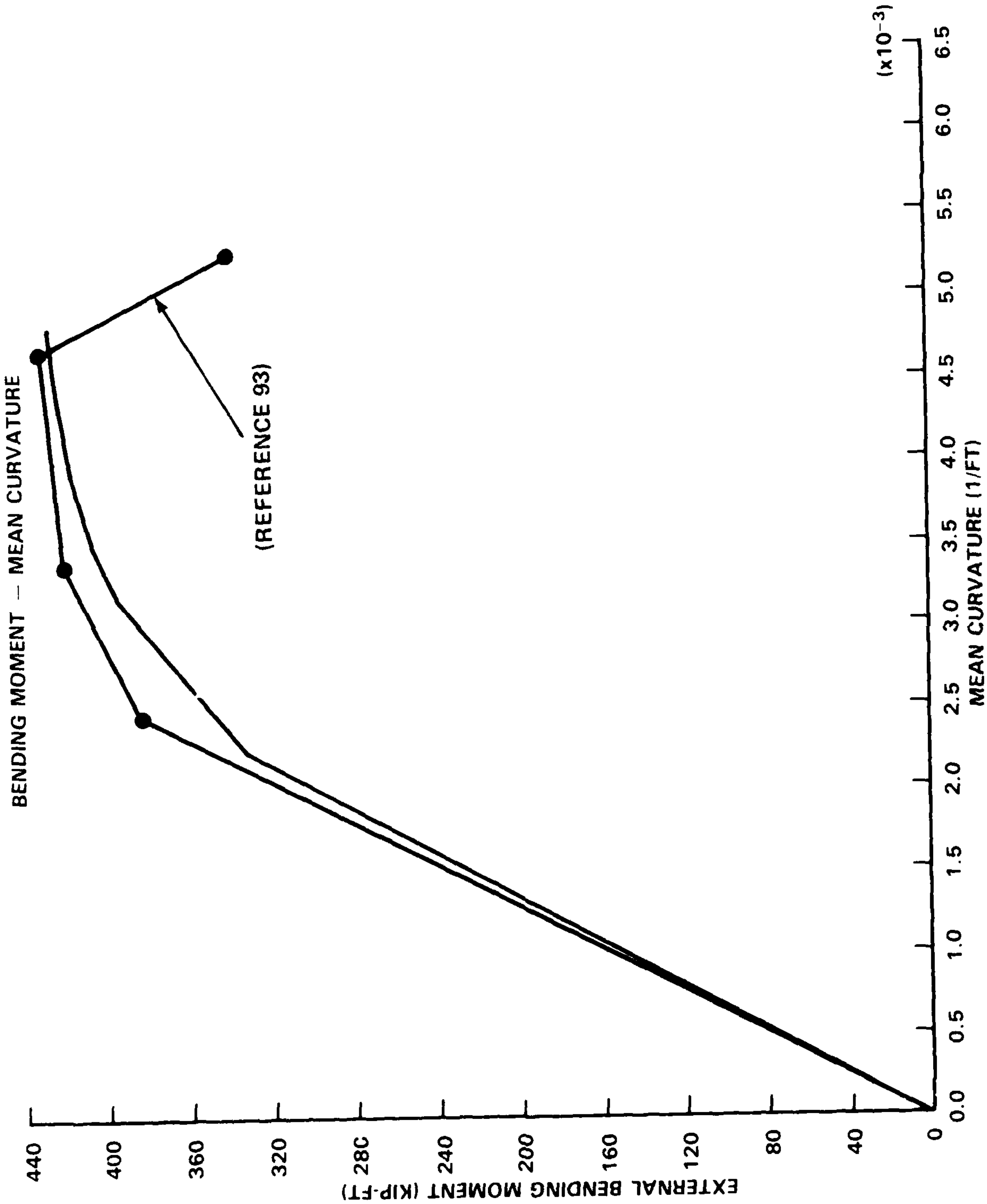

FIGURE 21. MOMENT-CURVATURE PLOTS FOR IMPERFECT VERSION OF MODEL 20A

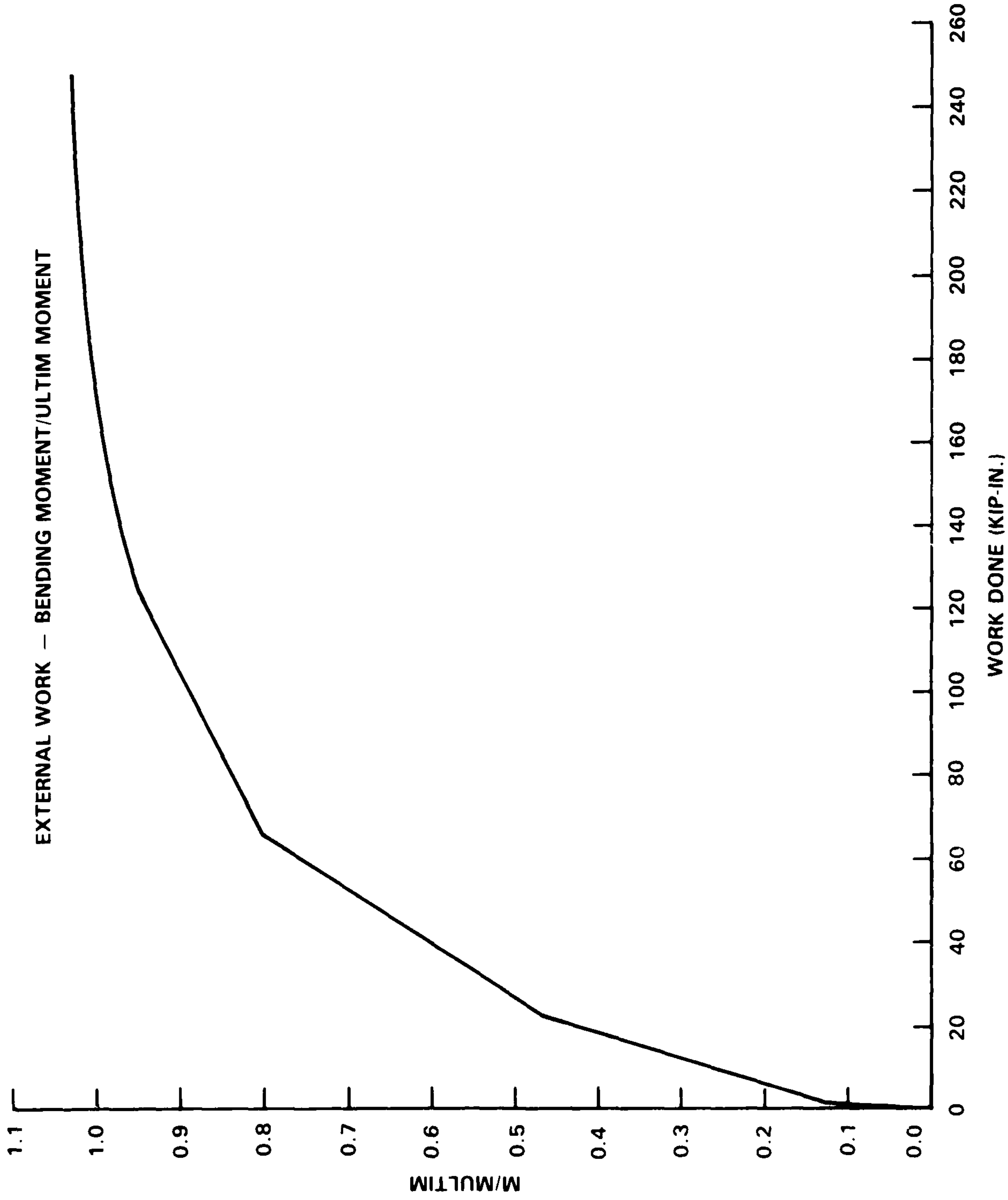

FIGURE 22. M/MULTIM ~ WORK DONE (KIP-IN.) FOR IMPERFECT VERSION OF MODEL 20A

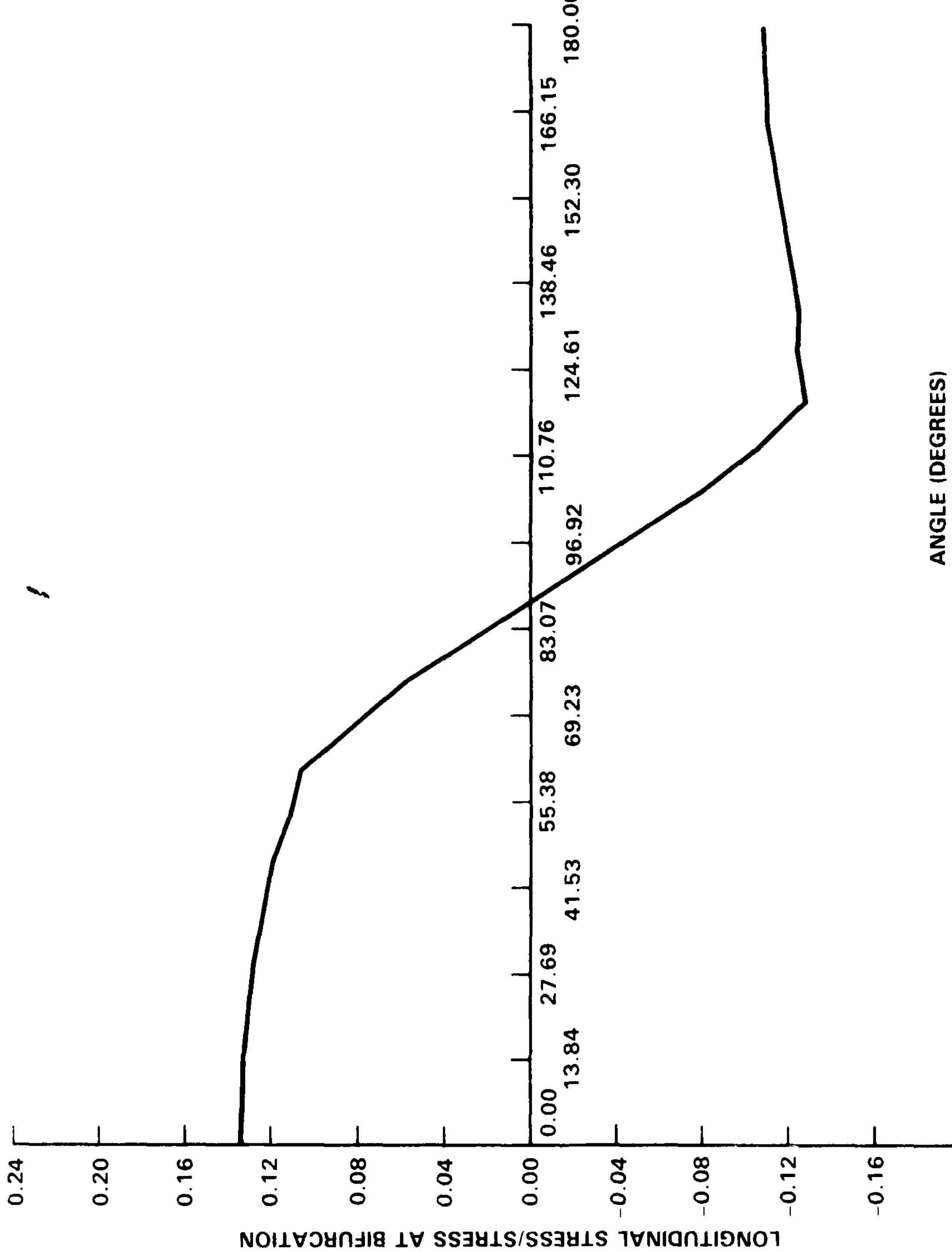

FIGURE 23. LONGITUDINAL STRESS (STEP 6, INCREMENT 2, WHICH CORRESPONDS TO FINAL PLOTTED POINT ON FIGURE 21) VERSUS ANGULAR POSITION FOR IMPERFECT VERSION OF MODEL 20A

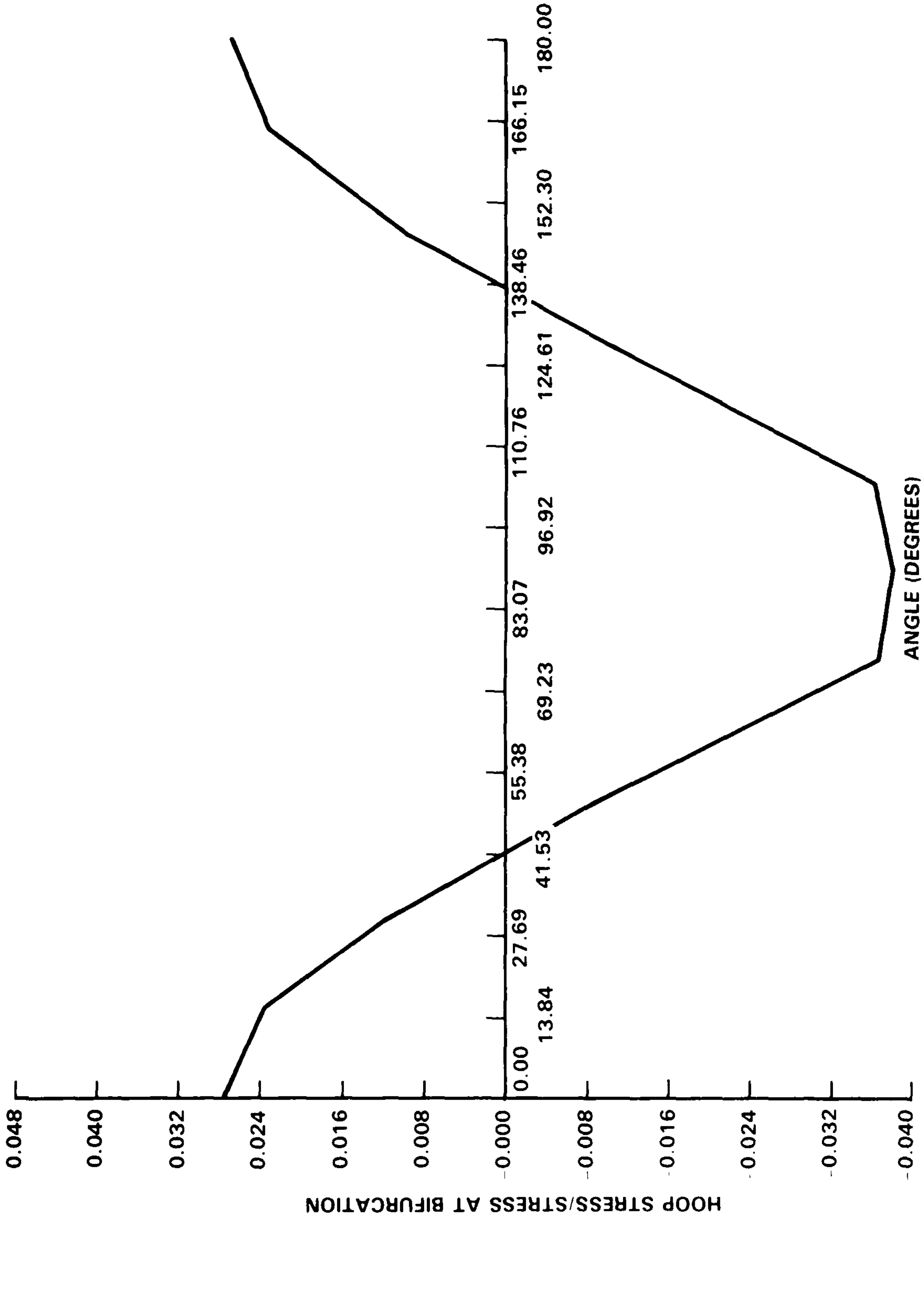

FIGURE 24. HOOP STRESS DISTRIBUTION (STEP 6, INCREMENT 2, WHICH CORRESPONDS TO FINAL PLOTTED POINT ON FIGURE 21) VERSUS ANGULAR POSITION FOR IMPERFECT VERSION OF MODEL 20A

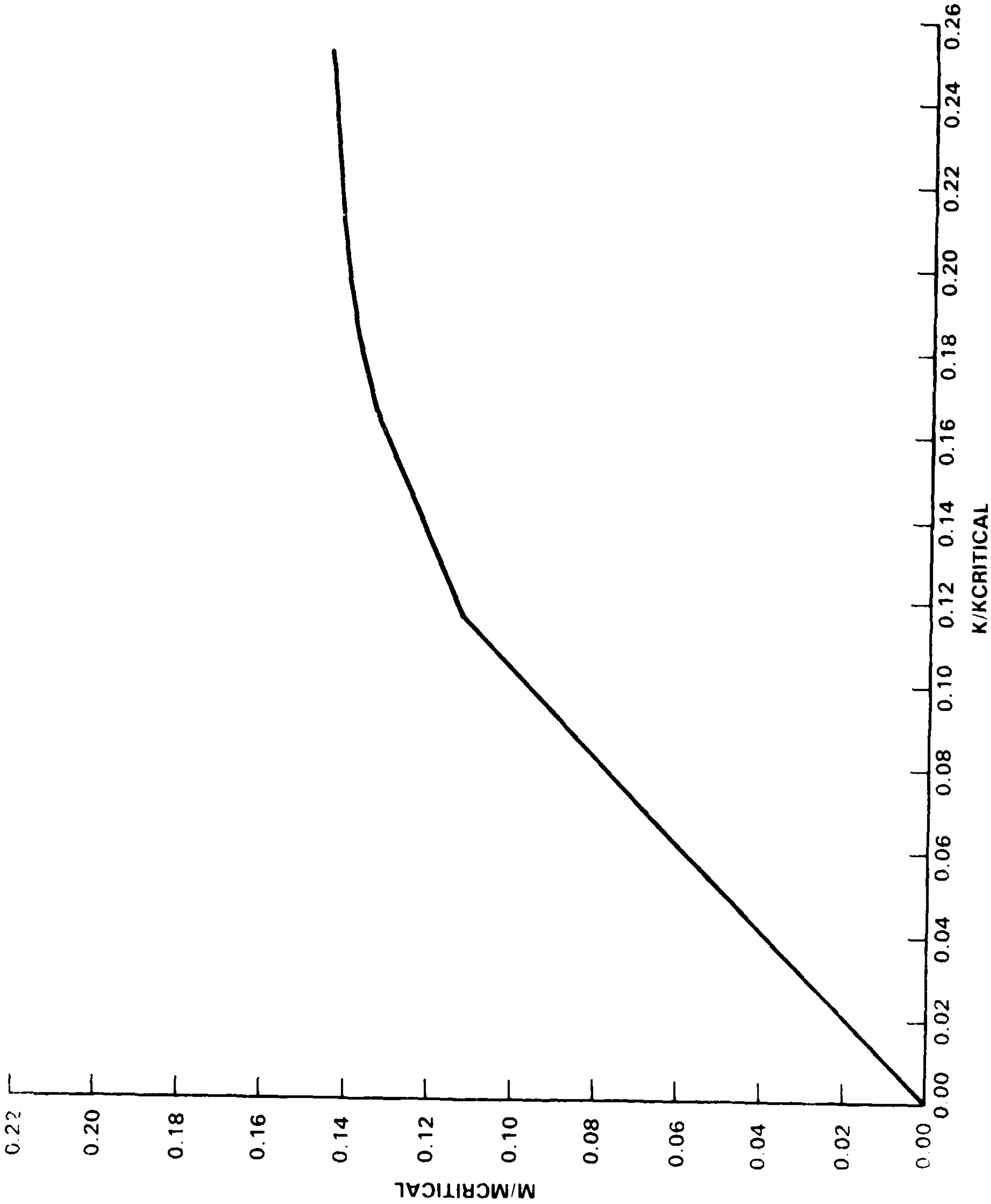

FIGURE 25. M/MCRITICAL VERSUS K/KCRITICAL FOR IMPERFECT VERSION OF MODEL 20A

At this point, note that the relevant figures corresponding to the perfect model 20A are 8, 11, 14, and 17, respectively. The imperfection in the radial displacement of the original surface from the mean radius R of imperfect model 20AI varied according to the formula

$$h \sin\left(\frac{\pi z}{L}\right) \cos(10\theta)$$

Imperfect model 20AI was generated with one-half wave axially and 10 waves peripherally.

Figure 26 presents superimposed moment-curvature curves for both models 20A and 20AI. Notice that since they are comparatively thick and fail by plastification, unlike ovalization or bifurcation failure, they are not imperfection sensitive. The response of the imperfect model 20AI is very similar to the perfect one.

Table 3 summarizes digitized results pertaining to bending moment, angle of rotation at the end, where the external load is applied, as well as strain energy, work done, and plastic dissipation for model 20A. Note that because of an existing error in ABAQUS, concerning how energies are computed, strain energy and plastic dissipation do not agree exactly with the work done (0.120489 + 0.290966 = 0.411455 compared with 0.417864). In fact, this difference decreases as we march along the load-deformation curve. Table 4 gives the stress distribution for load step 20 of model 20A. Tables 5 and 6 give the corresponding information for model 20AI, and Tables 7 and 8 give the actual points plotted in Figure 26 for both models 20A and 20AI.

Finally, a fine and extremely important point pertaining to the modeling issue must be addressed. The experimental set up involved the analysis of a three span beam (in all cases) subject to vertical self-equilibrating shear loads, to simulate overall bending over the two end spans. The middle span had no loads applied. In this analysis, one end span and half of the center span (symmetry) were modeled. A rotation was enforced through the "auxiliary node" concept and the MPC constraints. Subsequent computations without the "additional" end span gave a slightly different response.

Consequently, what constitutes an adequate additional span to be included for proper response has not been determined but is of major importance in this analysis. In addition, to complete studies on the bend-buckling modeling of cylindrical shells, "short" and "medium" length tubes with or without ring stiffeners must be addressed.

In closing this discussion it must be stressed that, by neglecting inertia effects, a reasonably successful first approximation of the problem of a long straight circular cylinder shell subject to end couples has been developed.

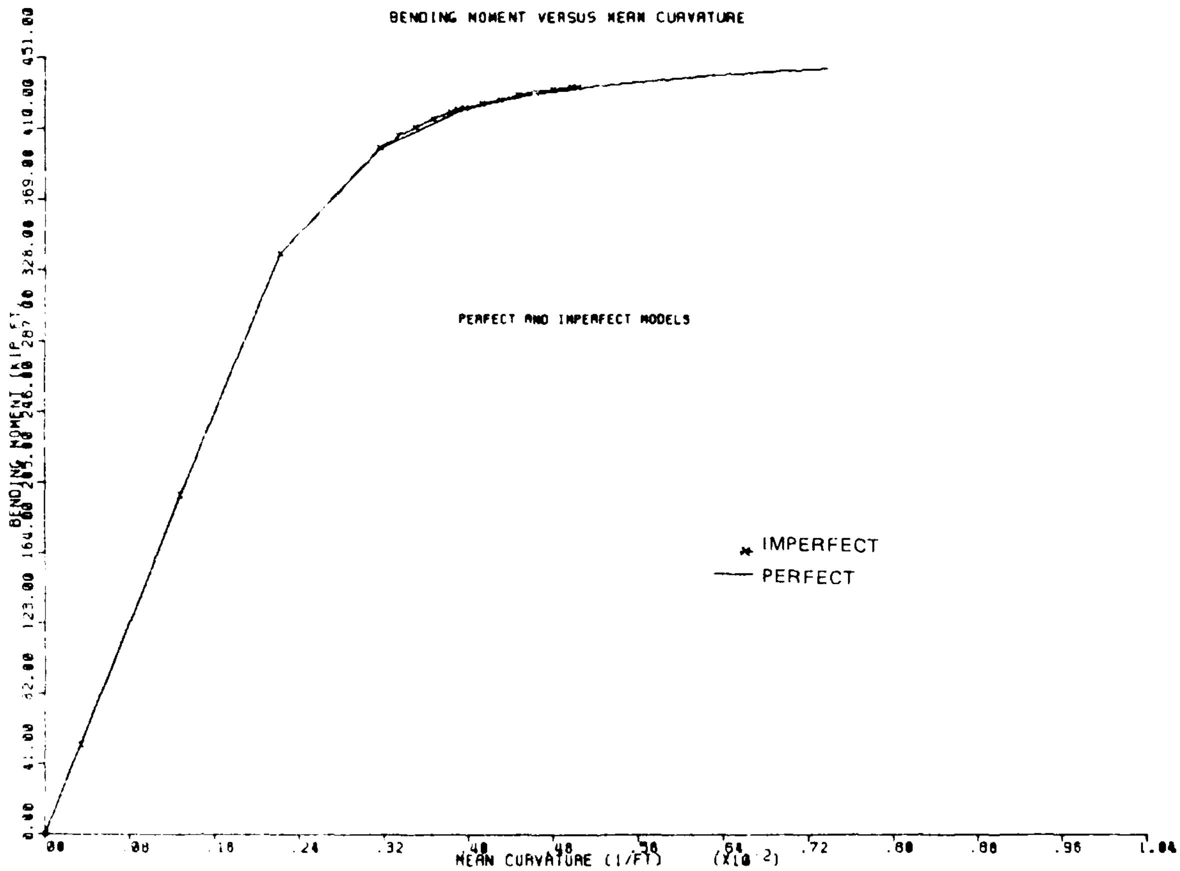

FIGURE 26. BENDING MOMENT DISTRIBUTION VERSUS MEAN CURVATURE FOR BOTH PERFECT AND IMPERFECT VERSIONS OF MODEL 20A

TABLE 3. POST-PROCESSING INFORMATION FROM ABAQUS FOR MODEL 20A

STEP NO.	TOTAL BENDING MOMENT AT AUXILIARY NODE (LB-IN)	ROTATION ABOUT GLOBAL Y-AXIS (DEGREES)
1	0.623339E+06	0.261412E+00
2	0.236641E+07	0.986562E+00
3	0.404768E+07	0.171171E+01
4	0.478507E+07	0.243686E+01
5	0.505084E+07	0.305324E+01
6	0.509211E+07	0.323453E+01
7	0.513190E+07	0.341581E+01
8	0.516604E+07	0.359710E+01
9	0.518940E+07	0.377839E+01
10	0.520879E+07	0.395968E+01
11	0.522644E+07	0.414096E+01
12	0.524388E+07	0.432225E+01
13	0.526043E+07	0.450354E+01
14	0.527557E+07	0.468482E+01
15	0.528840E+07	0.486511E+01
16	0.530105E+07	0.504740E+01
17	0.531590E+07	0.522669E+01
18	0.532418E+07	0.540997E+01
19	0.533412E+07	0.559126E+01
20	0.534003E+07	0.569097E+01

INCREMENT NO	STRAIN ENERGY	EXTERNAL WORK DONE	PLASTIC DISSIPATION	ABAQUS STEP	ABAQUS INCREMENT
1	0.143355E+04	0.178984E+04	0.000000E+00	1	5
2	0.203964E+05	0.229520E+05	0.000000E+00	1	10
3	0.500974E+05	0.658929E+05	0.111234E+04	1	15
4	0.559165E+05	0.123413E+06	0.316443E+05	1	20
5	0.982309E+05	0.176822E+06	0.725563E+05	1	25
6	0.100536E+06	0.192983E+06	0.862532E+05	1	30
7	0.102974E+06	0.209070E+06	0.100634E+06	1	35
8	0.105190E+06	0.225375E+06	0.114103E+06	1	40
9	0.106832E+06	0.241766E+06	0.128835E+06	1	45
10	0.108307E+06	0.256224E+06	0.143801E+06	1	50
11	0.109742E+06	0.274738E+06	0.158862E+06	1	55
12	0.111208E+06	0.291308E+06	0.173945E+06	1	60
13	0.112557E+06	0.307932E+06	0.189095E+06	1	65
14	0.114052E+06	0.324605E+06	0.204348E+06	1	70
15	0.115345E+06	0.341322E+06	0.219743E+06	1	75
16	0.116649E+06	0.358079E+06	0.235162E+06	1	80
17	0.117740E+06	0.374876E+06	0.250633E+06	1	85
18	0.118980E+06	0.391710E+06	0.266388E+06	1	90
19	0.119954E+06	0.408575E+06	0.282236E+06	1	95
20	0.120489E+06	0.417864E+06	0.290966E+06	1	100

TABLE 4. POST-PROCESSING INFORMATION (STRESS DISTRIBUTION) FROM ABAQUS FOR MODEL 20A

STEP NO 20 FOR STRESSES

ANGLE (DEGREES)	LONGITUDINAL MEMBRANE STRESS (PSI)	NONDIMENSIONAL MEMBRANE LONGITUDINAL STRESS	HOOP STRESS (PSI)	NONDIMENSIONAL HOOP STRESS
0.000	0.632128E+05	0.139699E+00	0.182834E+05	0.404057E-01
7.702	0.627863E+05	0.138756E+00	0.169217E+05	0.373965E-01
15.331	0.623718E+05	0.137840E+00	0.155168E+05	0.342917E-01
23.030	0.609195E+05	0.134630E+00	0.116398E+05	0.257237E-01
30.633	0.594624E+05	0.131410E+00	0.772034E+04	0.170617E-01
38.188	0.567114E+05	0.125331E+00	0.213745E+04	0.472371E-02
45.684	0.538930E+05	0.119102E+00	-.348791E+04	-.770818E-02
53.130	0.499846E+05	0.110465E+00	-.940137E+04	-.207768E-01
60.535	0.464282E+05	0.102605E+00	-.153252E+05	-.338684E-01
67.898	0.410452E+05	0.907087E-01	-.198203E+05	-.438023E-01
75.236	0.356993E+05	0.788944E-01	-.248881E+05	-.550020E-01
82.552	0.133819E+05	0.295737E-01	-.274967E+05	-.607669E-01
89.864	-.941319E+04	-.208029E-01	-.293937E+05	-.649592E-01
97.178	-.310386E+05	-.685944E-01	-.274463E+05	-.606556E-01
104.499	-.549397E+05	-.121415E+00	-.260129E+05	-.574879E-01
111.845	-.599972E+05	-.132592E+00	-.212607E+05	-.469856E-01
119.222	-.620184E+05	-.137059E+00	-.158268E+05	-.349768E-01
126.644	-.593842E+05	-.131238E+00	-.952565E+04	-.210514E-01
134.112	-.572913E+05	-.126612E+00	-.328290E+04	-.725511E-02
141.636	-.545373E+05	-.120526E+00	0.225880E+04	0.499188E-02
149.221	-.517689E+05	-.114408E+00	0.776267E+04	0.171553E-01
156.857	-.494856E+05	-.109362E+00	0.114913E+05	0.253954E-01
164.542	-.472357E+05	-.104389E+00	0.151840E+05	0.335562E-01
172.259	-.463326E+05	-.102394E+00	0.164973E+05	0.364585E-01
180.000	-.454807E+05	-.100511E+00	0.177748E+05	0.392819E-01

TABLE 5. POST-PROCESSING INFORMATION FROM ABAQUS FOR IMPERFECT VERSION OF MODEL 20AI

STEP NO.	TOTAL BENDING MOMENT AT AUXILIARY NODE (LB-IN)	ROTATION ABOUT GLOBAL Y-AXIS (DEGREES)
1	0.629773E+06	0.261412E+00
2	0.237180E+07	0.986562E+00
3	0.405516E+07	0.171171E+01
4	0.479309E+07	0.243686E+01
5	0.486891E+07	0.256792E+01
6	0.493186E+07	0.269897E+01
7	0.498622E+07	0.283003E+01
8	0.503512E+07	0.296108E+01
9	0.505118E+07	0.301245E+01
10	0.506491E+07	0.306373E+01
11	0.509419E+07	0.319165E+01
12	0.512270E+07	0.331957E+01
13	0.514996E+07	0.344749E+01
14	0.517342E+07	0.357541E+01
15	0.519202E+07	0.370333E+01
16	0.520742E+07	0.383125E+01
17	0.521293E+07	0.388088E+01

INCREMENT NO	STRAIN ENERGY	EXTERNAL WORK DONE	PLASTIC DISSIPATION	ABAQUS STEP	ABAQUS INCREMENT
1	0.14368[illegible]E+04	0.179[illegible]E+04	0.000000E+00	1	5
2	0.20442[illegible]E+05	0.23004[illegible]E+05	0.000000E+00	1	10
3	0.5016[illegible]E+05	[illegible]	0.11[illegible]E+04	1	15
4	0.660105E+05	[illegible]	0.3[illegible]037E+05	1	20
5	0.8[illegible]1544E+05	0.1347[illegible]	0.3[illegible]105E+05	2	5
6	0.[illegible]9452E+05	0.1457[illegible]	0.43[illegible]72E+05	2	10
7	[illegible]E+05	0.157332E+0[illegible]	0.5[illegible]819E+05	2	15
8	[illegible]E+05	0.16880[illegible]E+06	0.660[illegible]17E+05	2	20
9	[illegible]E+05	0.17[illegible]E+06	0.697452E+05	3	2
10	[illegible]E+05	0.1778[illegible]E+06	0.735243E+05	4	2
11	0.10[illegible]E+06	0.189209E+06	0.8[illegible]1935E+05	5	5
12	0.10[illegible]E+06	0.200621E+06	0.9[illegible]9125E+05	5	10
13	0.1035[illegible]E+06	0.212095E+06	0.10[illegible]704E+06	5	15
14	0.105151E+06	0.223625E+06	0.112689E+06	5	20
15	0.106427E+06	0.23520[illegible]E+06	0.122979E+06	5	25
16	0.107538E+06	0.246814E+06	0.133471E+06	5	30
17	0.107951E+06	0.251328E+06	0.137568E+06	6	2

TABLE 6. POST-PROCESSING INFORMATION (STRESS DISTRIBUTION) FROM ABAQUS FOR IMPERFECT VERSION OF MODEL 20AI

STEP NO 17 FOR STRESSES

ANGLE (DEGREES)	LONGITUDINAL MEMBRANE STRESS (PSI)	NONDIMENSIONAL MEMBRANE LONGITUDINAL STRESS	HOOP STRESS (PSI)	NONDIMENSIONAL HOOP STRESS
0.000	0.607271E+05	0.134205E+00	0.126331E+05	0.279188E-01
7.610	0.603679E+05	0.133411E+00	0.117107E+05	0.258804E-01
15.222	0.600186E+05	0.132639E+00	0.107918E+05	0.238496E-01
22.803	0.589542E+05	0.130287E+00	0.819050E+04	0.181008E-01
30.336	0.578366E+05	0.127817E+00	0.543694E+04	0.120155E-01
37.857	0.559761E+05	0.123706E+00	0.172225E+04	0.380612E-02
45.380	0.543367E+05	0.120083E+00	-.176146E+04	-.389277E-02
52.876	0.508672E+05	0.112415E+00	-.536827E+04	-.118637E-01
60.310	0.483576E+05	0.106869E+00	-.927398E+04	-.204952E-01
67.714	0.379751E+05	0.839238E-01	-.131977E+05	-.291666E-01
75.119	0.256496E+05	0.566849E-01	-.167934E+05	-.371128E-01
82.525	0.967097E+04	0.213726E-01	-.170584E+05	-.376986E-01
89.913	-.552706E+04	-.122146E-01	-.174408E+05	-.385437E-01
97.302	-.204710E+05	-.452402E-01	-.170163E+05	-.376056E-01
104.712	-.356946E+05	-.788840E-01	-.166135E+05	-.367153E-01
112.123	-.479357E+05	-.105936E+00	-.133175E+05	-.294314E-01
119.535	-.578694E+05	-.127890E+00	-.955361E+04	-.211132E-01
126.980	-.559483E+05	-.123644E+00	-.525418E+04	-.116116E-01
134.420	-.559580E+05	-.123666E+00	-.150316E+04	-.332195E-02
142.030	-.541790E+05	-.119734E+00	0.189382E+04	0.418529E-02
149.571	-.523666E+05	-.115729E+00	0.5[illegible]4892E+04	0.122630E-01
157.126	-.508176E+05	-.112305E+00	0.818455E+04	0.180876E-01
164.729	-.493716E+05	-.109110E+00	0.106620E+05	0.235627E-01
172.365	-.488732E+05	-.106208E+00	0.114846E+05	0.253807E-01
180.000	-.483773E+05	-.106912E+00	0.123154E+05	0.272168E-01

TABLE 7. MOMENT-CURVATURE RESULTS FOR PERFECT VERSION OF MODEL 20A

CURVATURE K (1/FT)	MOMENT M (KIP-FT)
0.00000000E+00	0.00000000E+00
0.33796293E-03	0.52361568E+02
0.12754640E-02	0.19720113E+03
0.22129680E-02	0.33730643E+03
0.31504813E-02	0.39875580E+03
0.39473758E-02	0.42090363E+03
0.41817576E-02	0.42434280E+03
0.44161407E-02	0.42765866E+03
0.46505262E-02	0.43050354E+03
0.48849112E-02	0.43215026E+03
0.51192953E-02	0.43406573E+03
0.53536799E-02	0.43553680E+03
0.55880644E-02	0.43698962E+03
0.58224513E-02	0.43836884E+03
0.60568429E-02	0.43963071E+03
0.62912297E-02	0.44069992E+03
0.65256148E-02	0.44175455E+03
0.67600049E-02	0.44282471E+03
0.69943932E-02	0.44368170E+03
0.72287684E-02	0.44451007E+03
0.73576709E-02	0.44500220E+03

TABLE 8. MOMENT-CURVATURE RESULTS FOR IMPERFECT VERSION OF MODEL 20A (MODEL 20AI)

CURVATURE K (1/FT)	MOMENT M (KIP-FT)
0.00000000E+00	0.00000000E+00
0.33796293E-03	0.52481121E+02
0.12754641E-02	0.19764960E+03
0.22129680E-02	0.33793011E+03
0.31504813E-02	0.39942395E+03
0.33199168E-02	0.40574283E+03
0.34893532E-02	0.41079804E+03
0.36587899E-02	0.41551855E+03
0.38282289E-02	0.41959351E+03
0.38946490E-02	0.42093170E+03
0.39609359E-02	0.42207605E+03
0.41263211E-02	0.42451611E+03
0.42917063E-02	0.42689178E+03
0.44570942E-02	0.42916224E+03
0.46224827E-02	0.43111819E+03
0.47878711E-02	0.43266830E+03
0.49532559E-02	0.43395139E+03
0.50174259E-02	0.43441101E+03

SUMMARY

A modeling strategy is established to obtain the moment-curvature relation as well as the relation between the work done and the applied moment for circular cylindrical shells. This is achieved by using the nonlinear finite element program ABAQUS in conjunction with preprocessing and postprocessing computer programs. The results compare favorably with experimental curves reported in the open literature. Such analysis is of potential use in predicting critical bending moments, ultimate moment for ship hulls, pipe bends in nuclear reactors, submarine pipelines, etc.

REFERENCES

1. Maurer, L., "Ueber die Deformation gekruemmter elastischer Platten," Archiv der Mathematik und Physik, Vol. 6, Part I, pp. 1-10; Part II, pp. 10-26; and Part III, 1904, pp. 260-283.

2. Bantlin, A., "Formaenderung und Beanspruchung federnder Ausgleichroehren," Zeitschrift des Vereines Deutscher Ingeniere, Vol. 54, No. 2, Jan 1910, pp. 43-49.

3. v.Karman, Th., "Ueber die Formaenderung duennwandiger Rohre, insbesondere federnder Ausgleichrohren," Zeitschrift des Vereines Deutscher Ingenieure, Vol. 55, No. 45, Nov 1911, pp. 1889-1895.

4. Lorenz, H., "Die Biegung krummer Rohre," Physik. Zeitschrift, XIII, 1912, pp. 768-774.

5. Timoshenko, S., "Bending Stresses in Curved Tubes of Rectangular Cross-Section," Transactions ASME, Vol. 45, 1923, pp. 135-140.

6. Sunatani, Chido, "The Theory of a Bourdon Tube Pressure Gauge and An Improvement in its Mechanism," Tohoku Imperial University, Japan, Vol. 4, No. 1, 1924-25, pp. 69-110.

7. Brazier, L. G., "On the Flexure of Thin Cylindrical Shells and other 'Thin' Sections," in Proceedings of Royal Society of London, Series A, Vol. 116, No. A27, Sep 1927, pp. 104-114.

8. Hovgaard, W., "The Elastic Deformation of Pipe Bends," Journal of Mathematics & Physics, VI, 1926-27, pp. 69-118, "Deformation of Plane Pipes," VII, 1927-28, pp. 198-238; "Further Research on Pipe Bends," VII, 1927-28, pp. 239-297.

9. Wahl, A. M., "Stresses and Reactions in Expansion Pipe Bends," Transactions ASME, Vol. 49-50, Part I, AER-FSP, 1927-28, pp. 241-262.

10. Mossman, R. W., and Robinson, R. G., "Bending Tests of Metal Monocoque Fuselage Construction," NACA Technical Note No. 357, Nov 1930.

11. Chwalla, E., "Elastostatische Probleme schlanker, duennwandiger Rohre mit gerader Achse," Sitzungsberichte Akademie der Wissenschaften, Mathematische Nat. Klasse, Wien, 140, 1931, pp. 163-198.

REFERENCES (Cont.)

12. Crocker, S., and McCutchan, A., "Frictional Resistance and Flexibility of Seamless-Tube Fittings Used in Pipe Welding," Transactions of ASME, Vol. 53, No. 14, FSP-53-17, Sep-Dec 1931, pp. 215-245.

13. Stange, K., "Der Spannungszustand einer Kreisringschale," Ingenieur Archiv, Vol. 2, 1931, pp. 47-91.

14. Cope, E. T., and Wert, E. A., "Load-Deflection Relations for Large, Corrugated, and Creased Pipe Bends," Transactions of ASME, Vol. 54, No. 16, FSP-54-12, Aug 1932, pp. 115-159.

15. Chwalla, E., "Reine Biegung schlanker duennwandiger Rohre mit gerader Achse," ZAMM, Vol. 13, No. 1, Feb 1933, pp. 48-53.

16. Lundquist, E. E., Strength Tests of Thin-Walled Duralumin Cylinders in Compression, NACA Report No. 473, 1933.

17. Lundquist, E. E., "Strength Tests of Thin-Walled Duralumin Cylinders in Pure Bending," NACA TN 479, Dec 1933.

18. Lundquist, E. E., Burke, W. F., "Strength Tests of Thin-walled Duralumin Cylinders of Elliptic Section," NACA TN 527, 1935.

19. Tueda, M., "Mathematical Theories of Bourdon Pressure Tubes and Bending of Curved Pipes," Mem. Coll. Engineering Kyoto Imperial University, Vol. 8, 1934, pp. 102-115; Vol. 9, 1936, pp. 132-152.

20. Heck, O. S., "Stability of Orthotropic Elliptic Cylinders in Pure Bending," NACA TN 834, 1937, pp. 1-33.

21. Osgood, W., "The Crinkling Strength and the Bending Strength of Round Aircraft Tubing," NACA TR 632, 1938.

22. Dean, W. R., "The Distorition of a Curved Tube due to Internal Pressure," Philosophical Magazine, No. 189, Vol. XXVIII, Seventh Series, Oct 1939, pp. 452-464.

23. Schubert, G., "Ueber Effekte zweiter Ordnung bei Biegung und Torsion duennwandiger Rohre elliptischer Querschnitts," Ingenieur Archiv, Vol. 12, 1941, pp. 53-63.

24. Lundquist, E. E., "Strength Tests on Thin-Walled Duralumin Cylinders," NACA TN 427, Aug 1932.

25. Lundquist, E. E., and Stowell, E. Z., "Strength Tests of Thin-Walled Elliptic Duralumin Cylinders in Pure Bending and in Combined Pure Bending and Torsion," NACA TN 861, Jun 1942.

26. Moore R. L., Marshall, H., "Beam and Torsion Tests of Aluminum Alloy 615-T Tubing," NACA TN 867, 1942.

REFERENCES (Cont.)

27. Karl, H., "Biegung gekruemmter, duennwandiger Rohre," ZAMM, Vol. 23, 1943, pp. 331-345.

28. Vingness, I., "Elastic Properties of Curved Tubes," Transactions ASME, Vol. 65, No. 2, Feb 1943, pp. 105-120.

29. Pardue, T. E., Symonds P. S., Vigness, I., "Characteristics of Short Radius Tube Bends," NRL First Partial Report 0-2317, 1944.

30. Beskin, L., "Bending of Curved Thin Tubes," J. Appl. Mech., 1945, pp. A-1 through A-7.

31. Salzmann, F., "Die Nachqiebiqkeit von Wellrohrexpansionen," Schweizerisches Bauzeitung, No. 11, Vol. 127, 1946, pp. 127-130.

32. Symond, P. S., and Pardue, T. E., "Characteristics of Short Radius Tube Bends," Second Partial Report, NRL Report 0-2761, 1946.

33. Wolf, A., "An Elementary Theory of the Bourdon Gage," Journal of Applied Mechanics, Vol. 68, Sep 1946, pp. A-207 through A-210. Discussion in Journal of Applied Mechanics, No. 2, Vol. 4, Jun 1947, pp. A-165 and A-166.

34. Reissner, E., "On Bending of Curved Thin-Walled Tubes," in Proceedings of National Academy of Sciences, Vol. 35, 1949, pp. 204-208.

35. Huber, M. T., "The Bending of the Curved Tube of Elliptic Section," in Proceedings of the Seventh Congress of Applied Mechanics, Vol. 1, 1949, pp. 322-328.

36. Clark, R. A., and Reissner, E., "Bending of Curved Tubes," Advances in Applied Mechanics, II, 1950, pp. 93-122.

37. Clark, R. A., Gilroy, T. I., and Reissner, E., "Stresses and Deformations of Toroidal Shells of Elliptical Cross Section with Applications to Problems of Bending of Curved Tubes and of the Bourdon Gage," J. Appl. Mech., Vol. 19, No. 1, Mar 1952, pp. 37-48. Discussion in Vol. 19, No. 4, 1952, pp. 565-566.

38. Gross, N., and Ford, H., "The Flexibility of a Short-Radius Pipe-Bend," in Proceedings of the Institution of Mechanical Engineers, 1B, 1952-53, pp. 480-491. (Discussion on pp. 492-497).

39. Gross, N., "Experiments on Short-Radius Bends," in Proceedings of Institution of Mechanical Engineers, 1B, 1952-53, pp. 465-479.

40. Moore, R. L., Clark, J. W., "Torsion, Compression, and Bending Tests of Tubular Sections Machined from 755-T6 Rolled Round Rod," NACA RM 52125, 1952, pp. 1-33.

REFERENCES (Cont.)

41. Pardue, T. E., and Vingness, I., "Characteristics of Pipe Bends Under Applied Moments," Summary Report, NRL 4253, 1953, pp. 1-20.

42. Anderson, R. A., Pride, R. A., Johnson, A. E. Jr., "Some Information on the Strength of Thick-skin wings with Multiweb and Multipost Stabilization," NACA RM L53F15, 1953, pp. 1-19.

43. Fralich, R. W., Mayers, J., Reissner, E., "Behavior in Pure Bending of a Long Monocoque Beam of Circular-Arc Cross Section," NACA TN 2875, 1953.

44. Wuest, W., "Einige Anwendungen der Theorie der Zylinderschale," ZAMM, Vol. 34, No. 12, Dec 1954, pp. 444-454.

45. Vissat, P. L., and Del Buono, A. J., "In-plate Bending Properties of Welding Elbows," Transactions ASME, Vol. 77, 1955, pp. 161-175.

46. Kafka, P. G. and Dunn, M. B., "Stiffness of Curved Circular Tubes with Internal Pressure," J. Appl. Mech., Jun 1956, pp. 247-254.

47. Peterson, J. P., "Bending Tests of Ring-Stiffened Circular Cylinders," NACA TN 3735, Jul 1956, pp. 1-14.

48. Ades, C. S., "Bending Strength of Tubing in the Plastic Range," Journal of Aeronautical Sciences, Vol. 24, Aug 1957, pp. 605-610.

49. Turner, C. E., and Ford, H., "Examination of the Theories for Calculating Stresses in Pipe Bends Subjected to In-Plane Bending," in Proceedings of the Institution of Mechanical Engineers, Vol. 171, 1957, pp. 513-525.

50. Rodbaugh, E. C., and George, H. H., "Effect of Internal Pressure on Flexibility and Stress-Intensification Factors of Curved Pipe or Welding Elbows," Transactions of American Society of Mechanical Engineers, Vol. 79, 1957, pp. 939-948.

51. Wood, J. D., "The Flexure of a Uniformly Pressurized, Circular, Cylindrical Shell," J. Appl. Mech., Dec 1958, pp. 453-458.

52. Suer, H. S, Harris, L. A., Skene, W. T., and Benjamin, R. J., "The Bending Stability of Thin-Walled Unstiffened Circular Cylinders Including the Effects of Internal Pressure," Journal of the Aeronautical Sciences, Vol. 25, No. 5, May 1958, pp. 281-287.

53. Reissner, E., "Rotationally Symmetric Problems in the Theory of Thin Elastic Shells," in Proceedings of 3rd U.S. National Congress of Applied Mechanics, Brown University, 1958, pp. 51-69.

54. Chernin, V. S., "On the System of Differential Equations of Equilibrium of Shells of Revolution under Bending Loads," PMM, Vol. 23, 1959, pp. 372-382.

55. Reissner, E., "On Finite Bending of Pressurized Tubes," J. Appl. Mech., Sep 1959, pp. 386-392.

REFERENCES (Cont.)

56. Turner, C. E., "Study of the Symmetrical Elastic Loading of Some Shells of Revolution with Special Reference to Toroidal Elements," Journal of Mechanical Engineering Science, Vol. 1, 1959, pp. 113-129.

57. Knowles, J. K., and Reisner, E., "On Stress-Strain Relations and Strain-Energy Expressions in the Theory of Thin Elastic Shells," Journal of Applied Mechanics, Mar 1960, pp. 104-106.

58. Dow, M. B., and Peterson, J. P., "Bending and Compression Tests of Pressurized Ring-Stiffened Cylinders," NASA Technical Note D-360, Apr 1960, pp. 1-27.

59. Seide, P., and Weingarten, V. I., "On the Buckling of Circular Cylindrical Shells Under Pure Bending," J. Appl. Mech., Mar 1961, pp. 112-116.

60. Reissner, E., "On Finite Pure Bending of Cylindrical Tubes," Oesterreichisches Ingenieur Archiv, Vol. 15, 1961, pp. 165-172.

61. Zender, G. W., "The Bending Strength of Pressurized Cylinders," Journal of the Aerospace Sciences, Vol. 29, Mar 1962, pp. 362-363.

62. Weingarten, V. I., "Effects of Internal Pressure on the Buckling of Circular-Cylindrical Shells Under Bending," Journal of the Aerospace Sciences, Jul 1962, pp. 804-807.

63. Akselrad, E. L., "Equations of Deformation for Shells of Revolution and for the Bending of Thin-Walled Tubes Subjected to Large Elastic Displacements," American Rocket Society, Vol. 32, Jul 1962, pp. 1147-1151.

64. Yao, J. C., "Large-Deflection Analysis of Buckling of a Cylinder under Bending," J. Appl. Mech., Dec 1962, pp. 708-714.

65. Reissner, E., and Weinitschke, H. J., "Finite Pure Bending of Circular Cylindrical Tubes," Quarterly of Applied Mathematics, Vol. XX, No. 4, Jan 1963, pp. 305-319. (Correction in Vol. XXIII, No. 4, 1965, p. 368).

66. Courtie, M. G., and Maunder, L., "Bend-Buckling of Pressurized Cylindrical Shells," in Proceedings of the Institution of Mechanical Engineers, Vol. 178, Part 3J, 1963-64, pp. 130-139.

67. Wittrick, W. H., "Non-linear Discontinuity Stresses in Shells of Revolution Under Internal Pressure," International Journal of Engineering Science, Vol. 2, 1964, pp. 155-177.

68. Thurston, G. A., "Newton's Method Applied to Problems in Nonlinear Mechanics," J. Appl. Mech., Vol. 32, Jun 1965, pp. 383-388.

REFERENCES (Cont.)

69. Schilling, C. G., "Buckling Strength of Circular Tubes," Journal of the Structural Division ASCE, Vol. 91, Oct 1965, pp. 325-348.

70. Akselrad, E. L., "Refinement of the Upper Critical Loading of Pipe Bending Taking Account of Geometrical Nonlinearity," Izvestiya Akademii Nauk SSSR, Mekhanika i Mash., Vol. 4, 1965, pp. 133-139 (in Russian).

71. Dow, D. A., "Buckling and Postbuckling Tests of Ring-Stiffened Circular Loaded by Uniform External Pressure," NASA TN D-3111 (N66-11255), Nov 1965, pp. 1-21.

72. Caldwell, J. B., "Ultimate Longitudinal Strength," Transactions of Royal Institution of Naval Architects, Vol. 107, 1965, pp. 411-430.

73. Johns, D. J., "On the Linear Buckling of Circular Cylindrical Shells Under Asymmetric Axial Compressive Stress Distributions," J. of the Royal Aeronautical Society, Vol. 70, 1966, pp. 1095-1097.

74. Aksel'rad, E. L., "Periodic Solutions of an Axially Symmetric Problem in the Theory of Shells," Mechanics of Solids, No. 2, 1966.

75. Jones, N., "On the Design of Pipe-Bends," Nuclear Engineering and Design, Vol. 4, 1966, pp. 399-405.

76. Aksel'rad, E. L., "Stability of a Curved Pipe of Circular Cross-Section Under External Pressure," Mechanics of Solids, No. 2, 1967, pp. 117-120 (Translation of Mekhanika Tverdogo Tela).

77. Lakshmikantham, C., and Gerard, G., "On the Bending Elastic Stability of Isotropic Cylinders," Journal of the Royal Aeronautical Society, Vol. 71, Feb 1967, pp. 136-138.

78. Aksel'rad, E. L., "Various Definitions of Curvature-Change Parameters for Shells and their Relation to the Strain-Compatibility Equations," Mechanics of Solids, Vol. 2, 1967, pp. 68-69.

79. Aksel'rad, E. L., "Stability of a Curved Pipe of Circular Cross-Section Under External Pressure," Mechanics of Solids, Vol. 2, 1967, pp. 117-120.

80. Jones, N., "In-Plane Bending of a Short-Radius Curved Pipe Bend," Journal of Engineering for Industry, May 1967, pp. 271-277.

81. Smith, R. T., "Theoretical Analysis of the Stresses in Pipe Bends Subjected to Out-Of-Plane Bending," Journal of Mechanical Engineering Science, Vol. 9, 1967, pp. 115-123.

82. Marcal, P. V., "Elastic-Plastic Behavior of Pipe Bends With In-Plane Bending," Journal of Strain Analysis, Vol. 2, 1967, pp. 84-90.

REFERENCES (Cont.)

83. Smith, R. T., and Ford, H., "Experiments on Pipe Lines and Pipe Bends Subjected to Three-Dimensional Loads," Journal of Mechanical Engineering Science, Vol. 9, No. 2, 1967, pp. 124-137.

84. Afendik, L. G., "Bending of Thin-Walled Tubes with Considerable Curvature Beyond the Elastic Limit," Prikladnaia Mekhanika, Kiev, Naukova Dumka, Vol. IV, 1968 (in Russian). (English Translation in Soviet Applied Mechanics by Plenum Press, pp. 27-30.)

85. Cheng, D. H., Thailer, H. J., "In-Plane Bending of Curved Circular Tubes," Journal of Engineering for Industry, Nov 1968, pp. 666-670.

86 Buckling of Thin-Walled Circular Cylinders, NASA SP-8007, Revised in Aug 1968, NASA Space Vehicle Design Criteria (Structures), pp. 7 and 19 for bending.

87. Ariaratnam, S. T., and Dubry, R. N., "Instability in an Elastic Plastic Cylindrical Shell Under Axial Compression," Journal of Applied Mechanics, Mar 1969, pp. 47-50.

88. Tenerelli, and Horton, W. H., "An Experimental Study of Local Buckling of Ring-Stiffened Cylinders Subject to Axial Compression," Israel Journal of Technology, Vol. 7, No. 1-2, 1969, pp. 181-194.

89. Afendik, L. G., "The Stability of a Circular Cylindrical Shell in Bending Beyond the Elastic Limit," Prikladnaia Mekhanika, Kiev, Naukova Dumka, Vol. VI, 1970, pp. 39-44 (in Russian). (English Translation in Soviet Applied Mechanics by Plenum Press, pp. 951-955.)

90. Weinitschke, H. J., "Die Stabilitaet elliptischer Zylinderschalen bei reiner Biegung," Zeitschrift fuer Angewandte Mathematik und Mechanik, Vol. 50, 1970, pp. 411-422.

91. Wilhoit, J. C. Jr., and Merwin, J. E., "The Effects of Axial Tension on Moment Carrying Capacity of Line Pipe Stressed Beyond the Elastic Limit," OTC Paper No. 1355, 3rd OTC Conference, 1971, pp. 1-293 - 1-296.

92. Perrone, N., Kao, R., "A General Nonlinear Relaxation Iteration Technique for Solving Nonlinear Problems in Mechanics," J. Appl. Mech., 1971, pp. 371-376.

93. Jirsa, J. O., Lee, F. H., Wilhoit, J. C. Jr., and Merwin, J. E., "Ovaling of Pipelines under Pure Bending," OTC paper No. 1569, Fourth OTC Conference, 1972, pp. I-573 - I-578.

94. Blomfield, J. A., Turner, C. E., "Theory of Thin Elastic Shells Applied to Pipe Bends Subjected to Bending and Internal Pressure," Journal of Strain Analysis, Vol. 7, No. 4, 1972, pp. 285-293.

REFERENCES (Cont.)

95. Dodge, W. G., and Moore, S. E., "Stress Indices and Flexibility Factors for Moment Loadings on Elbows and Curved Pipe," Welding Research Bulletin No. 179, 1972, pp. 1-20.

96. Dodge, W. G., Moore, S. E., ELBOW: A Fortran Program for the Calculation of Stresses, Stress Indices, and Flexibility Factors for Elbows and Curved Pipes, ORNL-TM-4098, 1973.

97. Koroleva, E. M., "Stability of Cylindrical Shells of Oval Cross Section in the Bending State of Stress," PMM, Vol. 37, 1973, pp. 901-904 (dates refer to translation).

98. Bowkamp, J. G., Stephen, R. M., "Large Diameter Pipe Under Combined Loading," Transportation Eng. J. ASCE, Vol. 99, No. 3, 1973, pp. 521-536.

99. Mello, R. M., Griffin, D. S., "Plastic Collapse Loads for Pipe Elbows Using Inelastic Analysis," J. Pressure Vessel Technology, ASME, 1974, pp. 177-183.

100. Almorth, B. O., and Starnes, J. H. Jr., "The Computer in Shell Stability Analysis," presented at the 1973 ASCE National Structural Engineering Meeting, San Francisco, California, 9-13 Apr 1973. Also in ASCE J. Eng. Mech., Vol. 101, EM6, Dec 1975, pp. 873-888.

101. Kempner, J., and Chen, Y. N., "Buckling and Initial Postbuckling of Oval Cylindrical Shells under Combined Axial Compression and Bending," Transactions of New York Academy of Sciences, Vol. 36, No. 2, 1974, pp. 171-191.

102. Schroeder, J., Srinivasaiah, K. R., and Graham, P., "Analysis of Test Data on Branch-Pipe Connections Exposed to Internal Pressure and/or External Couples," WRC Bulletin No. 200, Nov 1974, pp. 1-26.

103. Na, T. Y., and Turski, C. E., "Solution of the Nonlinear Differential Equations for Finite Bending of a Thin-Walled Tube by Parameter Differentiation," Aeronautical Quarterly, Vol. XXV, No. 1, Feb 1974, pp. 14-18.

104. Sherman, D. R., and Glass, A. M., "Ultimate Bending Capacity of Circular Tubes," OTC paper No. 2119, in Proceedings of Sixth OTC Conference, 1974, pp. 901-910.

105. Aksel'rad, E. L., and Kvasnikov, B. N., "Semi-Zero-Moment Theory of Curvilinear Bar-Shells," Mechanics of Solids, Vol. 2, 1974, pp. 125-133.

106. Wilhoit, J. C. Jr., and Merwin, J. E., "Critical Plastic Buckling Parameters for Tubing in Bending Under Axial Tension," in Proceedings of 5th Offshore Technology Conference, OTC 1974, Vol. 2, pp. 11-465.

107. Calladine, C. R., "Limit Analysis of Curved Tubes," Journal of Mechanical Engineering Science, Vol. 16, No. 2, 1974, pp. 85-87.

REFERENCES (Cont.)

108. Stephens, W. B., Starnes, J. H. Jr., and Almorth, B. O., "Collapse of Long Cylindrical Shells Under Combined Bending and Pressure Loads," AIAA Journal, Vol. 13, No. 1, Jan 1975, pp. 20-25.

109. Storakers, B., "On Buckling of Axisymmetric Thin Elastic-Plastic Shells," Intr. J. Solids and Structures, Vol. 11, 1975, pp. 1329-1346.

110. Johns, J. G., Mesloh, R. E., Winegarter, R., and Sorenson, J. E., "Inelastic Buckling of Pipelines under Combined Loads," OTC paper No. 2209, in Proceedings of Seventh OTC Conference, 1975, pp. 635-646.

111. Chen, Y. N., and Kempner, J., "Buckling of Oval Cylindrical Shells under Compression and Asymmetric Bending," AIAA Journal, Vol. 14, No. 9, Sep 1976, pp. 1235-1240.

112. Grinenko, N. I., and Khishchenko, Y. M., "Experimental Study of Stability of Reinforced Cylindrical Shells Under Pure Bending," Soviet Applied Mechanics, Vol. 12, May 1976, pp. 468-472.

113. Sherman, D. R., "Tests of Circular Steel Tubes in Bending," ASCE J. Strl. Div., Nov 1976, pp. 2181-2195.

114. Fabian, O., "Collapse of Cylindrical, Elastic Tubes under Combined Bending, Pressure and Axial Loads," Intl. J. Solids & Structures, Vol. 13, 1977, pp. 1257-1270.

115. Remseth, S. N., Holthe, K., Bergan, P. G., and Holand, I., "Tube Buckling Analysis by the Finite Element Method," in Proceedings of Finite Elements in Nonlinear Mechanics, International Conf., Geilo, Norway, Tapir, Aug 1977, pp. 671-694.

116. Weller, J., and Singer, J., "Experimental Studies on the Buckling Under Axial Compression of Integrally Stringer-Stiffened Circular Cylindrical Shells," Journal of Applied Mechanics, Dec 1977, pp. 721-730.

117. Sobel, L. H., "In-Plane Bending of Elbows," J. Computers and Structures, Vol. 7, No. 6, 1977, pp. 701-715.

118. Thurston, G. A., "Critical Bending Moment of Circular Cylindrical Tubes," J. Appl. Mech., 1977, pp. 173-175.

119. Gudramovich V. S., Gaiduchenko, A. P., Demeshko, M. F., Konovalenkov, V. S., "Plastic Buckling of Cylindrical Shells in the Case of Complex Loading Paths," Prikladnaia Mekhanika, Kiev, Naukova Dumka, 1977, Translation in Soviet Applied Mechanics, Plenum Press, 1980, pp. 19-24.

120. Harding, J. E., "The Elasto-Plastic Analysis of Imperfect Cylinders," in Proceedings of Institution of Civil Engineers, Part 2, Vol. 65, Dec 1978, pp. 875-892.

REFERENCES (Cont.)

121. Axelrad, E. L., "Flexible Shell-Theory and Buckling of Toroidal Shells and Tubes," Ingenieur Archiv, Vol. 47, 1978, pp. 95-104.

122. Reddy, B. D., and Calladine, C. R., "Classical Buckling of a Thin-Walled Tube Subjected to Bending Moment and Internal Pressure," Intl. J. Mech. Science, Vol. 20, 1978, pp. 641-650.

123. Korol, R. M., "Inelastic Buckling of Circular Tubes," ASCE J. Eng. Mech. Div., (EM4) Aug 1978, pp. 939-950.

124. Spence, J., and Toh, S. L., "Collapse of Thin Orthotropic Elliptical Cylindrical Shells under Combined Bending and Pressure Loads," J. Appl. Mech., Vol. 46, Jun 1979, pp. 363-371.

125. Reddy, B. D., "Plastic Buckling of a Cylindrical Shell in Pure Bending," Intl. J. Mech. Sciences, Vol. 21, 1979, pp. 671-679.

126. Tugcu, P., and Schroeder, J., "Plastic Deformation and Stability of Pipes exposed to External Couples," Intl. J. Solids and Structures, Vol. 15, 1979, pp. 643-658.

127. Khalig, A. A., and Schilling, C. G., "Plastic Buckling Strength of Seamless Steel Tubes under Bending Loads," U.S. Steel Bulletin, Feb 1979.

128. Reddy, B. D., "An Experimental Study of the Plastic Buckling of Circular Cylinders in Pure Bending," Intl. J. Solids and Structures, Vol. 15, 1979, pp. 669-683.

129. Boyle, J. T., Spence, J., "A Simple Analysis for Oval Presesurized Pipe Bends Under External Bending," in Proceedings of Intl. Conf. on Pressure Vessel Technology, London, paper C87/80, 1980, pp. 201-207.

130. Axelrad, E. L., "Flexible Shells," IUTAM Proceedings 15th Congress, University of Toronto, Aug 1980, pp. 45-56.

131. Gellin, S., "The Plastic Buckling of Long Cylindrical Shells under Pure Bending," Intl. J. Solids and Structures, Vol. 16, 1980, pp. 397-407.

132. Boyle, J. T., "The Finite Bending of Curved Pipes," Intl. J. Solids and Structures, Vol. 17, 1981, pp. 515-529.

133. Harding, J. E., "Ring-Stiffened Cylinders Under Axial and External Pressure Loading," in Proceedings of Institution of Civil Engineers, Part 2, Vol. 71, Sep 1981, pp. 863-878.

134. Emmerling, F. A., "Nichtlineare Biegung eines schach gekruemmten Rohres," ZAMM, Vol. 61, 1981, pp. T86 - T89.

135. Fabian, O., "Elastic-Plastic Collapse of Long Tubes Under Combined Bending and Pressure Load," Ocean Engineering, Vol. 8, No. 3, 1981, pp. 295-330.

REFERENCES (Cont.)

136. Bushnell, D., "Elastic-Plastic Bending and Buckling of Pipes and Elbows," J. of Computers and Structures, Vol. 13, 1981, pp. 241-248.

137. Reissner, E., "On Finite Pure Bending of Curved Tubes," Intl. J. Solids and Structures, Vol. 17, No. 9A, 1981, pp. 839-844.

138. Lang, H. A., "Pure Bending of Elliptic Ring Sector," Journal of Applied Mechanics, Vol. 49, Jun 1982, pp. 456-458.

139. Emmerling, F. A., "Nichtlineare Biegung und Beulen von Zylindern und krummen Rohren," Ingenieur Archiv, Vol. 52, 1982, pp. 1-16.

140. Kyriakides, S., and Shaw, P. K., "Response and Stability of Elastoplastic Circular Pipes under Combined Bending and External Pressure," Intl. J. Solids and Structures, Vol. 18, No. 11, 1982, pp. 957-973.

141. Kitching, R., Hussain, D., and Jones, N., "Limit Loads for Cylindrical Shells Subjected to Local Longitudinal Bending Moments," Intl. J. Mech. Sciences, Vol. 24, No. 11, 1982, pp. 673-690.

142. Obraztsov, I. F., Vol'mir, A. S., "Toroidal Shells, Stability, and Catastrophes," Sov. Phys. Dokl., Vol. 27, No. 10, 1982; English Translation in American Institute of Physics, 1983.

143. Bannister, K., "Large Deformation Analysis of a Cylindrical Shell Under Pure Bending and Pressurization," Ph.D. Thesis, Penn. State University May 1983.

144. Villhard, V. C., Bang, C., and Paluzotto, A. N., "Instability of Short Stiffened Composite Cylindrical Shells Under Bending with Prebuckling Displacements," J. Computers and Structures, Vol. 16, No. 6, 1983, pp. 773-775.

145. Kecman, D., "Bending Collapse of Rectangular & Square Section Tubes," Intl. J. Mech. Sciences, Vol. 25, No. 9, 1983, pp. 623-636.

146. Suqimoto, H. and Chen, W. F., "Inelastic Post Buckling Behavior of Tubular Members," Preprint SC-5, ASCE, Structures Congress Houston, Texas, 17-19 Oct 1983, pp. 1-14.

147. Chen, W. F., Suqimoto, H., "Moment-Curvature-Axial Compression-Pressure Relationship of Structural Tubes," Preprint SC-6, Structures Congress, Houston, ASCE, Oct 1983, pp. 1-14.

148. Benson, R. C., "Nonlinear Bending and Collapse of Long, Thin, Open Section Beams and Corrugated Panels," Journal of Applied Mechanics, Vol. 51, Mar 1984, pp. 141-145.

149. Rimrott, F., Draisey, S. H., "Critical Bending Moment of Double-Slit Tubing," J. of Spacecraft, Vol. 21, No. 3, 1984, pp. 316-318.

REFERENCES (Cont.)

150. Wu, J., Gould, Ph. L., "Pure Bending of Thin-Walled Beams," J. of Eng. Mechs. ASCE, Vol. 110, No. 7, 1984, pp. 1076-1085.

151. Fluegge, W., "Die Stabilitaet der Kreiszylinderschale," Ingenieur Archiv, Vol. 3, 1932, pp. 463-506.

152. Hibbitt, Karlsson and Sorensen, ABAQUS User's Manual, Version 4, Jul 1982, "ABAQUS Example Problems," Oct 1982.

153. Love, A. E., A Treatise on the Mathematical Theory of Elasticity, Fourth Edition, Dover Publications, Chapter V, Arts 87-89, 1944, pp. 129-132.

154. Washizu, K., Variational Methods in Elasticity and Plasticity, Third Edition, Pergamon Press, 1982, p. 8.

155. Wempner, G., "Mechanics of Solids with Applications to Thin Bodies," Sijthoff & Noordhoff, 1981, p. 62.

NOMENCLATURE

$\underline{a}_1, \underline{a}_2, \underline{a}_3$ = Local vectors along the local Y, Z, and X axes. Local z-axis is parallel to global y. Initially, local y is not parallel, but is coplanar with global x and in the same direction. Initially, local X is coplanar with global z and points in the same direction (Figure 2).

E = Young's Modulus

F_0 = Axial force based on yield stress

k_{CR} = Critical curvature at bifurcation (see Table 2)

h = Shell thickness

I = Moment of inertia of undeformed section (Table 2)

k = Subscript in nodal values u_k, u_{k+1}, u_{k+2} (Eq. (24)). Mean curvature defined as the sum of absolute value of direct axial strains at the top and bottom of the cylinder divided by the undeformed diameter of the shell.

L = Total length of cylindrical shell (Figure 1). In Equation (25), L is total arc length of end section ABC (Figure 2) prior to deformation.

ℓ_i = Length of side of element i on arc where end rotation is applied (undeformed side ABC on Figure 2)

M_{BR} = Critical bending moment by Brazier (Table 2)

M_{CR} = Critical bending moment of bifurcation (Table 2)

M, M_{EXT} = External bending moment calculated in the form of a reaction in this analysis

M_0 = Plastic moment or ultimate moment based on yield stress (Table 2)

N = Total number of equal elements on undeformed arc ABC (Figure 2)

NOMENCLATURE (Cont.)

$\underline{r}$	= Final position vector on arc A'B'C' (Figure 2, after deformation)
r_o	= Initial position vector of any point on periphery of shell (arc ABC on Figure 2) at which the end rotation will be applied
$\underline{r}_o^b$	= Initial position vector of auxiliary node
R	= Mean shell radius
$\underline{u}$	= In the "APPLIED LOADING" section, $\underline{u}$ is the vector displacement after deformation; it is not to be confused with u
$\underline{u}^b$	= In the context of analysis given in "APPLIED LOADING," vector displacement of auxiliary node after deformation; it is not to be confused with u
u_x, u_y, u_z	= Vertical, transverse and longitudinal translations (along global X, Y, Z axes). Also referred to as u, v, and w.
(u)	= Vertical displacement at any point ξ on an element side
u_k, u_{k+1}, u_{k+2}	= Nodal values of displacement $u(\xi)$ at end node k, midside node k+1, end node k+2.
u_s	= Nodal value at s (point on arc where end rotation is being applied)
u	= Translation along global x-axis
v	= Translation along global y-axis
w	= Translation along global z-axis
θ	= Angle from vertical global x-axis up to end of arc to be analyzed
ν	= Poisson's ratio
ξ	= Local normalized variable in interval (0, 1) employed in describing vertical displacement distribution $u(\xi)$.
σ_{CR}	= Critical stress at bifurcation (Table 2)
σ_Y	= Yield stress of material
φ_o	= Initial inclination of cylindrical shell about y-axis. For straight tubes (present case) $\varphi_o = 0$
φ_x	= Rotation about global x-axis

NOMENCLATURE (Cont.)

φ_y	= Rotation about global y-axis
φ_y^b	= Prescribed end rotation about y-axis
φ_z	= Prescribed end rotation about z-axis

DISTRIBUTION

	Copies
Chief of Naval Technology	
Office of Naval Technology	
Attn: ASW-14	1
Dr. A. J. Faulstich (Code 023)	1
Navy Department	
Arlington, VA 22217-5000	
Commander	
Naval Sea Systems Command	
Attn: SEA-03B	1
SEA-05B (P. Palermo)	1
SEA-55B (J. B. O'Brian)	1
SEA-55Y1 (S. G. Arntson)	1
SEA-55Y2 (R. E. Provencher)	1
SEA-63R32 (D. Houser)	1
SEA-9G32	1
SEA-32R (C. Pohler)	1
PMS-402	1
PMS-406	1
PMS-407	1
Department of the Navy	
Washington, DC 20362	
Commander	
David W. Taylor Naval Ship Research and Development Center	
Attn: Code 17 (M. Krenzke)	1
Code 175 (J. Sykes)	1
Code 175.2 (B. Whang)	1
Code 175.2	1
Code 175.2 (T. Gilbert)	1
Code 175.3 (W. Conley)	1
Code 175.3 (P. Manny)	1
Code 184.4 (M. Hurwitz)	1
Code 172	1
Code 1620.3 (R. Jones)	1
Code 1720.6 (A. E. Dadley)	1
Code 1730.5 (J. C. Adamchak)	1
Bethesda, MD 20084	

	Copies
David W. Taylor Naval Ship Research and Development Center	
Attn: Code 177 (R. Fuss)	1
Code 177.1 (V. Bloodgood)	1
Code 177.1 (M. Riley)	1
Code 177.1 (R. Higginbotham)	1
Underwater Explosion Research Division	
Portsmouth, VA 23709	
Naval Coastal Systems Center	
Attn: Code 4210 (J. Rumbough)	1
Panama City, FL 32407	
Lockheed Palo Alto Laboratory	
Lockheed Missiles and Space Company Labs	
Attn: Dr. John DeRuntz	1
3251 Hanover Street	
Palo Alto, CA 94304	
Commander	
Naval Weapons Center	
Attn: Code 533 (Technical Library)	1
China Lake, CA 93555	
Commander	
Naval Ocean Systems Center	
Attn: Technical Library	1
San Diego, CA 92152	
Commanding Officer	
Naval Underwater Systems Center	
Attn: D. J. Lepore	1
Newport, RI 02840	

DISTRIBUTION (Cont.)

	Copies
Massachusetts Institute of Technology Attn: Prof. T. Wierzbicki Department of Ocean Engineering Cambridge, MA 02139	1
Massachusetts Institute of Technology Attn: Prof. T. H. Pian Prof. E. A. Witmer Department of Aeronautics and Astronautics Cambridge, MA 02139	1 1
Massachusetts Institute of Technology Attn: Prof. K. J. Bathe Department of Mechanical Engineering Cambridge, MA 02139	1
Massachusetts Institute of Technology Attn: Prof. J. J. Connor Department of Civil Engineering Cambridge, MA 02139	1
Purdue University Attn: Prof. W. F. Chen School of Civil Engineering West Lafayette, IN 47907	1
Office of Naval Research Attn: Code 432 (A. Kushner) 800 North Quincy Street Arlington, VA 22217	1
Defense Nuclear Agency Attn: SPSS (C. McFarland) Washington, DC 20305	1
Defense Technical Information Center Cameron Station Alexandria, VA 22314	12

	Copies
Weidlinger Associates Weidlinger Consultant Attn: M. Bowen A. Misovich 110 East 58th Street New York, NY 10022	1 2
Hibbitt, Karlson & Sorensen, Inc. Attn: Dr. B. Karlson Dr. P. Sorensen 35 South Angell Street Providence, RI 02906	1 1
American Bureau of Shipping Attn: Mr. Stanley G. Stiansen, Vice President Dr. Y. K. Chen Dr. D. Liu 65 Broadway New York, NY 10006	1 1 1
Stevens Institute of Technology, Castle Point Attn: Prof. David Nicholson Department of Mechanical Engineering Hoboken, NJ 07030	1
Library of Congress Attn: Gift and Exchange Division Washington, DC 20540	4
Westinghouse Electric Corporation Attn: Dr. Aspi K. Dhalla Advanced Energy Systems Division P. O. Box 158 Madison, PA 15663	1
Lockheed Palo Alto Research Laboratory Attn: Dr. David Bushnell Department 52-33, Building 205 3251 Hanover Street Palo Alto, CA 94304	1

DISTRIBUTION (Cont.)

	Copies
Internal Distribution:	
R10	1
R10 (D. Phillips)	1
R10 (M. Marshall)	1
R10 (H. Huang)	1
R102	2
R14	20
R14 (M. Moussouros)	20
R14 (K. Bannister)	1
R14 (K. Kiddy)	1
R14 (G. Harris)	1
R14 (S. Wilkerson)	1
R14 (F. Bandak)	1
R14 (D. Bendt)	1
R14 (J. Shaker)	1
E231	9
E232	3
E35	1
U01	1

END

DTIC

7-86

AD-A169 009 AN ANALYSIS OF EXPLOSION-INDUCED BENDING DAMAGE IN SUBMERGED SHELL TARGETS(U) NAVAL SURFACE WEAPONS CENTER DAHLGREN VA M MOUSSOUROS DEC 84 NSWC/TR-84-380 1/1

UNCLASSIFIED F/G 19/4 NL

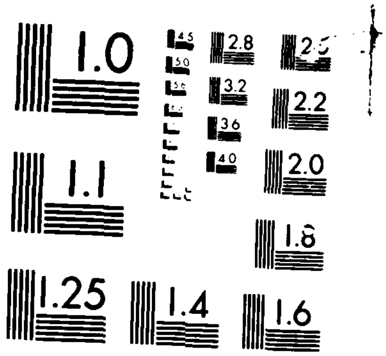

MICROCOP

NSWC TR 84-380

(12)

AN ANALYSIS OF EXPLOSION-INDUCED BENDING DAMAGE IN SUBMERGED SHELL TARGETS

BY MINOS MOUSSOUROS

RESEARCH AND TECHNOLOGY DEPARTMENT

DECEMBER 1984

NAVAL SURFACE WEAPONS CENTER

Dahlgren, Virginia 22448 • Silver Spring, Maryland 20910

UNCLASSIFIED

SECURITY CLASSIFICATION OF THIS PAGE (When Data Entered)

REPORT DOCUMENTATION PAGE		READ INSTRUCTIONS BEFORE COMPLETING FORM
1. REPORT NUMBER NSWC TR 84-380	2. GOVT ACCESSION NO. A169009	3. RECIPIENT'S CATALOG NUMBER
4. TITLE (and Subtitle) AN ANALYSIS OF EXPLOSION-INDUCED BENDING DAMAGE IN SUBMERGED SHELL TARGETS		5. TYPE OF REPORT & PERIOD COVERED 6. PERFORMING ORG. REPORT NUMBER
7. AUTHOR(s) MINOS MOUSSOUROS		8. CONTRACT OR GRANT NUMBER(s)
9. PERFORMING ORGANIZATION NAME AND ADDRESS Naval Surface Weapons Center (Code R14) 10901 New Hampshire Avenue Silver Spring, MD 20903-5000		10. PROGRAM ELEMENT, PROJECT, TASK AREA & WORK UNIT NUMBERS 62633N; F33327; SF33327; R19BA
11. CONTROLLING OFFICE NAME AND ADDRESS		12. REPORT DATE December 1984 13. NUMBER OF PAGES 73
14. MONITORING AGENCY NAME & ADDRESS (if different from Controlling Office)		15. SECURITY CLASS. (of this report) UNCLASSIFIED 15a. DECLASSIFICATION/DOWNGRADING SCHEDULE

16. DISTRIBUTION STATEMENT (of this Report)

Approved for public release; distribution unlimited.

17. DISTRIBUTION STATEMENT (of the abstract entered in Block 20, if different from Report)

18. SUPPLEMENTARY NOTES

19. KEY WORDS (Continue on reverse side if necessary and identify by block number)

Finite element
Bend-buckling
Cylindrical
Explosion analysis

20. ABSTRACT (Continue on reverse side if necessary and identify by block number)

An underwater explosion gives rise to a violently oscillating bubble containing detonation gases. The oscillations cause pulses to impinge on a nearby submerged structure which, under some conditions, produce low frequency bending motion. The amplitude of the bending motion frequently is large enough to correspond to severe plastic deformation and bend-buckling. An analysis for this problem can be performed by treating the structure as a cylindrical shell subjected to two end couples set up by longitudinal membrane stresses.

DD FORM 1 JAN 73 1473 EDITION OF 1 NOV 65 IS OBSOLETE

S N 0102-LF-014-6601

UNCLASSIFIED

SECURITY CLASSIFICATION OF THIS PAGE (When Data Entered)

20. (Cont.)

Such stresses are known to induce axial buckling and/or ovalization or plastification of the cross-section. As a first approximation, and in view of the low frequency response, inertia is neglected in this analysis.

Bending moment and work done on the structure are determined as a function of mean curvature. Computational results are presented for several shell geometries and published experimental data for these models compare favorably with the computations.

FOREWORD

This study represents the initial effort aimed at addressing the bend buckling of circular cylindrical shells subject to two self-equilibrating end moments and zero net axial loading. Such conditions may arise in the flexural response of a submerged cylinder excited by an underwater explosion bubble. The inertia forces are neglected here in view of the low frequency nature of the response. Both material and geometrical nonlinearities are included.

This analysis uses the nonlinear finite element program ABAQUS. Analytical predictions from ABAQUS are validated by comparison of results to experimental data available in the open literature.

Approved by:

Kurt F. Mueller

KURT F. MUELLER, Head
Energetic Materials Division

A1

CONTENTS

ILLUSTRATIONS

ILLUSTRATIONS (Cont.)

TABLES

INTRODUCTION

The problem of the deformation of a straight or curved shell, subject to end bending moments and possibly internal pressure, has been addressed in numerous articles.[1-151]

This report addresses numerically the problem of a straight circular tube subject to external end bending moments without internal pressure, allowing for geometric and material nonlinearities. The nonlinear finite element program ABAQUS[152] is used. Experimental results from the open literature[93] are compared with the numerical results in order to validate ABAQUS for problems of this category.

References 3, 4, 30, and 36 are essentially concerned with the linear bending of tubes subject to end bending moments. In modern terminology, they are referred to as "geometrically linear" analyses. The first "geometrically nonlinear" analyses are due to Brazier,[7] Chwalla,[11,15] Wood,[51] Reissner,[55,60] Reissner and Weinitschke,[65] and Weinitschke,[90] to mention a few.

Ades,[48] assuming that the cross-sections of a long cylinder remain elliptical after deformation, accounted for geometric and material nonlinearities. Afendik[84,89] presented an approximate analysis incorporating plasticity. References 131 and 140 allowed for geometrical and material nonlinearities, while Reference 135 extended an earlier analysis[114] to elastoplastic behavior of imperfect cylinders. References 100, 108, 115, and 152 are the only numerical papers (as applied to straight cylindrical shells) by the finite element method of which the author is aware.

Interest in this problem stems from the fact that during an underwater explosion, external vertical forces are set up on a submerged structure and cause it to bend, as if subjected to end couples. An analysis could be of potential use to ship designers when questions of quantifying ultimate longitudinal strength arise (see Caldwell[72]). Another potential problem is related to curved pipes between fixed supports.[4,8,9,19,27,28,30,34,35,36,37,46] When a temperature increase occurs, the curved part is subjected to terminal couples, which reduce the radius of curvature.

METHOD

As mentioned previously, the dynamic problem will be approximated by a static equivalent in view of the low frequency of the motions. The complexity of the problem necessitates the use of a numerical procedure. The nonlinear finite element program ABAQUS[152] is used in this work.

First, we establish a global right-handed coordinate (x,y,z) system (Figures 1 and 2) with z the longitudinal axis of the cylindrical shell, x the vertical, and y the transverse direction. Next, we discretize the structure by modeling only one-half the length and one-half the periphery, i.e., we employ a quarter model. It is assumed that the cylinder is perfectly circular (without imperfections due to fabrication and residual strains) and the end loads are symmetrical with respect to the x-z plane, with the bending couples lying on the global y-axis. The cylindrical surface is replaced by ABAQUS S8R shell elements with 3 integration points across the thickness. Geometric and material nonlinearities are allowed. Perfect plasticity, von Mises isotropic yield, and an associated normal flow rule are used by ABAQUS. The employed mesh, including midside nodes, was 25 x 25 excluding an auxiliary node. Figure 18 displays a 13 x 13 mesh which excludes all midnodes.

BOUNDARY CONDITIONS

All boundary conditions are given in the global Cartesian frame of reference. Along both generators, AA' ($\theta = 0°$) and CC' ($\theta = 180°$), owing to symmetry, we have

$$v = \varphi_x = \varphi_z = 0$$

Along the half-circle ABC, symmetry implies that (half length analyzed only)

$$w = \varphi_x = \varphi_y = 0$$

Note that up to this point, the vertical rigid body motion has not yet been removed, and it must be constrained prior to solution. This will be done in conjunction with the method of exerting the external loading.

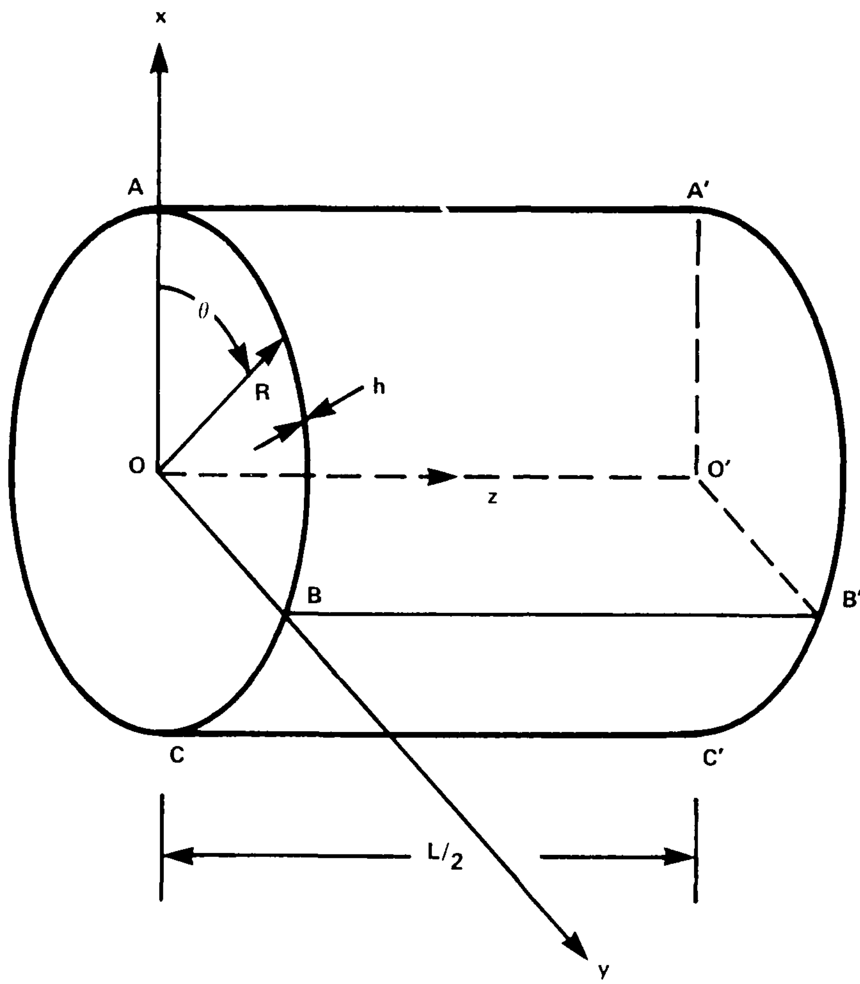

FIGURE 1. STRAIGHT CYLINDRICAL SHELL OF HALF LENGTH $L/_2$, MEAN RADIUS R, THICKNESS h, AND ASSOCIATED GLOBAL CARTESIAN COORDINATE SYSTEM (x, y, z)

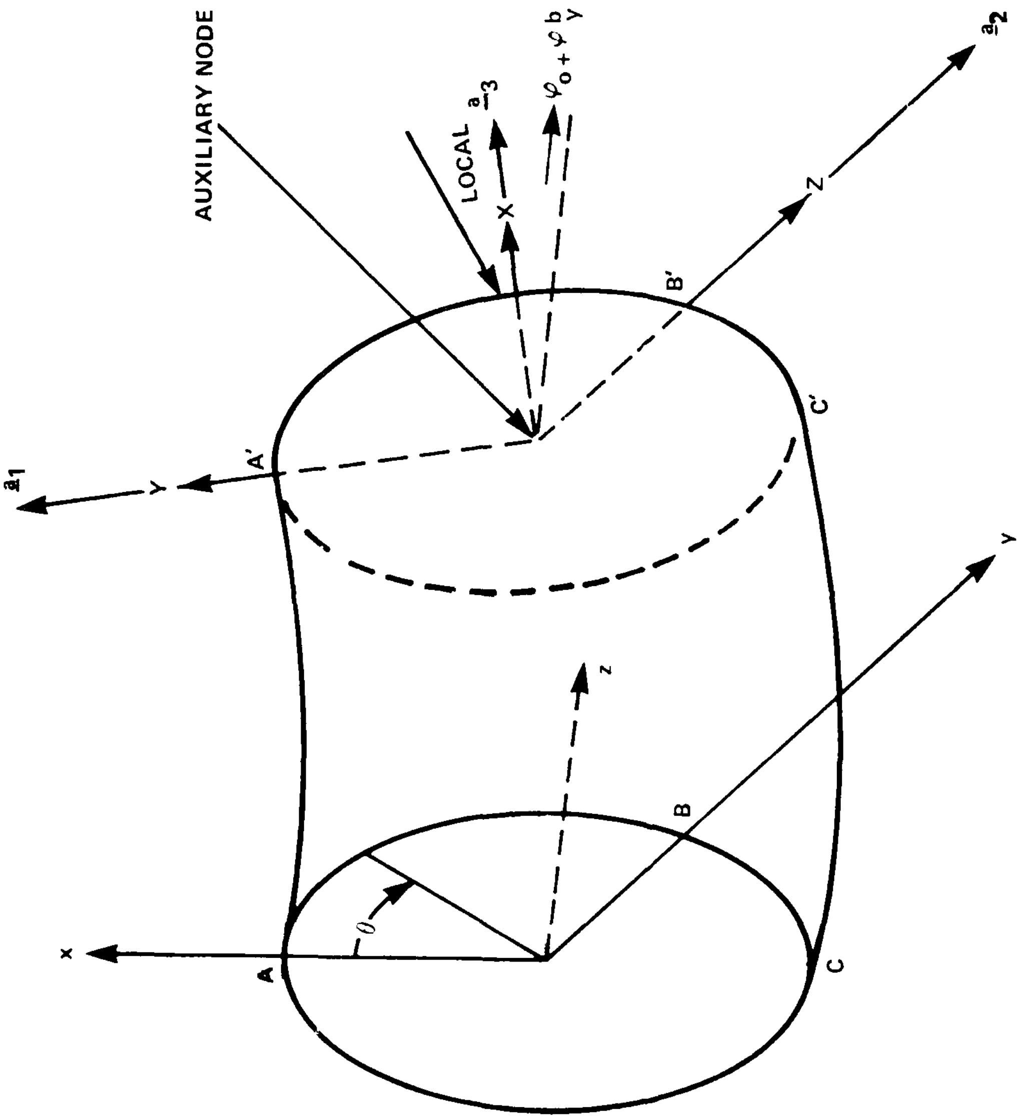

FIGURE 2. CYLINDRICAL SHELL WITH ASSOCIATED END SECTION A' B' C' AND AUXILIARY NODE AFTER DEFORMATION (LOCAL FRAME OF REFERENCE (X, Y, Z))

APPLIED LOADING

ABAQUS has a particularly attractive feature: a nonlinear multiple constraint capability (MPC).* The loading on the structure from the underwater explosion is approximated through an overall bending moment set up by the action of longitudinal membrane stresses. This will be modeled through a prescribed end rotation about the Y-axis applied incrementally. For small deformations, the vertical coordinate of the neutral axis from the center of the circular cross-section is extremely small. Consequently, the shift is approximately zero. However, for larger deformations this shift is substantial, necessitating an iteration if we are to assume that initially a linear distribution of forces produces a net applied moment. To avoid the above, the following method is used.

There are three conditions that must be fulfilled in this approach and are summarized here for clarity:

1. Plane sections remain plane at A'B'C' arc (Figure 2) (at the end where the external loading would have been applied).

2. There will be no rotation of A'B'C' plane (Figure 2) about the local Y-axis.

3. An end rotation about the global y (or local Z) is incrementally applied.

Condition 3 gives rise to a distribution of external longitudinal inplane forces along the local X-axis, which causes a bending moment.

An auxiliary node is set up to coincide with the center of the original undeformed plane. The terminal couple is applied at this section. After deformation, it is assumed that plane sections remain plane. By St. Venant's Principle of "elastic equivalence of statically equipollent systems of load,"[153,154] we conclude that for lengths larger than the cylinder diameter, the stress distribution away from the load, due to a zero net axial force and a terminal bending moment, does not depend on the traction distribution, except perhaps locally in the neighborhood of the point of application of the load. This condition can be fulfilled if vector $\underline{a}_3$ (Figure 2) of the local frame of reference, located on the deformed plane, is orthogonal to any vector on that plane.

The position vectors before deformation of nodes on the periphery of the shell, where the end couple is applied, are $\underline{r}_o$, and $\underline{r}_o^b$ for the auxiliary node. After displacements $\underline{u}$ of the peripheral nodes and $\underline{u}^b$ of the auxiliary node, we obtain

$$\underline{r} = \underline{r}_o + \underline{u} \tag{1}$$

$$\underline{r}^b = \underline{r}_o^b + \underline{u}^b \tag{2}$$

*MPC = Multiple Point Constraints

$$\underline{r} - \underline{r}^b = [\underline{r}_o - \underline{r}_o^{\,b}] + [\underline{u} - \underline{u}^b] \tag{3}$$

Therefore,

$$[\underline{r} - \underline{r}^b] \cdot \underline{a}_3 = 0 \tag{4}$$

where, in component notation,

$$\underline{r} - \underline{r}^b = [(x - x_b), (y - y_b), (z - z_b)] \tag{5}$$

and all quantitites are given with respect to the global undeformed frame. Now, if the original local x-axis (along vector $\underline{a}_3$) had an initial inclination φ_o with respect to the global y-axis, after deformation the angle would be $\varphi_o + \varphi_y{}^b$. Therefore, after deformation the direction cosines of the local vectors $\underline{a}_1$, $\underline{a}_2$, and $\underline{a}_3$ with respect to the global system would be

$$\underline{a}_1 = [\cos(\varphi_o + \varphi_y{}^b), \quad 0, \quad -\sin(\varphi_o + \varphi_y{}^b)] \tag{6}$$

$$\underline{a}_2 = [0, \quad 1, \quad 0] \tag{7}$$

$$\underline{a}_3 = [\sin(\varphi_o + \varphi_y{}^b), \quad 0, \quad \cos(\varphi_o + \varphi_y{}^b)] \tag{8}$$

Therefore,

$$(\underline{r} - \underline{r}^b) \cdot \underline{a}_3 = (x - x_b)\sin(\varphi_o + \varphi_y{}^b) + (z - z_b)\cos(\varphi_o + \varphi_y{}^b) = 0 \tag{9}$$

This can be further expanded by means of the trigonometric identities

$$\cos(\varphi_o + \varphi_y{}^b) = \cos\varphi_o \cos\varphi_y{}^b - \sin\varphi_o \sin\varphi_y{}^b \tag{10}$$

$$\sin(\varphi_o + \varphi_y{}^b) = \sin\varphi_o \cos\varphi_y{}^b + \cos\varphi_o \sin\varphi_y{}^b \tag{11}$$

Since our solution process is incremental and our constraints are nonlinear, our boundary conditions must be cast in incremental form. Consequently, we note that φ_o is a constant angle (which for straight tubes is zero). The incremental form of the left-hand side of Equation (3) can be obtained from the difference of the incremental forms of Equations (1) and (2), since

$$\underline{r} + \Delta\underline{r} = \underline{r}_o + \underline{u} + \Delta\underline{u} \tag{12}$$

$$\underline{r}^b + \Delta\underline{r}^b = \underline{r}_o{}^b + \underline{u}^b + \Delta\underline{u}^b \tag{13}$$

$$\begin{aligned}(\underline{r} + \Delta\underline{r}) - (\underline{r}^b + \Delta\underline{r}^b) &= (\underline{r}_o - \underline{r}_o{}^b) + (\underline{u} - \underline{u}^b) \\ &\quad + (\Delta\underline{u} - \Delta\underline{u}^b)\end{aligned} \tag{14}$$

In view of Equation (3),

$$\Delta\underline{r} - \Delta\underline{r}^b = \Delta\underline{u} - \Delta\underline{u}^b \tag{15}$$

The incremental form of the righthand side of Equation (9) with respect to increments of the displacements u_z, u_x, $\varphi_y{}^b$, $u_z{}^b$, and $u_x{}^b$, by means of Equation (15) becomes

$$\begin{aligned}&(\Delta u_z - \Delta u_z{}^b)[\cos\varphi_o \cos\varphi_y{}^b - \sin\varphi_0 \sin\varphi_y{}^b] \\ &\quad + (\Delta u_x - \Delta u_x{}^b)[\sin\varphi_o \cos\varphi_y{}^b + \cos\varphi_o \sin\varphi_y{}^b] \\ &\quad + (z - z_b)[-\cos\varphi_o \sin\varphi_y{}^b - \sin\varphi_o \cos\varphi_y{}^b]\Delta\varphi_y{}^b \\ &\quad + (x - x_b)\ [-\sin\varphi_o \sin\varphi_y{}^b + \cos\varphi_o \cos\varphi_y{}^b]\Delta\varphi_y{}^b = 0\end{aligned} \tag{16}$$

or

$$(\Delta u_z - \Delta u_z{}^b)\cos(\varphi_o + \varphi_y{}^b) + (\Delta u_x - \Delta u_x{}^b)\sin(\varphi_o + \varphi_y{}^b)$$

$$+ \Delta\varphi_y^b \left\{(z - z_b)\sin(\varphi_o + \varphi_y^b) + (x - x_b)\cos(\varphi_o + \varphi_y^b)\right\} = 0 \tag{17}$$

Next, we note the end plane does not rotate about the local Y-axis, i.e., there will be no component of rotation about vector $\underline{a}_1$. A small rotation about the local Y-axis can be obtained by a rotation vector with respect to the global system

$$\underline{\Omega} = (\varphi_x, \varphi_y, \varphi_z) \tag{18}$$

If this vector is normal to vector $\underline{a}_1$, then it has no rotational component about $\underline{a}_1$, i.e.,

$$\underline{\Omega} \cdot \underline{a}_1 = [\varphi_x, \varphi_y, \varphi_z] \cdot [\cos(\varphi_y + \varphi_y{}^b), \quad 0,$$

$$-\sin(\varphi_o + \varphi_y{}^b)] = 0 \tag{19}$$

or

$$\varphi_x\cos(\varphi_o + \varphi_y{}^b) - \varphi_z\sin(\varphi_o + \varphi_y{}^b) = 0 \tag{20}$$

The incremental form of Equation (20) becomes

$$\Delta\varphi_x\cos(\varphi_o + \varphi_y{}^b) - \Delta\varphi_z\sin(\varphi_o + \varphi_y{}^b)$$

$$- \Delta\varphi_y{}^b \left\{\varphi_x\sin(\varphi_o + \varphi_y{}^b) + \varphi_z\cos(\varphi_o + \varphi_y{}^b)\right\} = 0 \tag{21}$$

Finally, the essential boundary condition is that the rotation φ_y of all nodes on the periphery must equal the rotation about the local Z-axis ($\underline{a}_2$ vector or global y-axis) of the auxiliary node, i.e.,

$$\varphi_y = \varphi_y^b \tag{22}$$

and in incremental form

$$\Delta\varphi_y = \Delta\varphi_y^b \tag{23}$$

The vertical (global x-axis) rigid body motion must be removed. This can be accomplished by coupling the average X-displacement of the shell nodes on the end section to the vertical displacement of the auxiliary node. This, in turn, is set to zero. For element i, S8R element displacements across an edge are quadratic, i.e. (with $0 \leq \xi \leq 1$) the vertical displacement $u(\xi)$ is given in terms of its nodal values (u_k, u_{k+1}, u_{k+2})

$$u(\xi) = [(2\xi - 1)(\xi - 1),\ 4\xi(1 - \xi),\ \xi(2\xi - 1)] \begin{bmatrix} u_k \\ u_{k+1} \\ u_{k+2} \end{bmatrix} \tag{24}$$

For uniform finite element grid, where s denotes arc length, s_i arc length of element i, and L total arc length,

$$\ell_i = \frac{L}{N} \tag{25}$$

$$ds_i = \ell_i d\xi = \frac{L}{N}\, d\xi \tag{26}$$

At the element level (element i), with nodal vertical displacements (u_k, u_{k+1}, u_{k+2})

$$\int_{s=0}^{s=s_i} u(\xi)ds_i = \int_{\xi=0}^{\xi=1} u(\xi)\ell_i d\xi = \ell_i \int_0^1 u(\xi)d\xi$$

$$= \frac{\ell_i}{6}\,[1,\ 4,\ 1] \begin{bmatrix} u_k \\ u_{k+1} \\ u_{k+2} \end{bmatrix} = \frac{L}{6N}\,[1,\ 4,\ 1] \begin{bmatrix} u_k \\ u_{k+1} \\ u_{k+2} \end{bmatrix} \tag{27}$$

Since there are N elements (with 2 corner and 1 midside nodes, i.e. 3 nodes total), there will be 2N+1 nodes and associated nodal values of vertical displacements. Therefore, by Equation (24)

$$\int_{s=0}^{s=L} u(s)ds = \sum_{i=1}^{i=N} \int_{\xi=0}^{\xi=1} u(\xi)\ell_i d\xi$$

$$= \underset{\{1x(2N+1)\}}{\frac{L}{6N}\,[1,\ 4,\ 2,\ 4,\ .\ .\ .,\ 2,\ 4,\ 1]} \underset{\{(2N+1)\ x\ 1\}}{\begin{bmatrix} u_s \\ u_{s+1} \\ \vdots \\ u_{s+2N-1} \\ u_{s+2N} \end{bmatrix}} \tag{28}$$

Consequently, the boundary condition

$$\frac{1}{L}\int_{s=0}^{s=L} u(s)ds = u_x{}^b \tag{29}$$

can be recast, in view of Equation (28), to

$$\frac{1}{6N}\underset{\{1\ \times\ (2N+1)\}}{[1,\ 4,\ 2,\ 4,\ .\ .\ .,\ 2,\ 4,\ 1]}\underset{\{(2N+1)\ \times\ 1\}}{\begin{bmatrix} u_s \\ u_{s+1} \\ \vdots \\ u_{s+2N-1} \\ u_{s+2N} \end{bmatrix}} = u_x^{\,b} \tag{30}$$

for a uniform grid, where the nodal vector of Equation (30) denotes vertical displacements of shell nodes at the end plane. The above constraints can be incorporated through the nonlinear MPC capability of ABAQUS.[152] Furthermore, from Equations (3) and (9), Equation (9) can be rewritten as

$$\begin{aligned}&[x_o + u_x - x_o^{\,b} - u_x^{\,b}]\sin(\varphi_o + \varphi_y^{\,b}) \\ &\quad + [z_o + u_z - z_o^{\,b} - u_z^{\,b}]\cos(\varphi_o + \varphi_y^{\,b}) = 0\end{aligned} \tag{31}$$

Following Reference 152, we eliminate u_z from Equation (31) first (i.e. at the shell node)

$$u_z = u_z^{\,b} + (z_o^{\,b} - z_o) - (x_o - x_o^{\,b} + u_x - u_x^{\,b})\tan(\varphi_o + \varphi_y^{\,b}) \tag{32}$$

Solving for φ_x from Equation (20)

$$\varphi_x = \varphi_z \tan(\varphi_o + \varphi_y^{\,b}) \tag{33}$$

and φ_y from Equation (22)

$$\varphi_y = \varphi_y^{\,b} \tag{34}$$

Furthermore, we eliminate the vertical translation u_x. This follows from constraints involving the elimination of u_z. All previous steps are explained in Reference 152 or can be found in the FORTRAN listing for MPC constraints.

APPLICATIONS AND RESULTS

Four unstiffened circular cylinders[93] have been analyzed using the finite element program ABAQUS[152]: models 10A, 16A, 20A of Reference 93, and 20AI, which is an imperfect version of model 20A. Note that they are comparatively thick to avoid premature collapse and to exhibit plasticity effects as the applied external moment increases past the yield moment. The above models fall in the range of "long cylinders." Their perfect discrete analogues would fail by ovalization or the "Brazier effect," or by plastic deformation. The experimentally imperfect models failed by buckling "failure"[93] as displayed on the moment-curvature curves.

Table 1 gives the geometrical and material properties of these models and the stress-strain curves can be obtained from Reference 93. In Reference 93, the external loading was applied by the use of a so-called "shear span" prior to the test section "bending span." To create the external moment in our research, we employed an additional span beyond the bending span, equal to the "shear" span, and then applied a fixed angle of rotation. Table 2 contains some parameters used in reducing the stresses, moments, curvatures, and forces in nondimensional form, and they can be used to determine relative magnitude for critical quantities such as yield moment, etc.

Mean curvature k is defined as the ratio of the sum of the absolute values of direct longitudinal strains at 0° (top of cylinder, i.e. tension side) and 180° (bottom of cylinder, i.e. compression side) divided by the undeformed diameter of the shell. Figures 3 through 5 are the relevant M vs. k curves for models 10A, 16A, and 20A, together with the corresponding experimental results of Reference 93. Agreement between experimental (dots) and computed results is good for all three cylinders. Imperfection sensitivity and the analysis of medium and short cylinders, where short-wave length buckling may control the collapse mechanism, will be addressed elsewhere.

Figures 6 through 8 display the work done versus the moment parameter $\mu = M_{EXT}/M_0$, where $M_0 = 4R^2 h\sigma_y$, R = mean radius of cylinder, E = Young's Modulus, M_{EXT} = external bending moment, h = shell thickness, and σ_y = material yield stress.

We define two parameters, longitudinal stress/stress at bifurcation and hoop stress/stress at bifurcation, where stress at bifurcation is

$$\sigma_{CR} = \frac{E}{\sqrt{3\,(1-\nu^2)}}\ \frac{h}{R}$$

Figures 9 through 11 represent plots of the longitudinal inplane stress parameter versus angular position. Additional local bending stresses across the shell thickness are not addressed. Note, however, that the longitudinal membrane stress distribution in Figures 9 through 11 does not follow simple beam theory. The stress distribution from the 0° and 180° points (top and bottom of

TABLE 1. GEOMETRICAL AND MATERIAL PROPERTIES OF MODELS [93]

MODEL No.	RADIUS R (IN)	THICKNESS h (IN)	YOUNG'S MODULUS E (ksi)	POISSON'S RATIO ν	YIELD STRESS σ_Y (ksi)	HALF LENGTH USED IN COMPUTATION L/2 (IN)	R/h	L/R
10A	5.258	0.233	28,947.0	0.3	50.000	108.0	22.566	41.08
16A	7.870	0.260	30,000.0	0.3	45.272	162.0	30.629	41.17
20A	9.873	0.255	28,947.0	0.3	50.000	162.0	38.717	32.82

TABLE 2. CHARACTERISTIC PARAMETERS OF MODELS

MODEL No.	(1) σ_{CR} (ksi)	(2) M_{CR} (k-in)	(3) K_{CR} (1/in)	(4) M_{BR} (k-in)	(5) M_o (k-in)	(6) F_o (k)	(7) I (in^4)
10A	776.35	15,711.0	0.510074×10^{-2}	8,552.0	1,288.33	384.88	106.40
16A	599.84	30,346.7	0.254063×10^{-2}	16,518.6	2,916.17	582.04	398.15
20A	452.49	35,334.7	0.158329×10^{-2}	19,233.8	4,971.28	790.93	770.97

NOTES:

(1) CRITICAL STRESS AT BIFURCATION $\sigma_{CR} = \frac{E}{\sqrt{3(1-\nu^2)}}\left(\frac{h}{R}\right)$

(2) CRITICAL MOMENT AT BIFURCATION $M_{CR} = \frac{\pi E}{\sqrt{3(1-\nu^2)}} Rh^2$

(3) CRITICAL CURVATURE AT BIFURCATION $k_{CR} = \frac{1}{\sqrt{3(1-\nu^2)}} \frac{h}{R^2}$

(4) CRITICAL BRAZIER MOMENT $M_{BR} = \frac{2\sqrt{2}}{9\sqrt{(1-\nu^2)}} \pi E Rh^2$

(5) PLASTIC MOMENT BASED ON YIELD STRESS $M_o = 4R^2 h\sigma_y$

(6) AXIAL FORCE BASED IN YIELD STRESS $F_o = 2Rh\sigma_y$

(7) MOMENT OF INERTIA OF UNDEFORMED CROSS-SECTION $I = \pi R^3 h$

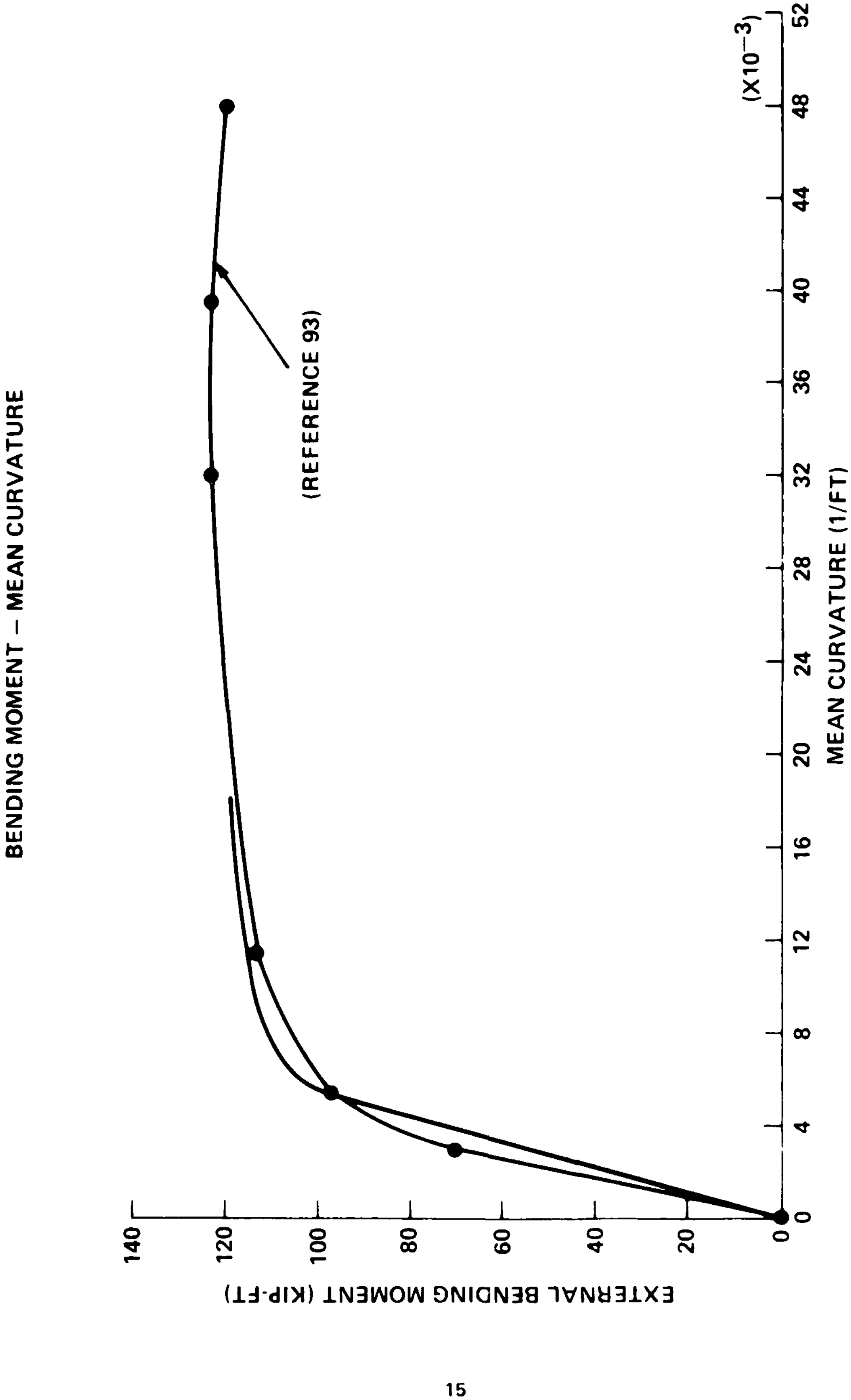

FIGURE 3. MOMENT – CURVATURE PLOTS FOR MODEL 10A

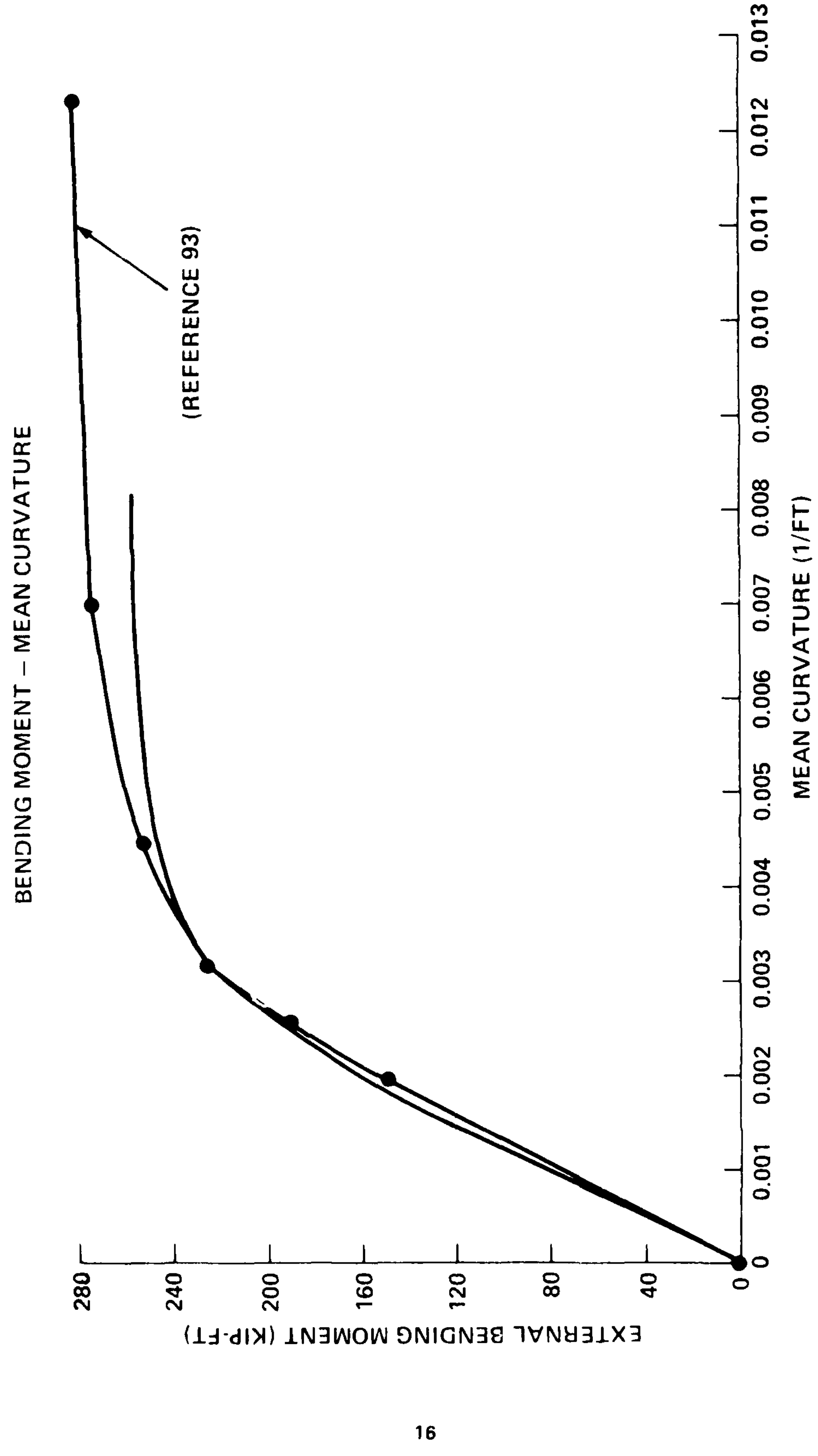

FIGURE 4. MOMENT – CURVATURE PLOTS FOR MODEL 16A

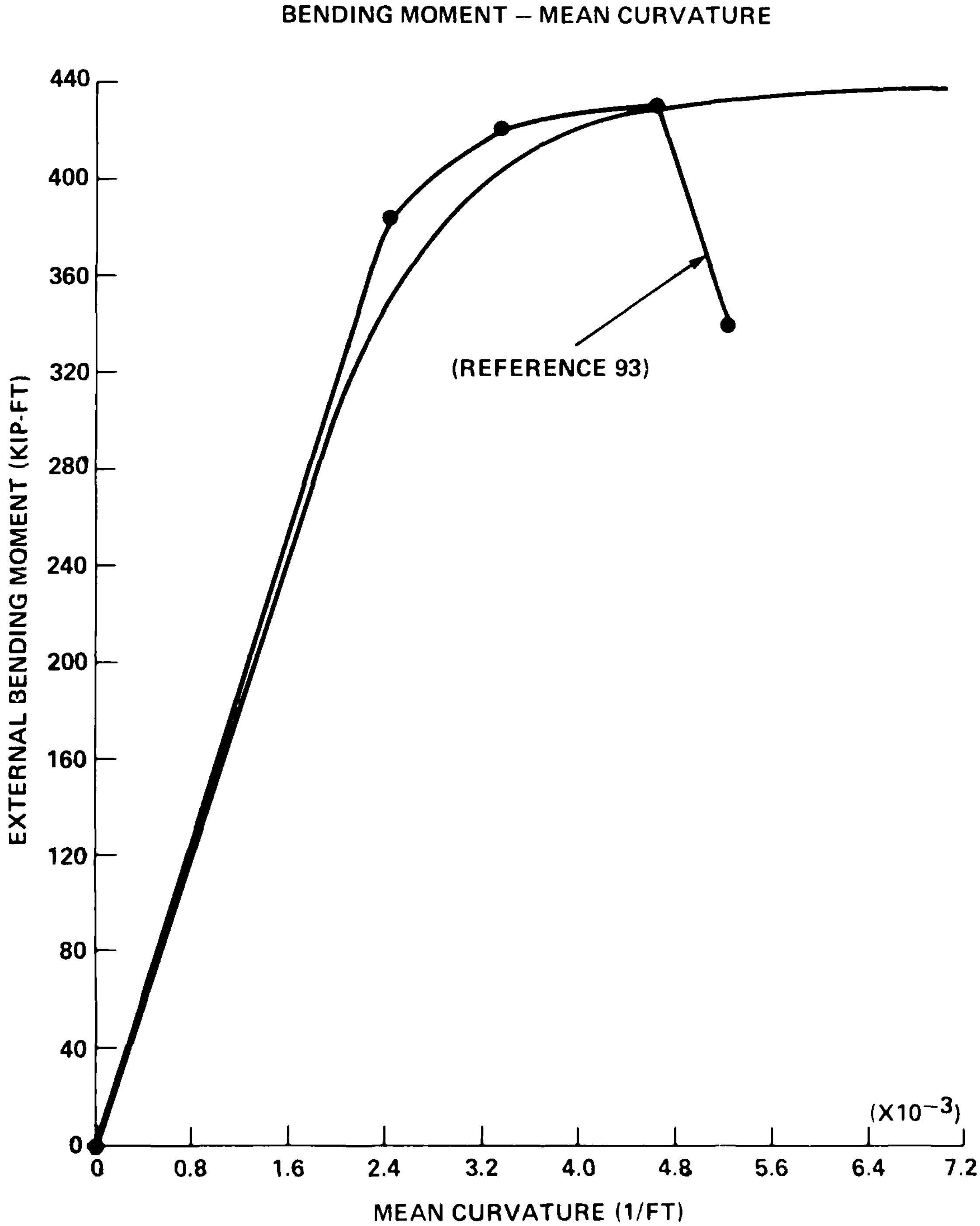

FIGURE 5. MOMENT – CURVATURE PLOTS FOR MODEL 20A

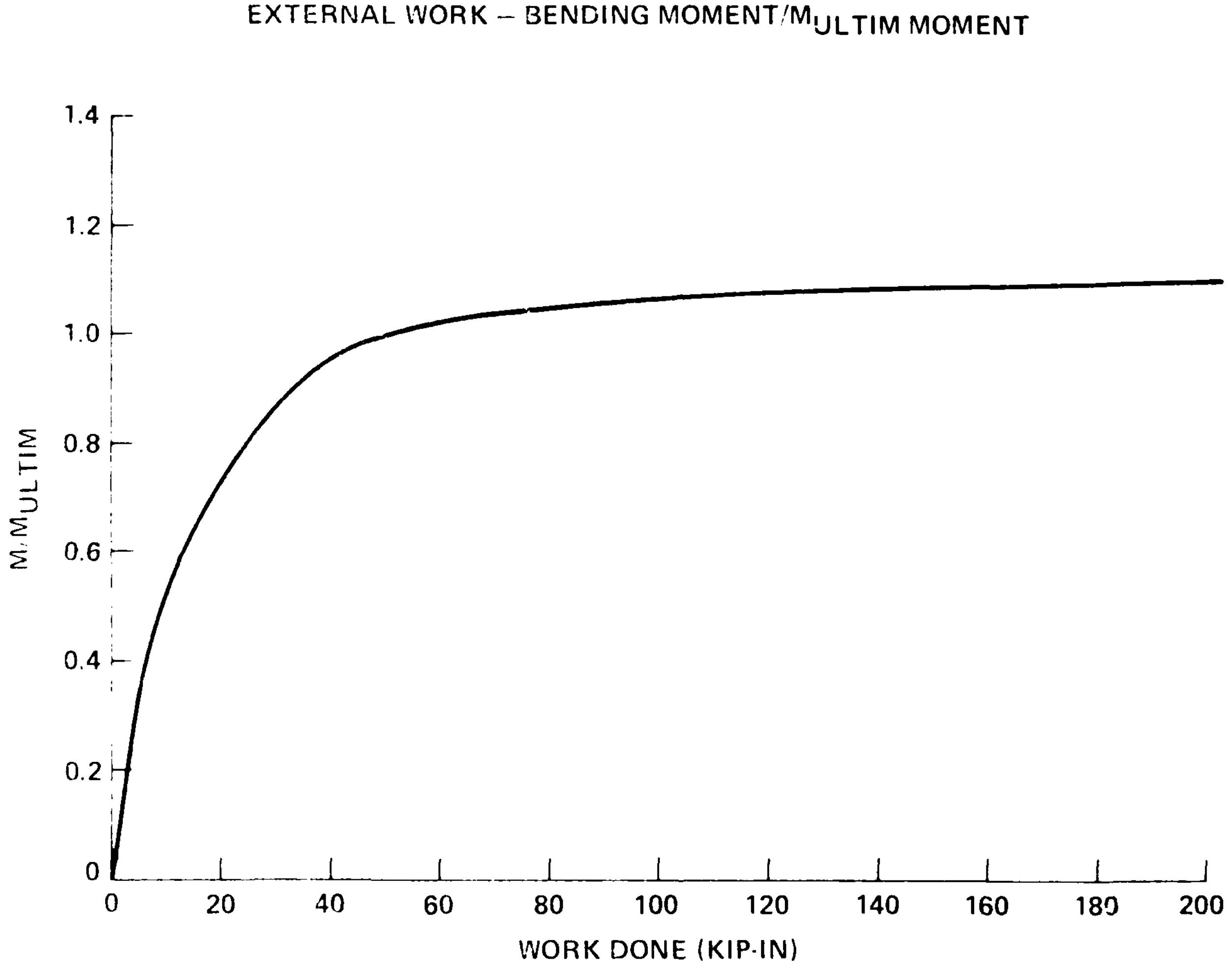

FIGURE 6. M/M_{ULTIM} WORK DONE (KIP-IN) FOR MODEL 10A

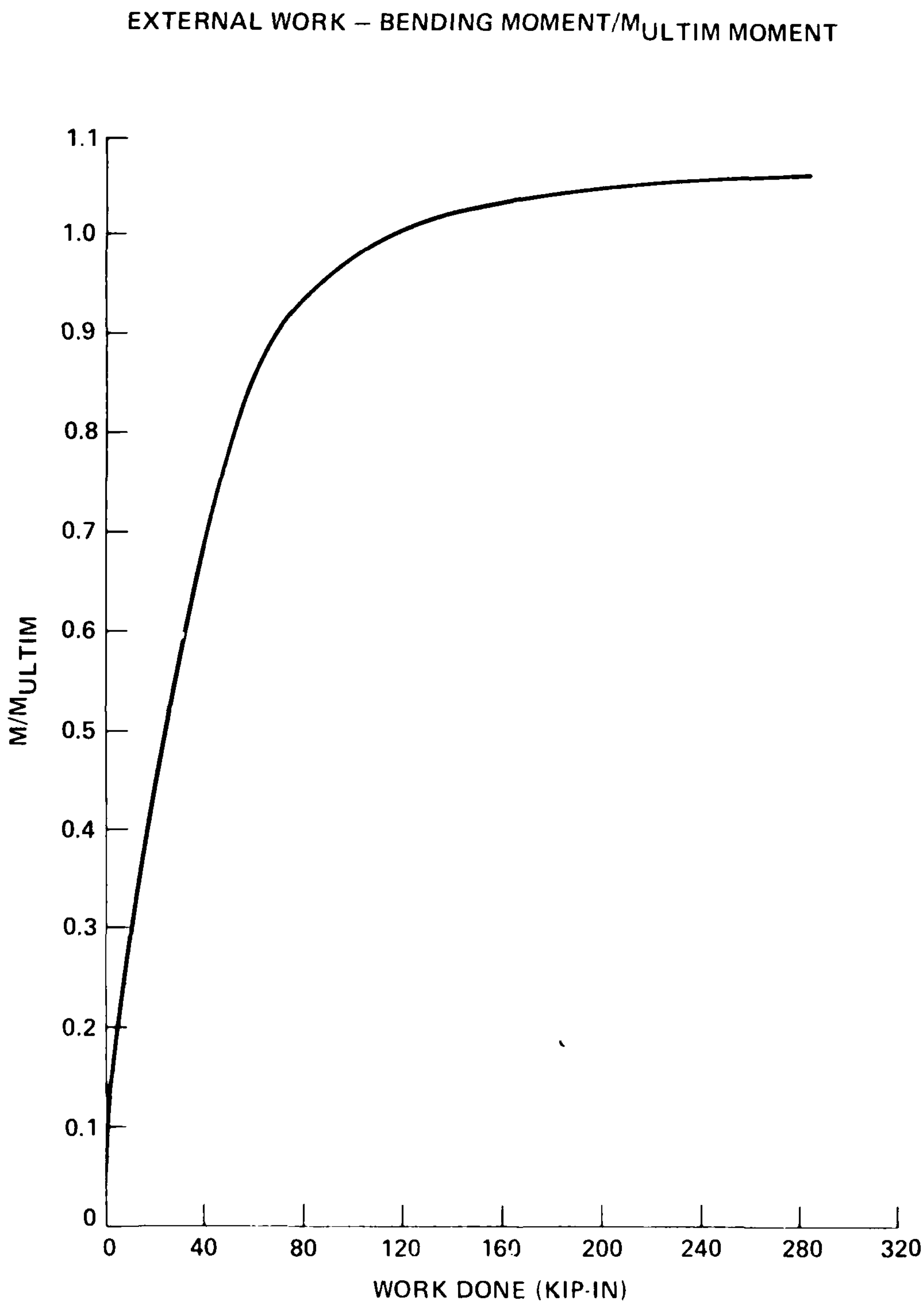

FIGURE 7. M/M_{ULTIM} WORK DONE (KIP·IN) FOR MODEL 16A

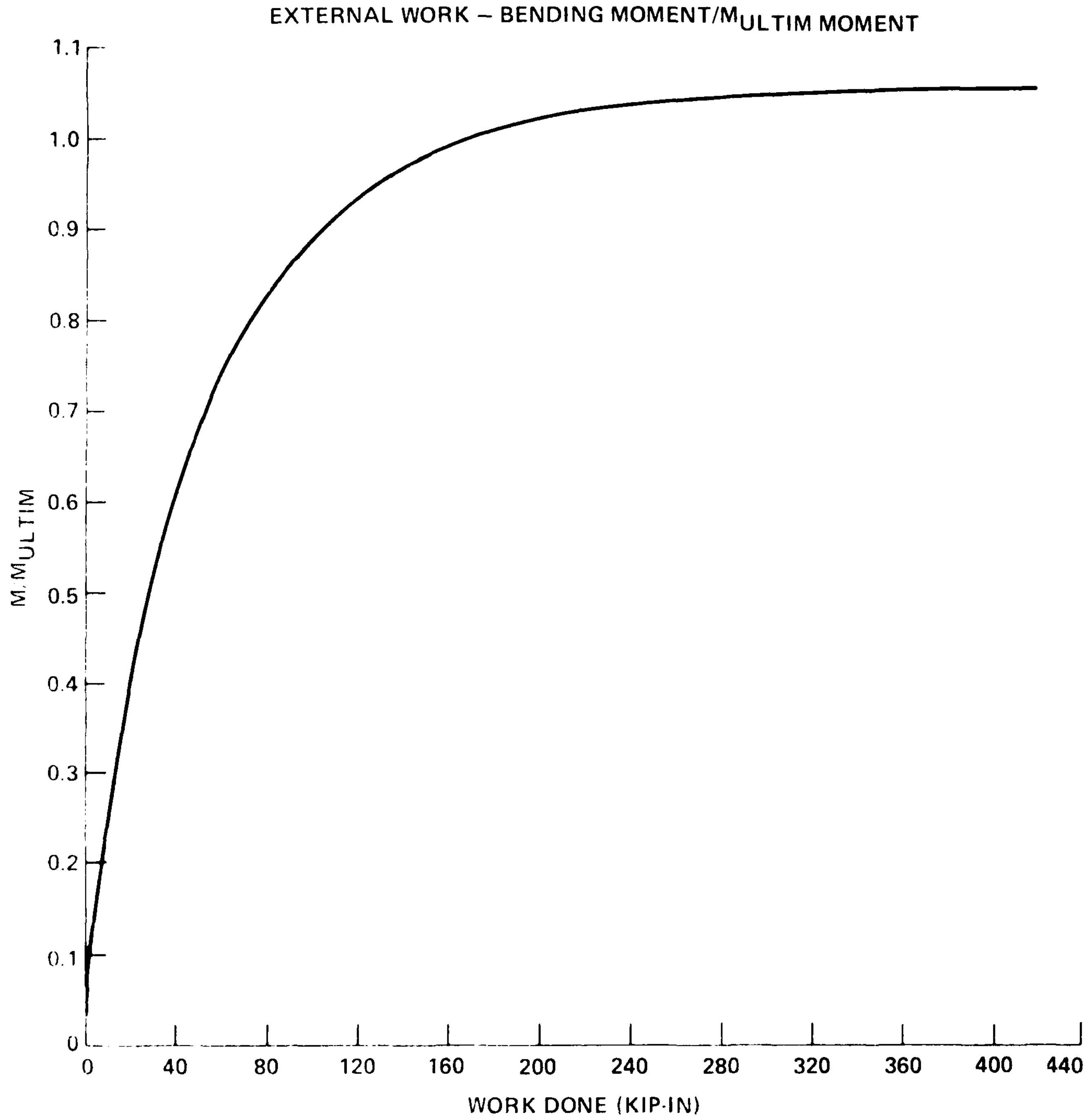

FIGURE 8. M/M_{ULTIM} WORK DONE (KIP-IN) FOR MODEL 20A

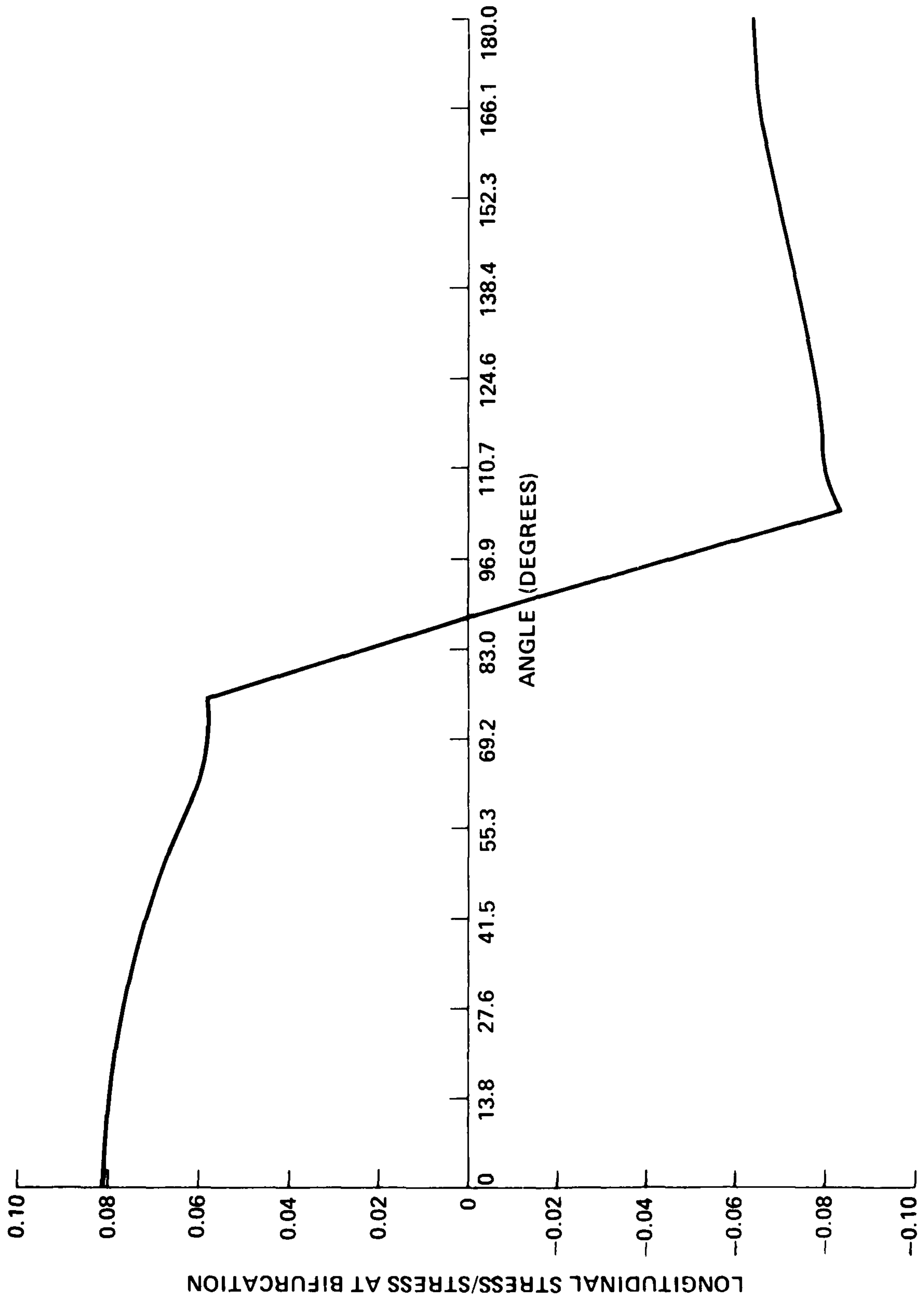

FIGURE 9. LONGITUDINAL STRESS (STEP 17) VERSUS ANGULAR POSITION FOR MODEL 10A

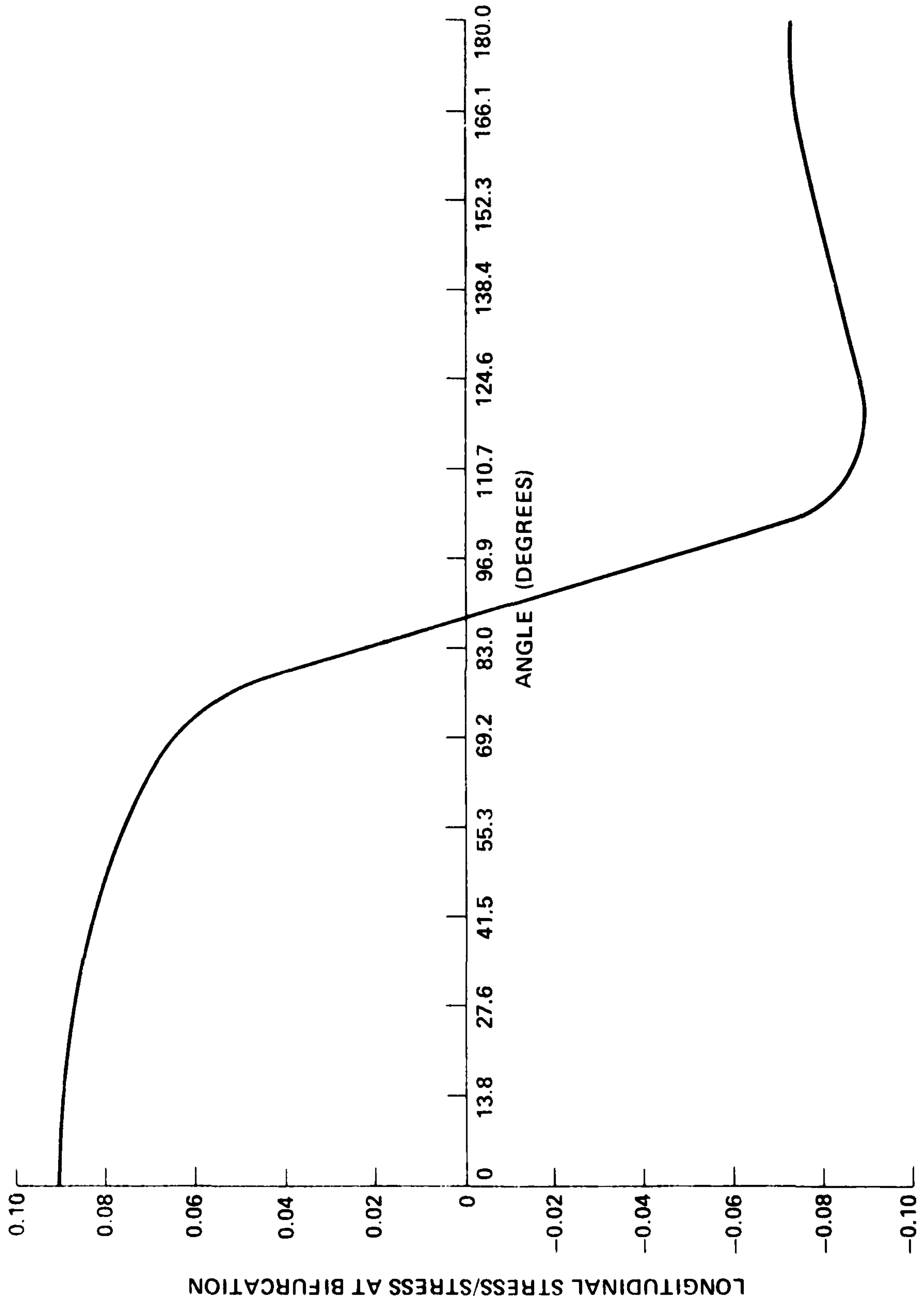

FIGURE 10. LONGITUDINAL STRESS (STEP 31) VERSUS ANGULAR POSITION FOR MODEL 16A

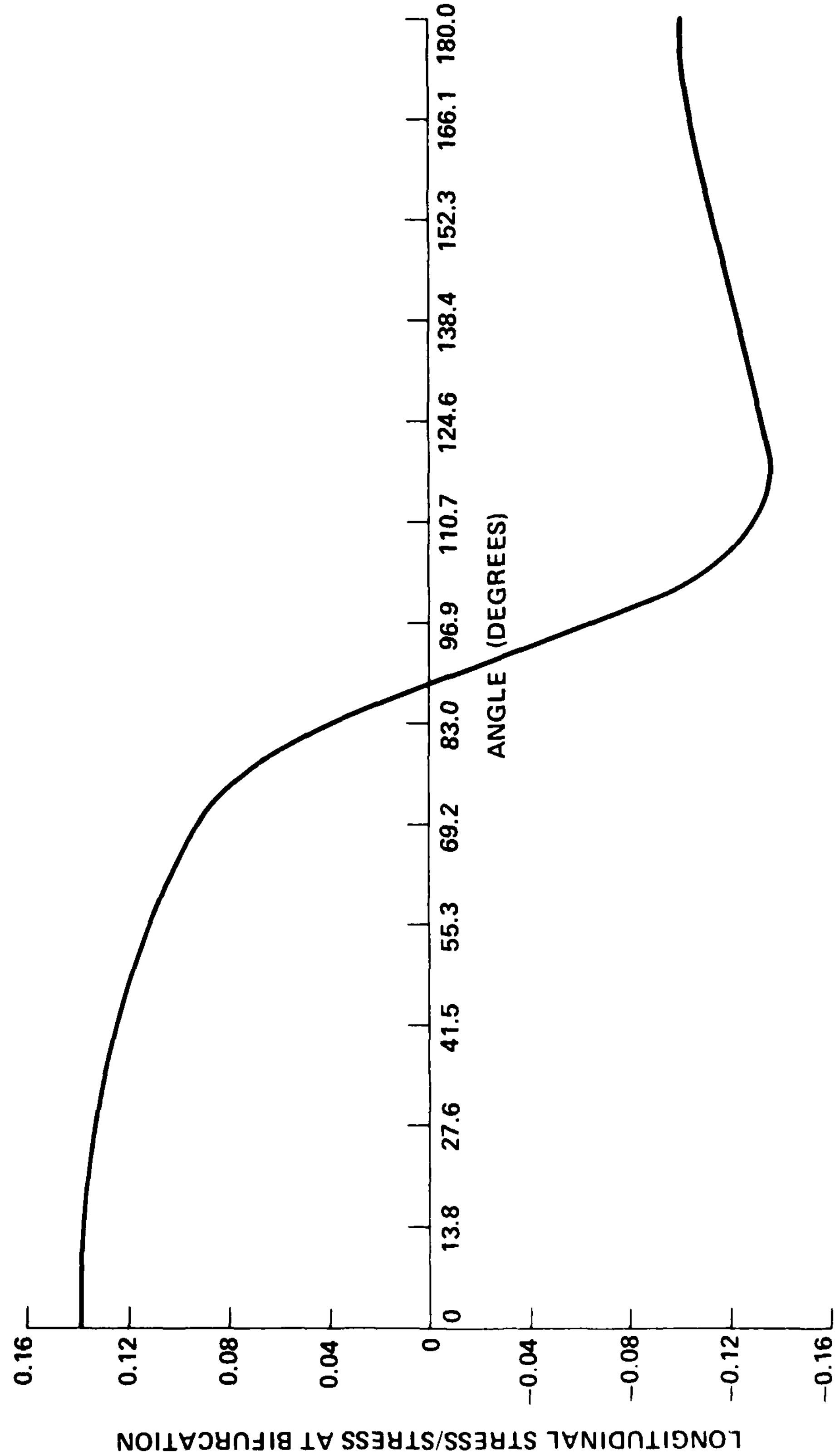

FIGURE 11. LONGITUDINAL STRESS (STEP 20) VERSUS ANGULAR POSITION FOR MODEL 20A

the half-section) is reduced (tension zone) or increased (compression zone) slightly before it assumes a linear form.

Figures 12 through 14 display the variation of the hoop stress parameter with angular location. The distribution of this stress over the half-section clearly indicates maximum compressive hoop stresses around the 90° location, with corresponding maximum tensile hoop stresses at 0° and 180°, respectively. These stresses, however, are smaller than the longitudinal membrane stresses by an order of magnitude. All stresses shown correspond to the final point of the moment-curvature plots.

Close examination of Figures 15 through 17 reveals that the M/M_{CR} vs. k/k_{CR} curves have a slope at the origin of approximately 1.0. This agrees fairly well with the initial slope predicted by Reissner's nonlinear theory[55] as well as Von Karman's linear analysis.[3] In the present notation, Reissner's relationship between M/M_{CR} and k/k_{CR} can be written as

$$M/M_{CR} = k/k_{CR}[1.0 - 0.5\,(k/k_{CR})^2 - (1/6)\,(k/k_{CR})^4 \;.\;.\;.\;.\;] \qquad (35)$$

with an obvious slope of 1.0 at the origin, maximum value of $M/M_{CR} = 0.5011$ at $k/k_{CR} = 0.71954$. The maximum value of 0.5011 is much higher than both experimental and numerical results, showing the effects of plasticity which Reissner's theory does not account for. Note that plots of $\mu = (M_{EXT}/M_0)$ versus work done (Figures 6 through 8) clearly display that ultimate moment is reached at $\mu \approx 1$ as predicted by beam plastic theory. Actually, it exceeds $\mu = 1$ by about 10 percent.

Figure 18 displays the deformed and undeformed profiles of cylindrical model 20A. Figure 19 represents the corresponding deformed and undeformed profiles of the imperfect version of model 20A, which from now on will be referred to as model 20AI. Figure 20 is an enlargement of the cross-sections at midlength before and after deformation of model 20AI. Figure 21 shows the moment-curvature plots of model 20AI compared with the experimental data (circled points). Similarly, Figures 22 through 25 show results for model 20AI of the following pairs of variables:

$\mu = M_{EXT}/M_0$ (or $M/M_{ULTIMATE}$) $\sim$ Work Done (kip-in.)

$\sigma^{LONG}_{INPLANE}/\sigma_{CR} \sim$ Angular Position

$\sigma^{HOOP}/\sigma_{CR} \sim$ Angular Position and $M/M_{CR} \sim k/k_{CR}$

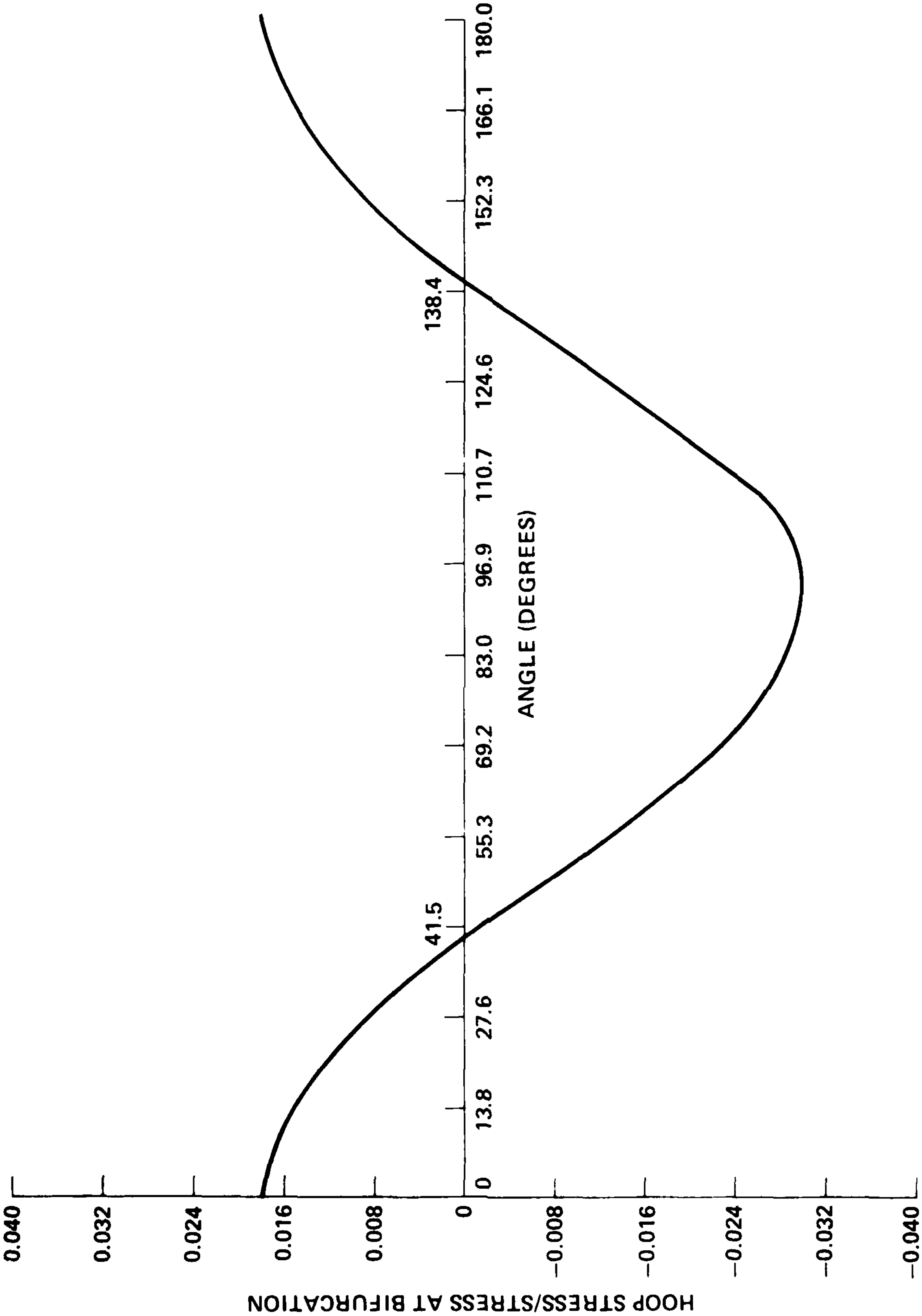

FIGURE 12. HOOP STRESS DISTRIBUTION (STEP 17) VERSUS ANGULAR POSITION FOR MODEL 10A

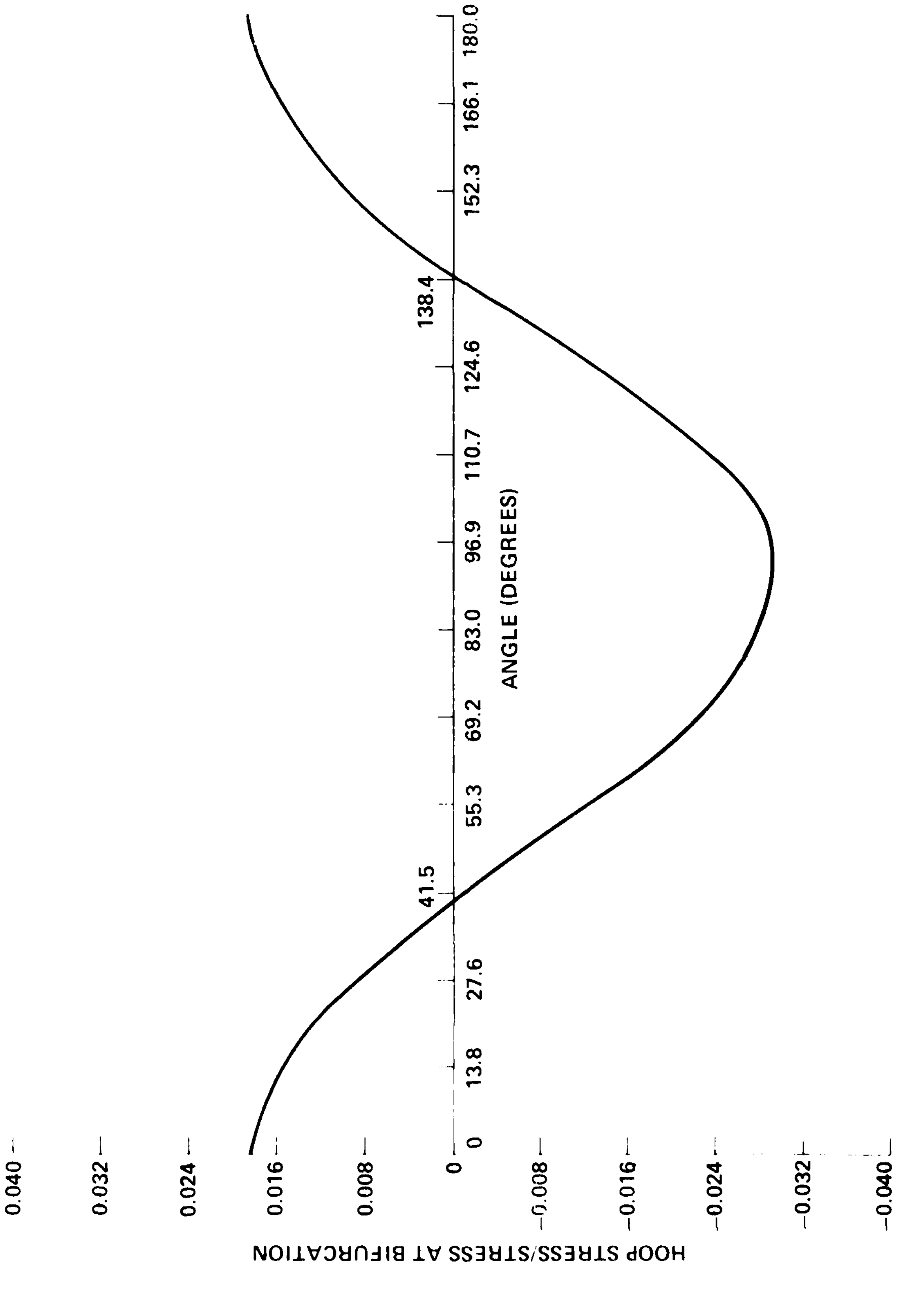

FIGURE 13. HOOP STRESS DISTRIBUTION (STEP 31) VERSUS ANGULAR POSITION FOR MODEL 16A

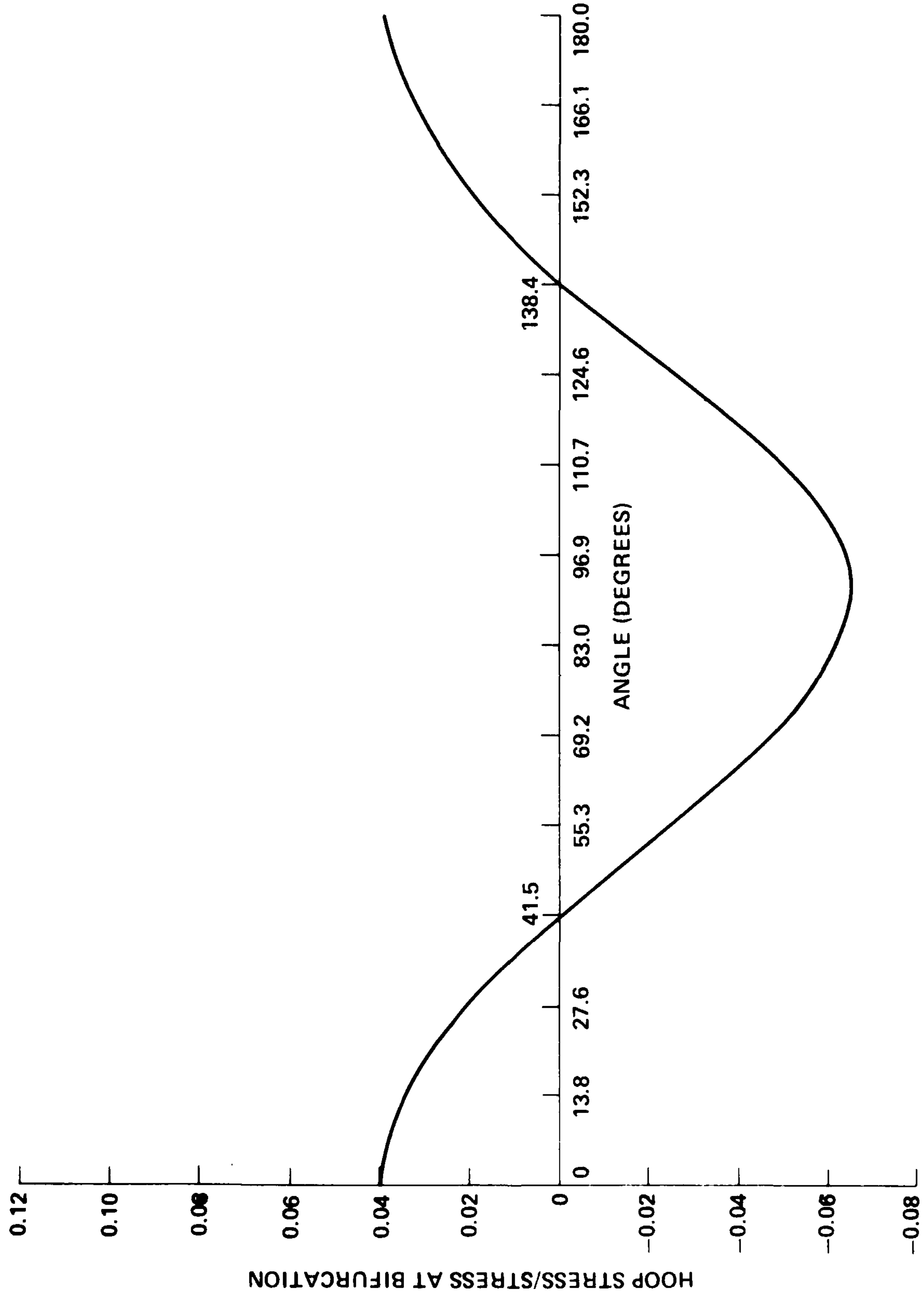

FIGURE 14. HOOP STRESS DISTRIBUTION (STEP 20) VERSUS ANGULAR POSITION FOR MODEL 20A

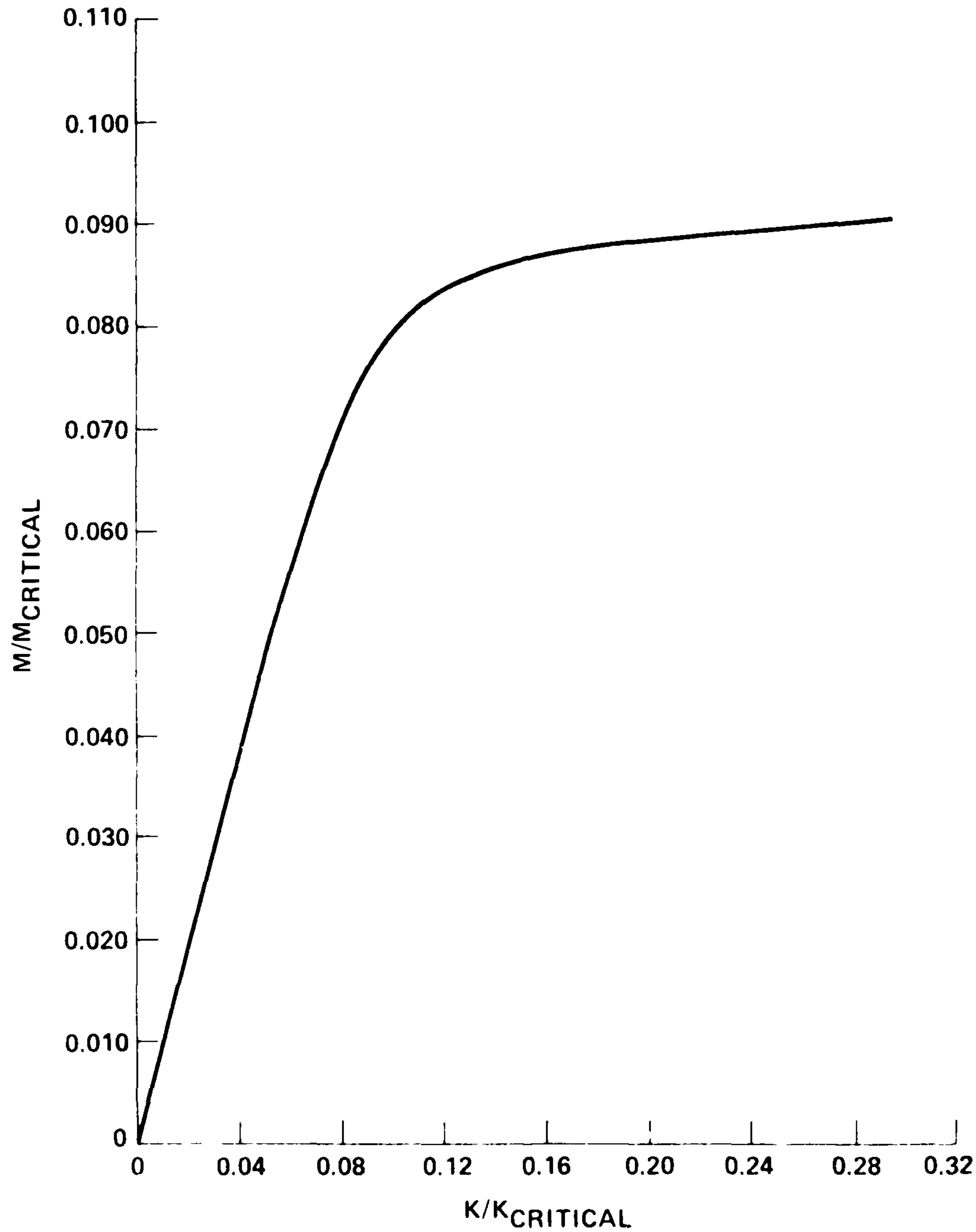

FIGURE 15. $M/M_{CRITICAL}$ VERSUS $K/K_{CRITICAL}$ FOR MODEL 10A

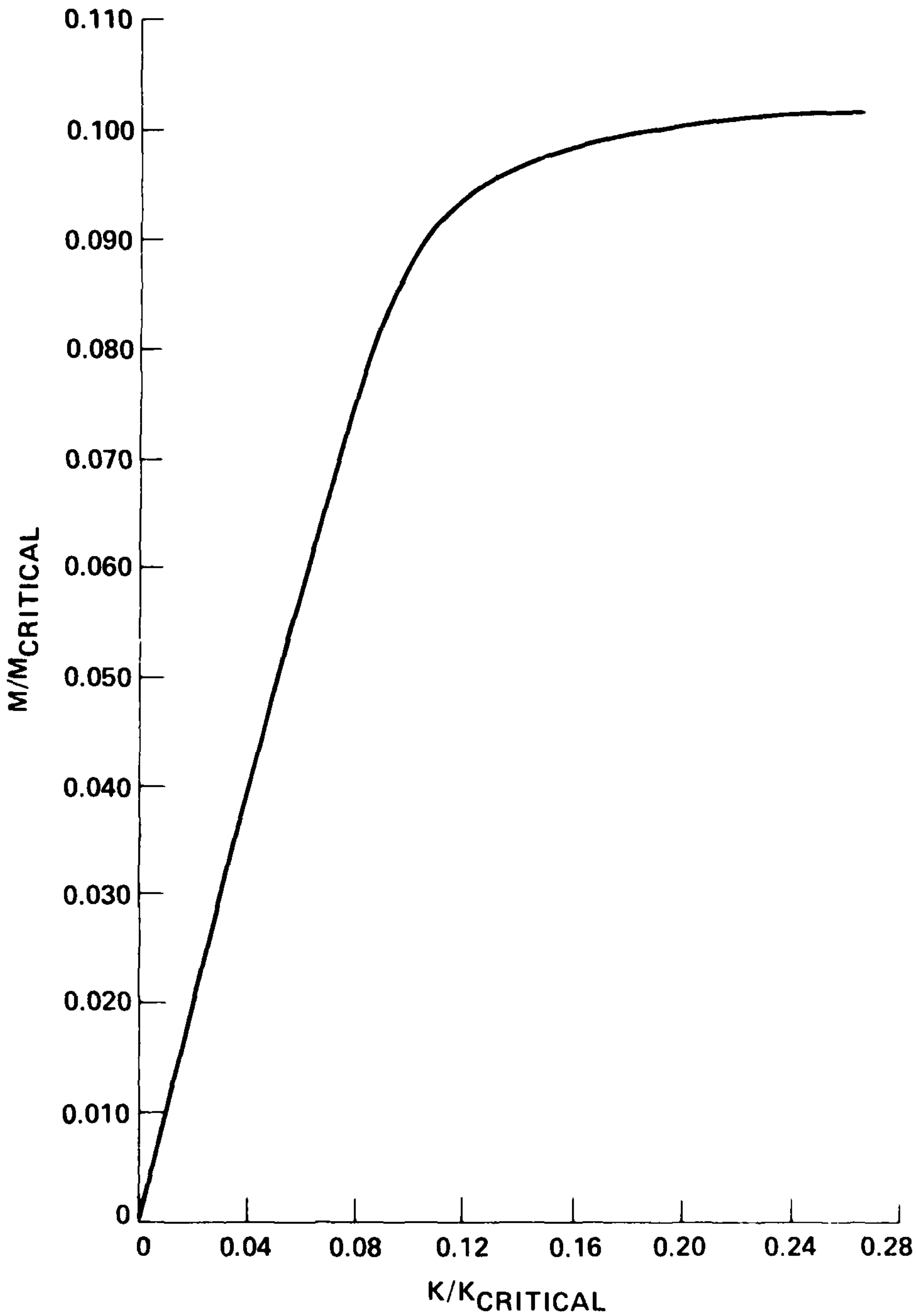

FIGURE 16. $M/M_{CRITICAL}$ VERSUS $K/K_{CRITICAL}$ FOR MODEL 16A

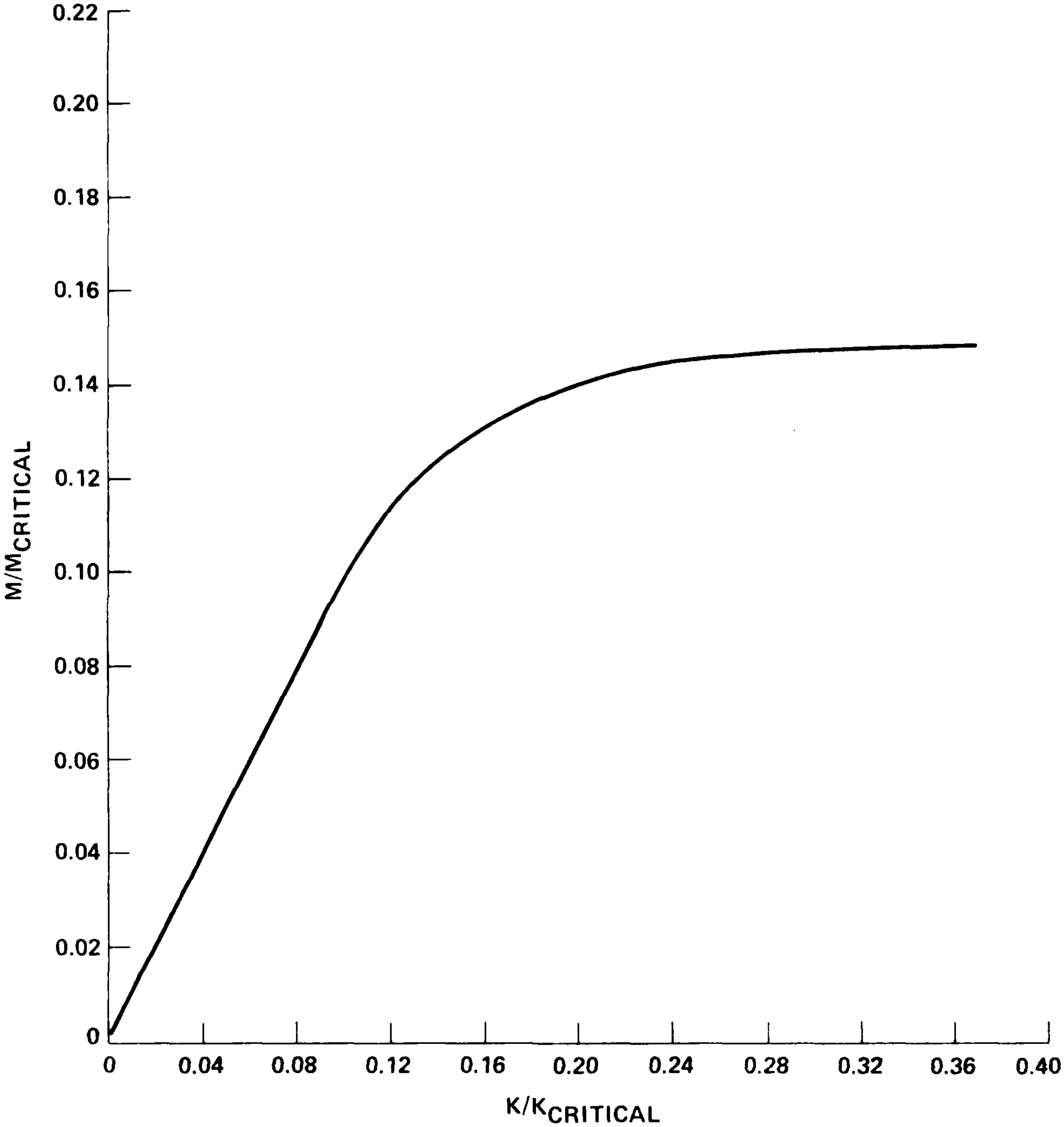

FIGURE 17. $M/M_{CRITICAL}$ VERSUS $K/K_{CRITICAL}$ FOR MODEL 20A

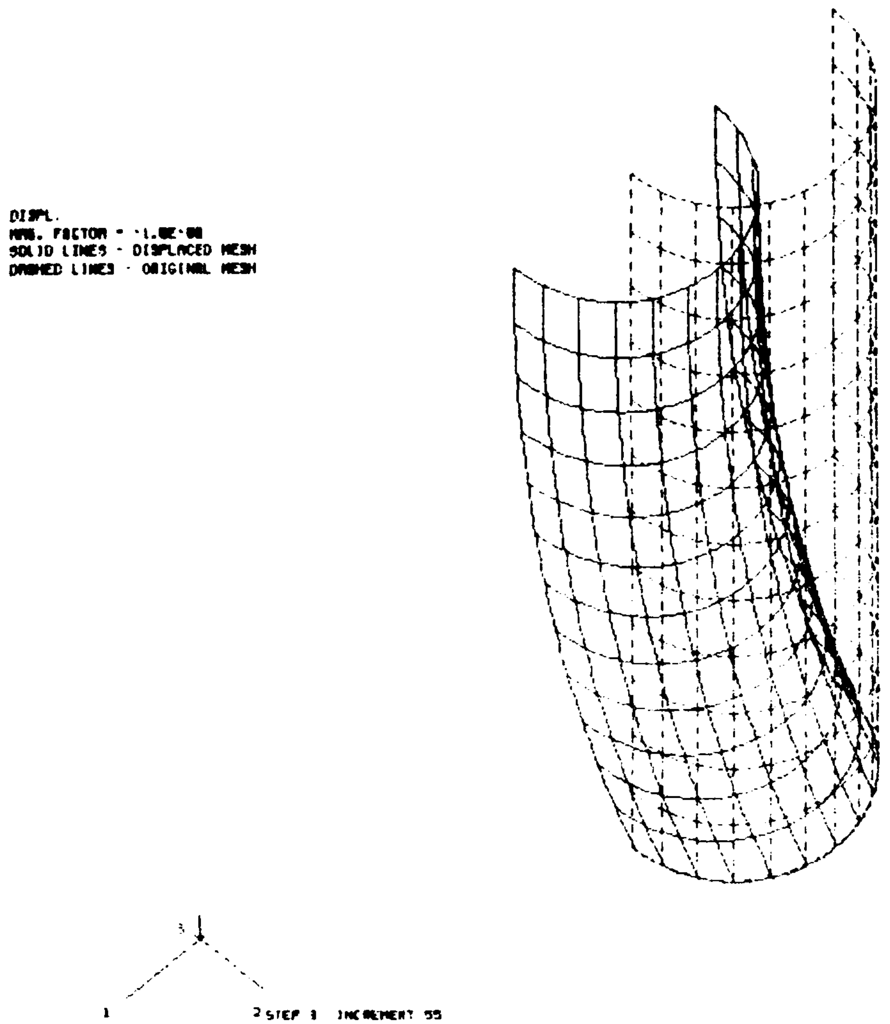

FIGURE 18. CYLINDRICAL SHELL (MODEL 20A) SUBJECT TO END BENDING MOMENT VIEWED FROM 100″,100″,500″ AT STEP 3, INCREMENT 55

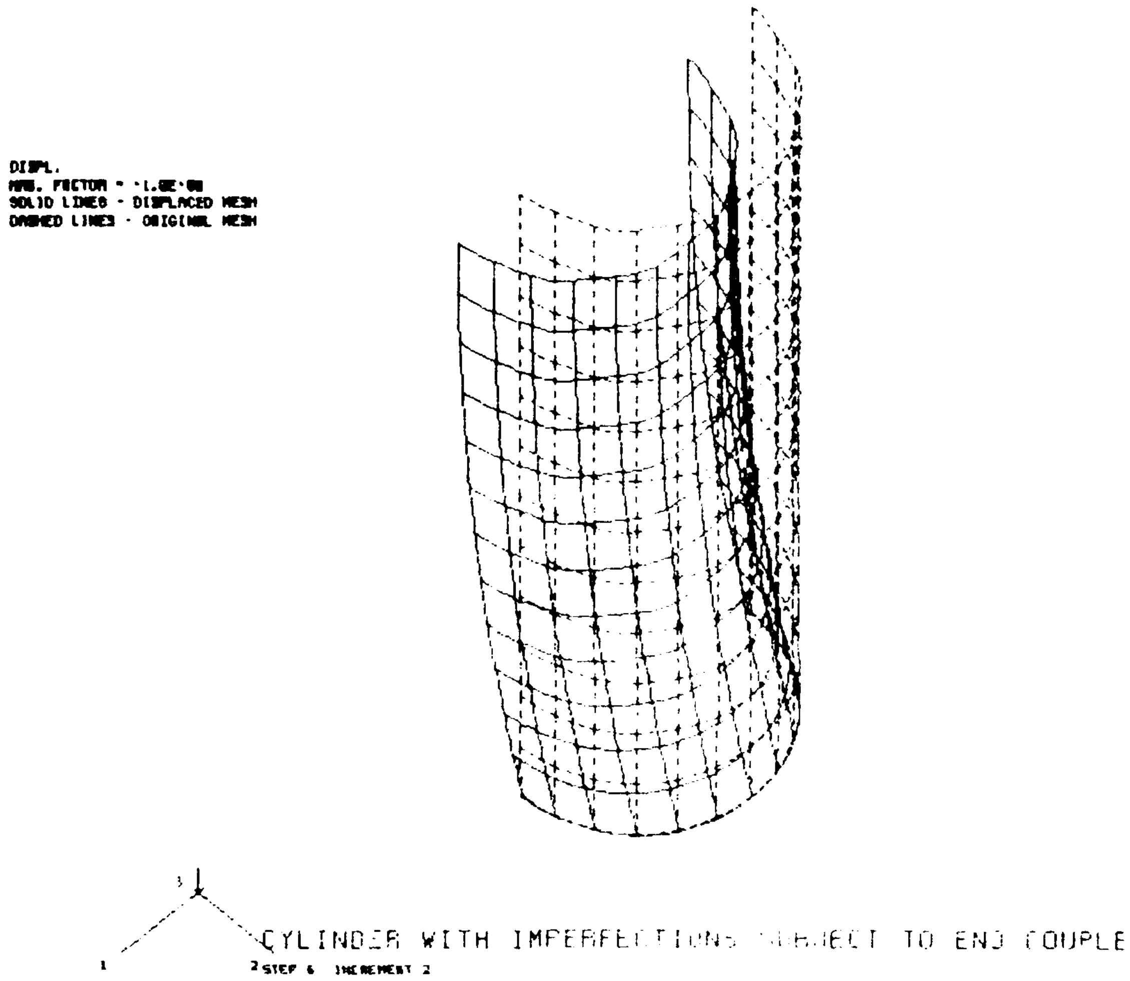

FIGURE 19. IMPERFECT CYLINDRICAL SHELL (VARIANT OF MODEL 20A) SUBJECT TO END BENDING MOMENT VIEWED FROM 100″,100″,500″ AT STEP 6, INCREMENT 2

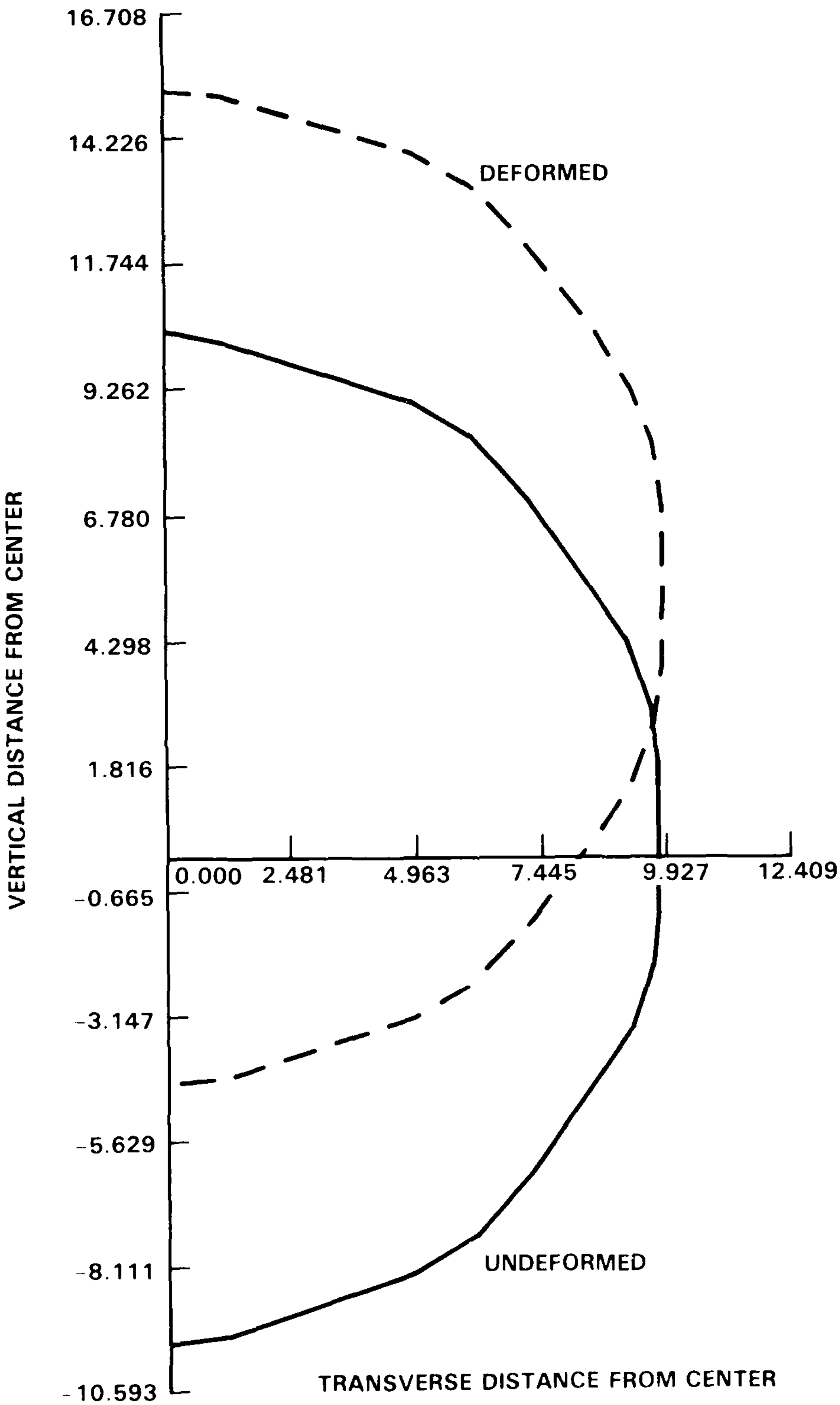

FIGURE 20. UNDEFORMED AND DEFORMED HALF-CROSS SECTION OF IMPERFECT VERSION OF MODEL 20A AT MIDLENGTH

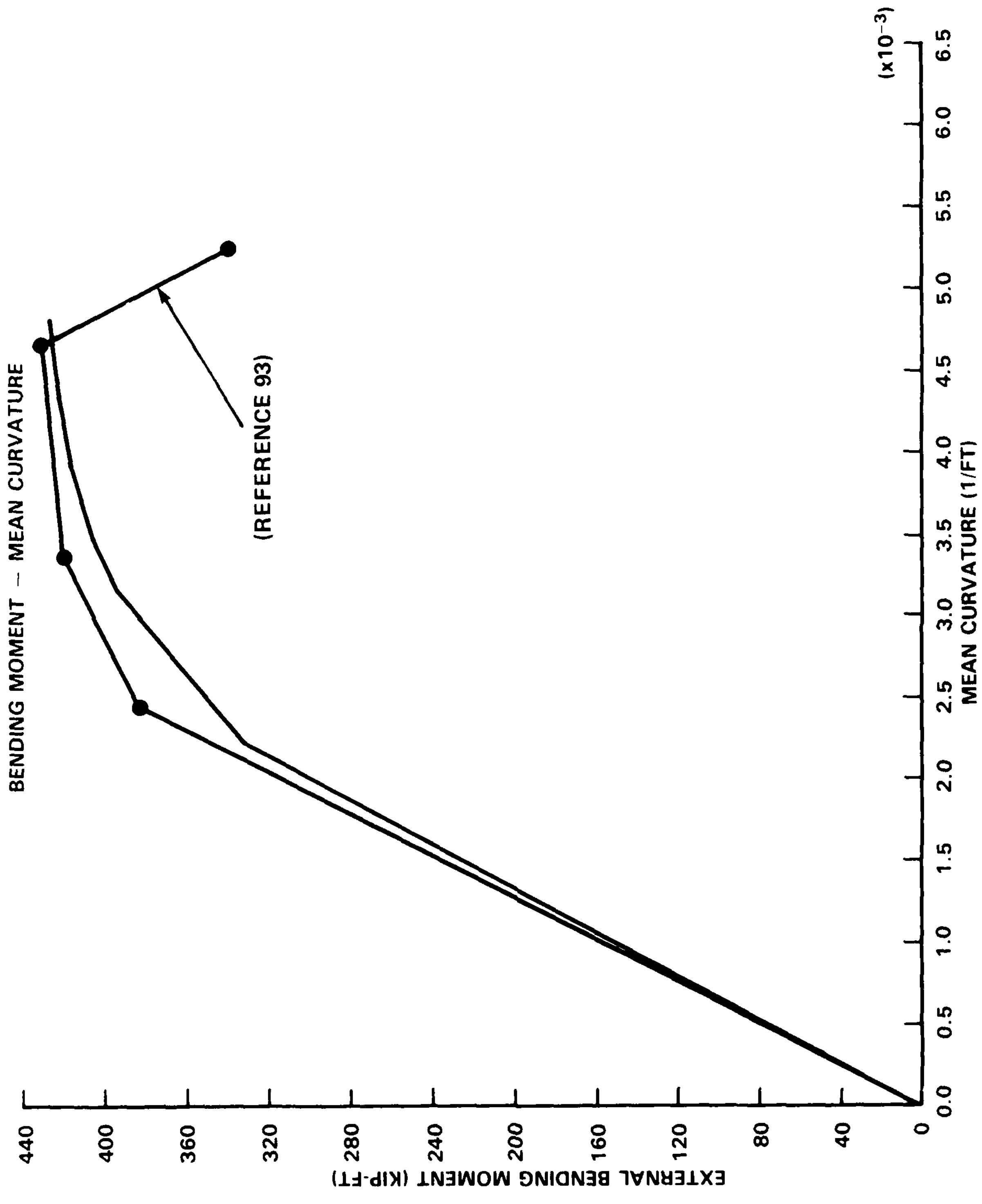

FIGURE 21. MOMENT-CURVATURE PLOTS FOR IMPERFECT VERSION OF MODEL 20A

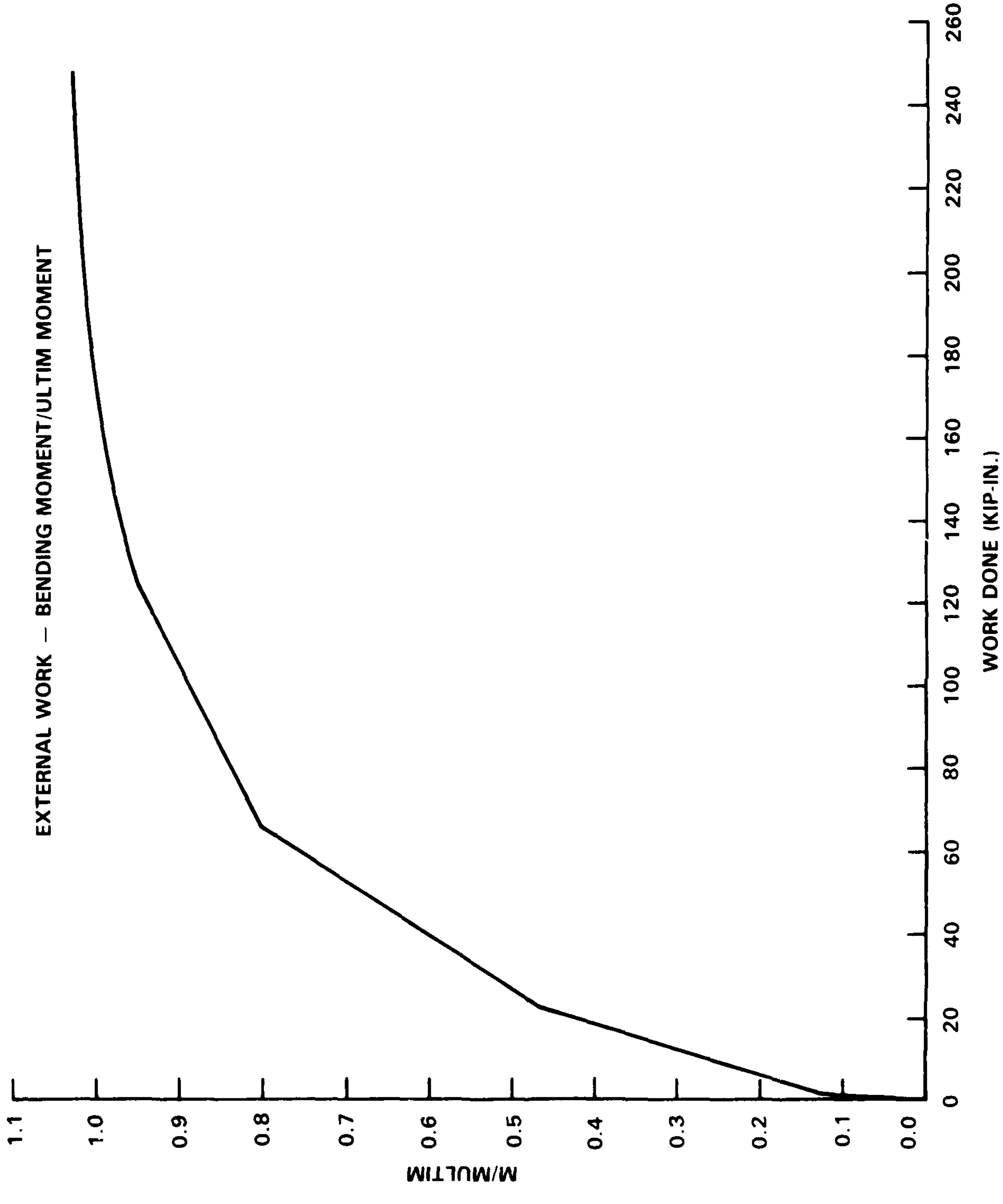

FIGURE 22. M/MULTIM ~ WORK DONE (KIP-IN.) FOR IMPERFECT VERSION OF MODEL 20A

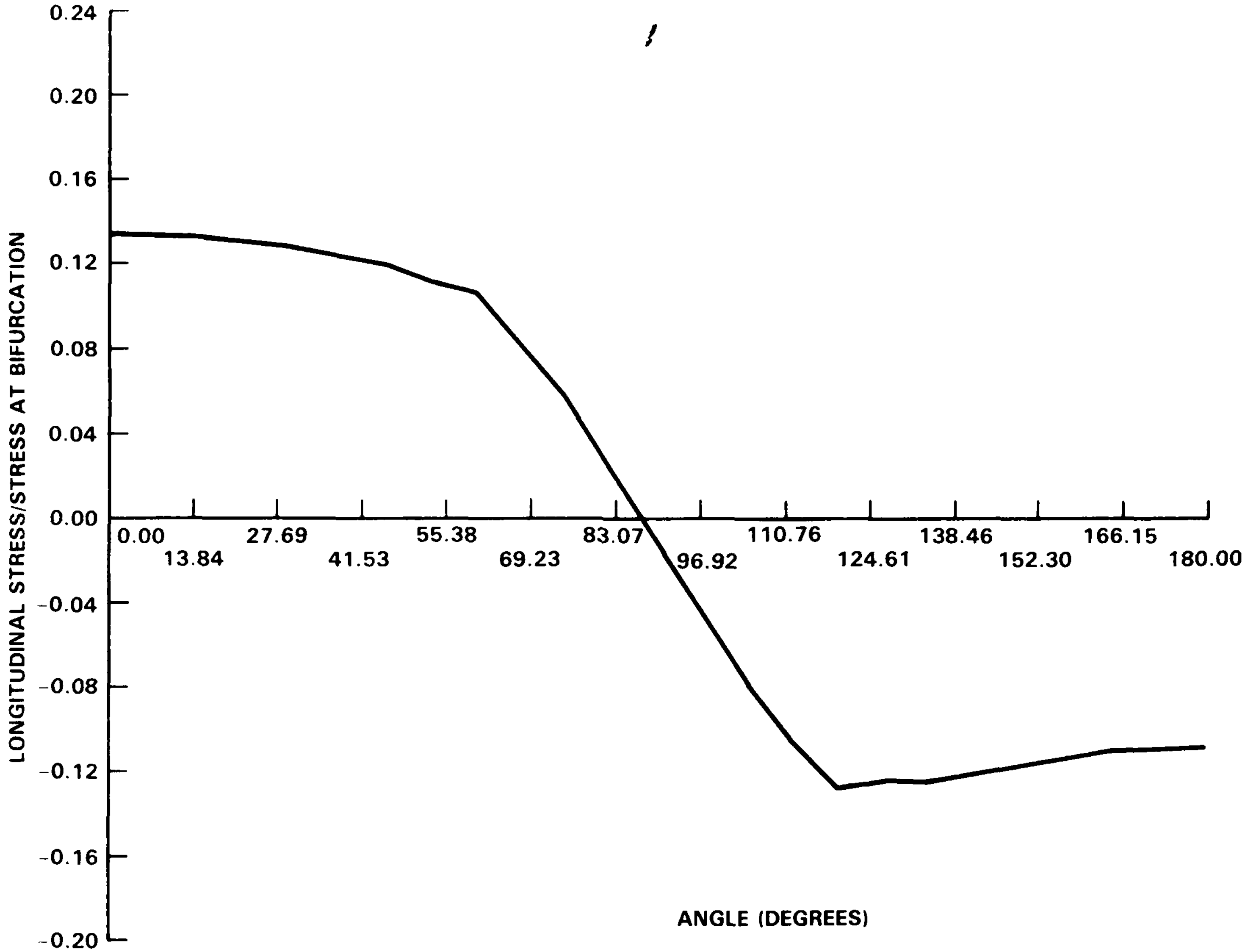

FIGURE 23. LONGITUDINAL STRESS (STEP 6, INCREMENT 2, WHICH CORRESPONDS TO FINAL PLOTTED POINT ON FIGURE 21) VERSUS ANGULAR POSITION FOR IMPERFECT VERSION OF MODEL 20A

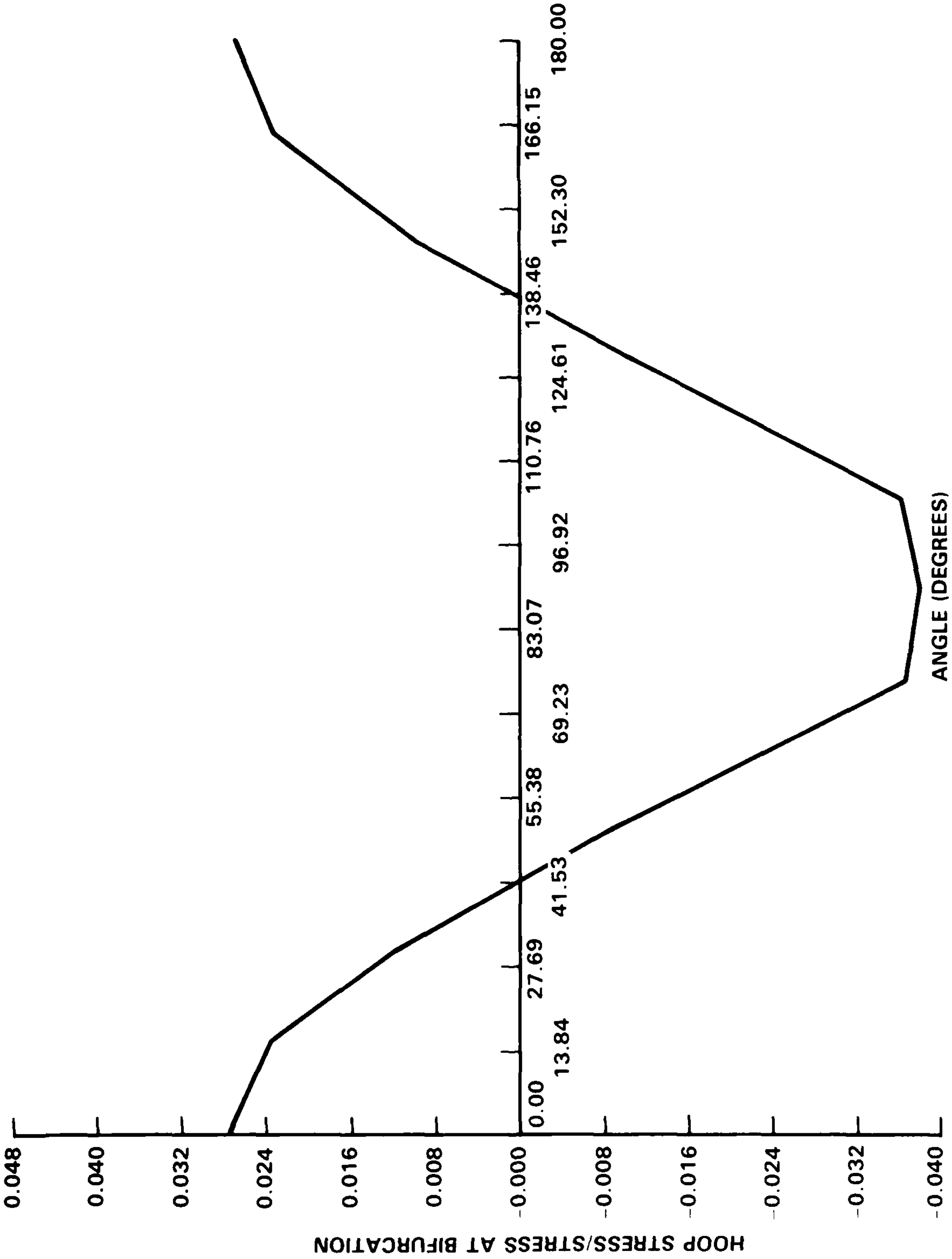

FIGURE 24. HOOP STRESS DISTRIBUTION (STEP 6, INCREMENT 2, WHICH CORRESPONDS TO FINAL PLOTTED POINT ON FIGURE 21) VERSUS ANGULAR POSITION FOR IMPERFECT VERSION OF MODEL 20A

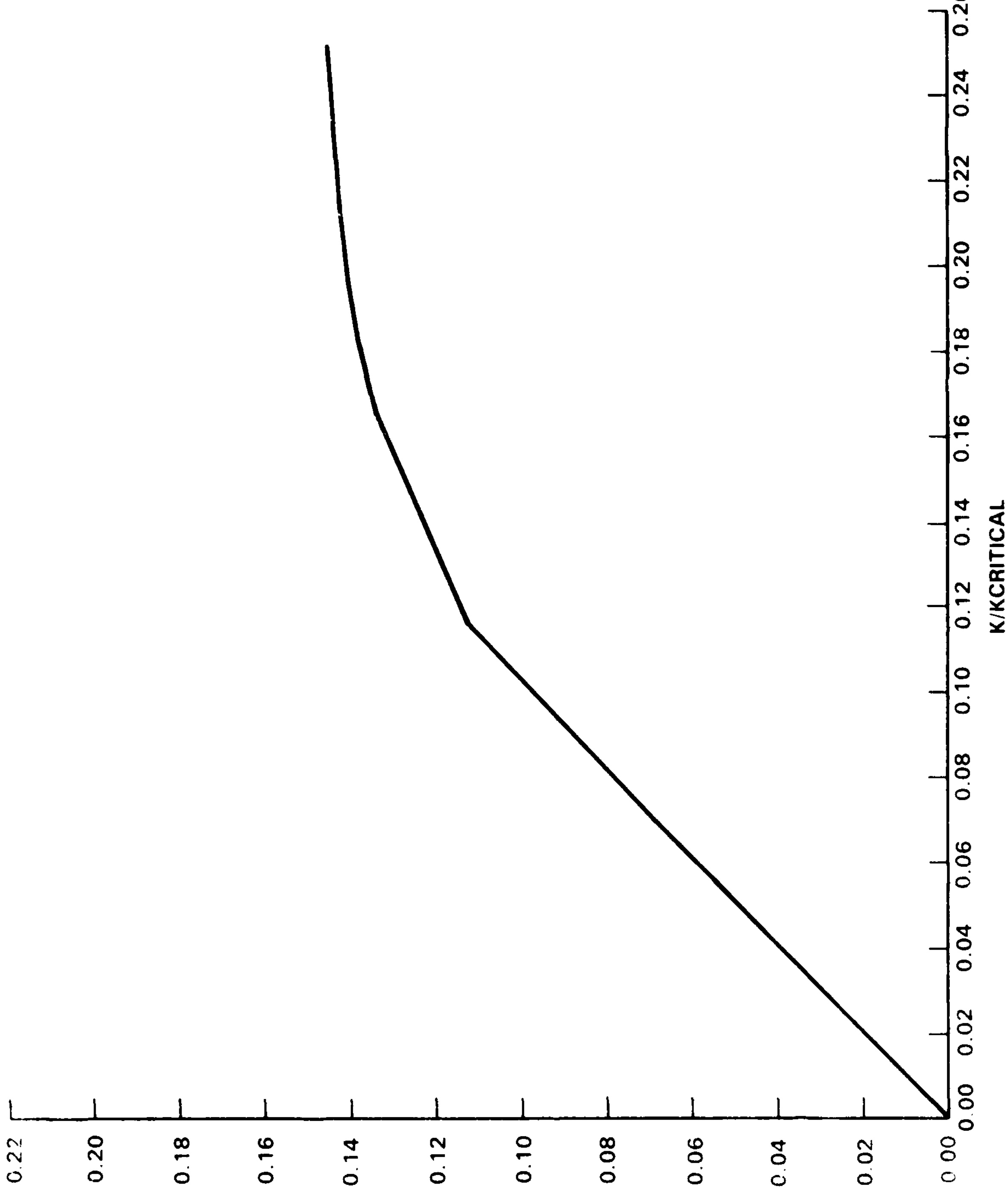

FIGURE 25. M/MCRITICAL VERSUS K/KCRITICAL FOR IMPERFECT VERSION OF MODEL 20A

At this point, note that the relevant figures corresponding to the perfect model 20A are 8, 11, 14, and 17, respectively. The imperfection in the radial displacement of the original surface from the mean radius R of imperfect model 20AI varied according to the formula

$$h \sin\left(\frac{\pi z}{L}\right) \cos(10\theta)$$

Imperfect model 20AI was generated with one-half wave axially and 10 waves peripherally.

Figure 26 presents superimposed moment-curvature curves for both models 20A and 20AI. Notice that since they are comparatively thick and fail by plastification, unlike ovalization or bifurcation failure, they are not imperfection sensitive. The response of the imperfect model 20AI is very similar to the perfect one.

Table 3 summarizes digitized results pertaining to bending moment, angle of rotation at the end, where the external load is applied, as well as strain energy, work done, and plastic dissipation for model 20A. Note that because of an existing error in ABAQUS, concerning how energies are computed, strain energy and plastic dissipation do not agree exactly with the work done (0.120489 + 0.290966 = 0.411455 compared with 0.417864). In fact, this difference decreases as we march along the load-deformation curve. Table 4 gives the stress distribution for load step 20 of model 20A. Tables 5 and 6 give the corresponding information for model 20AI, and Tables 7 and 8 give the actual points plotted in Figure 26 for both models 20A and 20AI.

Finally, a fine and extremely important point pertaining to the modeling issue must be addressed. The experimental set up involved the analysis of a three span beam (in all cases) subject to vertical self-equilibrating shear loads, to simulate overall bending over the two end spans. The middle span had no loads applied. In this analysis, one end span and half of the center span (symmetry) were modeled. A rotation was enforced through the "auxiliary node" concept and the MPC constraints. Subsequent computations without the "additional" end span gave a slightly different response.

Consequently, what constitutes an adequate additional span to be included for proper response has not been determined but is of major importance in this analysis. In addition, to complete studies on the bend-buckling modeling of cylindrical shells, "short" and "medium" length tubes with or without ring stiffeners must be addressed.

In closing this discussion it must be stressed that, by neglecting inertia effects, a reasonably successful first approximation of the problem of a long straight circular cylinder shell subject to end couples has been developed.

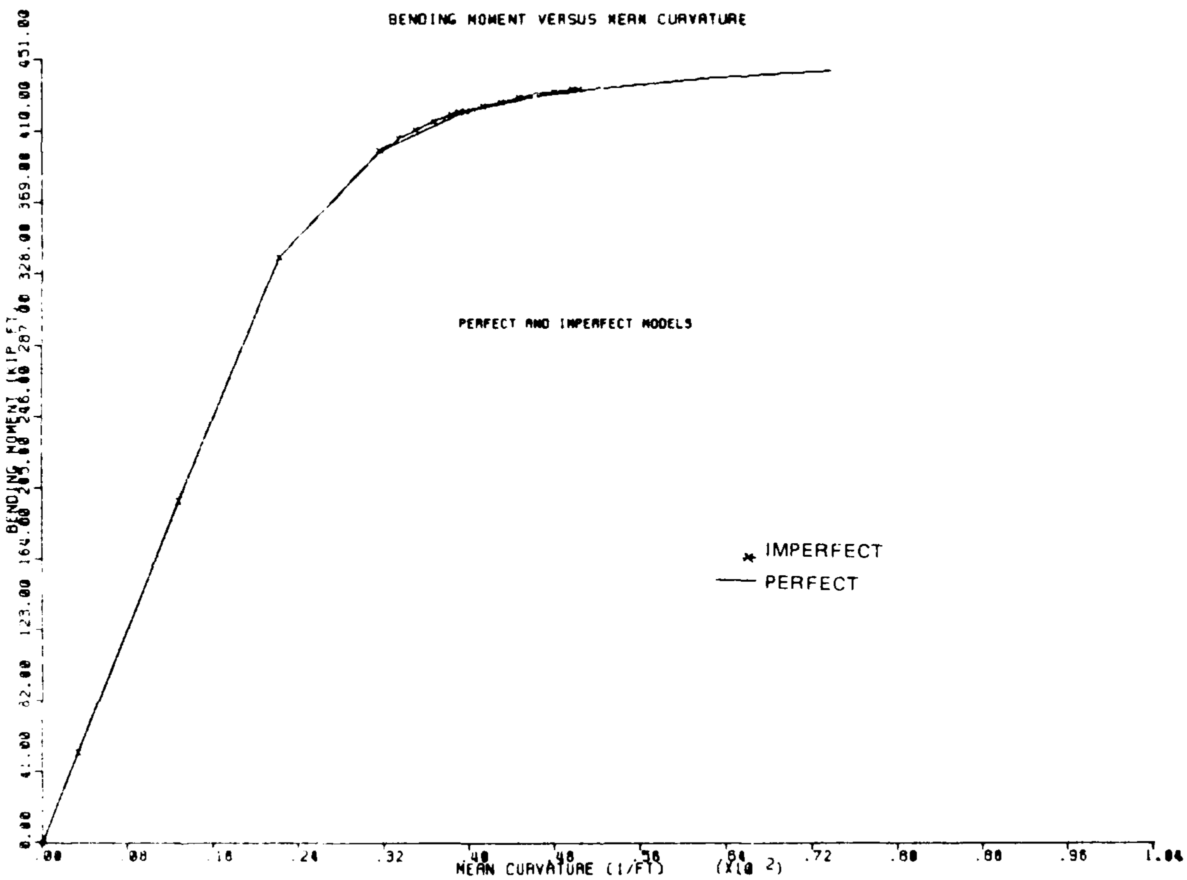

FIGURE 26. BENDING MOMENT DISTRIBUTION VERSUS MEAN CURVATURE FOR BOTH PERFECT AND IMPERFECT VERSIONS OF MODEL 20A

TABLE 3. POST-PROCESSING INFORMATION FROM ABAQUS FOR MODEL 20A

STEP NO.	TOTAL BENDING MOMENT AT AUXILIARY NODE (LB-IN)	ROTATION ABOUT GLOBAL Y-AXIS (DEGREES)
1	0.623339E+06	0.261412E+00
2	0.236641E+07	0.986562E+00
3	0.404768E+07	0.171171E+01
4	0.478507E+07	0.243686E+01
5	0.505084E+07	0.305324E+01
6	0.509211E+07	0.323453E+01
7	0.513190E+07	0.341581E+01
8	0.516604E+07	0.359710E+01
9	0.518940E+07	0.377839E+01
10	0.520879E+07	0.395968E+01
11	0.522644E+07	0.414096E+01
12	0.524388E+07	0.432225E+01
13	0.526043E+07	0.450354E+01
14	0.527557E+07	0.468482E+01
15	0.528840E+07	0.486611E+01
16	0.530105E+07	0.504740E+01
17	0.531390E+07	0.522869E+01
18	0.532418E+07	0.540997E+01
19	0.533412E+07	0.559126E+01
20	0.534003E+07	0.569097E+01

INCREMENT NO	STRAIN ENERGY	EXTERNAL WORK DONE	PLASTIC DISSIPATION	ABAQUS STEP	ABAQUS INCREMENT
1	0.143355E+04	0.178939E+04	0.000000E+00	1	5
2	0.203964E+05	0.229520E+05	0.000000E+00	1	10
3	0.600974E+05	0.659929E+05	0.111234E+04	1	15
4	0.559185E+05	0.123413E+06	0.316443E+05	1	20
5	0.982309E+05	0.176822E+06	0.725563E+05	1	25
6	0.100586E+06	0.192983E+06	0.862532E+05	1	30
7	0.102974E+06	0.209070E+06	0.100034E+06	1	35
8	0.105190E+06	0.225375E+06	0.114103E+06	1	40
9	0.106832E+06	0.241766E+06	0.128635E+06	1	45
10	0.108307E+06	0.256224E+06	0.143801E+06	1	50
11	0.109742E+06	0.274738E+06	0.158862E+06	1	55
12	0.111203E+06	0.291308E+06	0.173945E+06	1	60
13	0.112557E+06	0.307932E+06	0.189095E+06	1	65
14	0.114052E+06	0.324605E+06	0.204348E+06	1	70
15	0.115345E+06	0.341322E+06	0.217743E+06	1	75
16	0.116649E+06	0.358079E+06	0.235162E+06	1	80
17	0.117940E+06	0.374876E+06	0.250633E+06	1	85
18	0.118980E+06	0.391710E+06	0.266388E+06	1	90
19	0.119954E+06	0.408575E+06	0.282236E+06	1	95
20	0.120489E+06	0.417864E+06	0.290966E+06	1	100

TABLE 4. POST-PROCESSING INFORMATION (STRESS DISTRIBUTION) FROM ABAQUS FOR MODEL 20A

STEP NO. 20 FOR STRESSES

ANGLE (DEGREES)	LONGITUDINAL MEMBRANE STRESS (PSI)	NONDIMENSIONAL MEMBRANE LONGITUDINAL STRESS	HOOP STRESS (PSI)	NONDIMENSIONAL HOOP STRESS
0.000	0.632128E+05	0.139699E+00	0.182834E+05	0.404057E-01
7.702	0.627863E+05	0.138756E+00	0.169217E+05	0.373965E-01
15.331	0.623718E+05	0.137840E+00	0.155168E+05	0.342917E-01
23.030	0.609195E+05	0.134630E+00	0.116398E+05	0.257237E-01
30.633	0.594624E+05	0.131410E+00	0.772034E+04	0.170617E-01
38.188	0.567114E+05	0.125331E+00	0.213745E+04	0.472371E-02
45.684	0.538930E+05	0.119102E+00	-.348791E+04	-.770818E-02
53.130	0.499846E+05	0.110465E+00	-.940137E+04	-.207768E-01
60.535	0.464282E+05	0.102605E+00	-.153252E+05	-.338684E-01
67.898	0.410452E+05	0.907087E-01	-.198203E+05	-.438023E-01
75.236	0.356993E+05	0.788944E-01	-.248881E+05	-.550020E-01
82.552	0.133819E+05	0.295737E-01	-.274967E+05	-.607669E-01
89.864	-.941319E+04	-.208029E-01	-.293937E+05	-.649592E-01
97.178	-.310386E+05	-.685944E-01	-.274463E+05	-.606556E-01
104.499	-.549397E+05	-.121415E+00	-.260129E+05	-.574879E-01
111.845	-.599972E+05	-.132592E+00	-.212607E+05	-.469856E-01
119.222	-.620184E+05	-.137059E+00	-.158268E+05	-.349768E-01
126.644	-.593842E+05	-.131238E+00	-.952565E+04	-.210514E-01
134.112	-.572913E+05	-.126612E+00	-.328290E+04	-.725511E-02
141.636	-.545373E+05	-.120526E+00	0.225880E+04	0.499188E-02
149.221	-.517689E+05	-.114408E+00	0.776267E+04	0.171553E-01
156.857	-.494856E+05	-.109362E+00	0.114913E+05	0.253954E-01
164.542	-.472357E+05	-.104389E+00	0.151840E+05	0.335562E-01
172.259	-.463326E+05	-.102394E+00	0.164973E+05	0.364585E-01
180.000	-.454807E+05	-.100511E+00	0.177748E+05	0.392819E-01

TABLE 5. POST-PROCESSING INFORMATION FROM ABAQUS FOR IMPERFECT VERSION OF MODEL 20AI

STEP NO.	TOTAL BENDING MOMENT AT AUXILIARY NODE (LB-IN)	ROTATION ABOUT GLOBAL Y-AXIS (DEGREES)
1	0.629773E+06	0.261412E+00
2	0.237180E+07	0.986562E+00
3	0.405516E+07	0.171171E+01
4	0.479309E+07	0.243686E+01
5	0.486891E+07	0.256792E+01
6	0.493186E+07	0.269897E+01
7	0.498622E+07	0.283003E+01
8	0.503512E+07	0.296108E+01
9	0.505118E+07	0.301245E+01
10	0.506491E+07	0.306373E+01
11	0.509419E+07	0.319165E+01
12	0.512270E+07	0.331957E+01
13	0.514996E+07	0.344749E+01
14	0.517342E+07	0.357541E+01
15	0.519202E+07	0.370333E+01
16	0.520742E+07	0.383125E+01
17	0.521293E+07	0.388088E+01

INCREMENT NO.	STRAIN ENERGY	EXTERNAL WORK DONE	PLASTIC DISSIPATION	ABAQUS STEP	ABAQUS INCREMENT
1	0.143682E+04	0.1793[illegible]6E+04	0.000000E+00	1	5
2	0.204422E+05	0.230043E+05	0.000000E+00	1	10
3	0.501662E+05	0.65038[illegible]E+05	0.116035E+04	1	15
4	0.660105E+05	0.123680E+06	0.320037E+05	1	20
5	0.8[illegible]1544E+05	0.1347[illegible]0E+06	0.3[illegible]9105E+05	2	5
6	0.719452E+05	0.1459[illegible]E+06	0.433[illegible]72E+05	2	10
7	0.[illegible]E+05	0.157332E+06	0.5[illegible]819E+05	2	15
8	0.[illegible]E+05	0.168806E+06	0.660717E+05	2	20
9	0.978[illegible]E+05	0.173332E+06	0.697452E+05	3	2
10	0.[illegible]E+05	0.177861E+06	0.735243E+05	4	2
11	0.1002[illegible]E+06	0.189209E+06	0.8[illegible]1935E+05	5	5
12	0.10194[illegible]E+06	0.200621E+06	0.929125E+05	5	10
13	0.10361[illegible]E+06	0.212095E+06	0.102704E+06	5	15
14	0.105151E+06	0.223625E+06	0.112689E+06	5	20
15	0.106427E+06	0.235201E+06	0.122979E+06	5	25
16	0.107538E+06	0.246814E+06	0.133471E+06	5	30
17	0.107951E+06	0.251328E+06	0.137568E+06	6	2

TABLE 6. POST-PROCESSING INFORMATION (STRESS DISTRIBUTION) FROM ABAQUS FOR IMPERFECT VERSION OF MODEL 20AI

STEP NO. 17 FOR STRESSES

ANGLE (DEGREES)	LONGITUDINAL MEMBRANE STRESS (PSI)	NONDIMENSIONAL MEMBRANE LONGITUDINAL STRESS	HOOP STRESS (PSI)	NONDIMENSIONAL HOOP STRESS
0.000	0.607271E+05	0.134205E+00	0.126331E+05	0.279188E-01
7.610	0.603679E+05	0.133411E+00	0.117107E+05	0.258804E-01
15.222	0.600186E+05	0.132639E+00	0.107918E+05	0.238496E-01
22.803	0.589542E+05	0.130287E+00	0.819050E+04	0.181008E-01
30.336	0.578366E+05	0.127817E+00	0.543694E+04	0.120155E-01
37.857	0.559761E+05	0.123706E+00	0.172225E+04	0.380612E-02
45.380	0.543367E+05	0.120083E+00	-.176146E+04	-.389277E-02
52.876	0.508672E+05	0.112415E+00	-.536827E+04	-.118637E-01
60.310	0.483576E+05	0.106869E+00	-.927398E+04	-.204952E-01
67.714	0.379751E+05	0.839238E-01	-.131977E+05	-.291666E-01
75.119	0.256496E+05	0.566849E-01	-.167934E+05	-.371128E-01
82.525	0.967097E+04	0.213726E-01	-.170584E+05	-.376986E-01
89.913	-.552706E+04	-.122146E-01	-.174408E+05	-.385437E-01
97.302	-.204710E+05	-.452402E-01	-.170163E+05	-.376056E-01
104.712	-.356946E+05	-.788840E-01	-.166135E+05	-.367153E-01
112.123	-.479357E+05	-.105936E+00	-.133175E+05	-.294314E-01
119.535	-.578694E+05	-.127890E+00	-.955361E+04	-.211132E-01
126.980	-.559483E+05	-.123644E+00	-.525418E+04	-.116116E-01
134.470	-.559580E+05	-.123666E+00	-.150316E+04	-.332195E-02
142.030	-.541790E+05	-.119734E+00	0.189382E+04	0.418529E-02
149.571	-.523666E+05	-.115729E+00	0.554892E+04	0.122630E-01
157.126	-.508176E+05	-.112305E+00	0.818455E+04	0.180876E-01
164.729	-.493716E+05	-.109110E+00	0.106620E+05	0.235627E-01
172.365	-.488732E+05	-.108008E+00	0.114846E+05	0.253807E-01
180.000	-.483773E+05	-.106912E+00	0.123154E+05	0.272168E-01

TABLE 7. MOMENT-CURVATURE RESULTS FOR PERFECT VERSION OF MODEL 20A

CURVATURE K (1/FT)	MOMENT M (KIP-FT)
0.00000000E+00	0.00000000E+00
0.33796293E-03	0.52361568E+02
0.12754640E-02	0.19720113E+03
0.22129680E-02	0.33730643E+03
0.31504813E-02	0.39875580E+03
0.39473758E-02	0.42090363E+03
0.41817576E-02	0.42434280E+03
0.44161407E-02	0.42765866E+03
0.46505262E-02	0.43050354E+03
0.48849112E-02	0.43245026E+03
0.51192953E-02	0.43406573E+03
0.53536799E-02	0.43553660E+03
0.55880644E-02	0.43693962E+03
0.58224513E-02	0.43836884E+03
0.60568429E-02	0.43963071E+03
0.62912297E-02	0.44069992E+03
0.65256148E-02	0.44175455E+03
0.67600049E-02	0.44282471E+03
0.69943932E-02	0.44368170E+03
0.72287684E-02	0.44451007E+03
0.73576709E-02	0.44500220E+03

TABLE 8. MOMENT-CURVATURE RESULTS FOR IMPERFECT VERSION OF MODEL 20A (MODEL 20AI)

CURVATURE K (1/FT)	MOMENT M (KIP-FT)
0.00000000E+00	0.00000000E+00
0.33796293E-03	0.52481121E+02
0.12754641E-02	0.19764960E+03
0.22129680E-02	0.33793011E+03
0.31504813E-02	0.39942395E+03
0.33199168E-02	0.40574283E+03
0.34893532E-02	0.41078804E+03
0.36557899E-02	0.41551855E+03
0.38282289E-02	0.41759351E+03
0.38946470E-02	0.42093170E+03
0.39609359E-02	0.42207605E+03
0.41263211E-02	0.42451611E+03
0.42917063E-02	0.42689178E+03
0.44570942E-02	0.42916224E+03
0.46224827E-02	0.43111819E+03
0.47878711E-02	0.43266830E+03
0.49532559E-02	0.43395139E+03
0.50174259E-02	0.43441101E+03

SUMMARY

A modeling strategy is established to obtain the moment-curvature relation as well as the relation between the work done and the applied moment for circular cylindrical shells. This is achieved by using the nonlinear finite element program ABAQUS in conjunction with preprocessing and postprocessing computer programs. The results compare favorably with experimental curves reported in the open literature. Such analysis is of potential use in predicting critical bending moments, ultimate moment for ship hulls, pipe bends in nuclear reactors, submarine pipelines, etc.

REFERENCES

1. Maurer, L., "Ueber die Deformation gekruemmter elastischer Platten," Archiv der Mathematik und Physik, Vol. 6, Part I, pp. 1-10; Part II, pp. 10-26; and Part III, 1904, pp. 260-283.

2. Bantlin, A., "Formaenderung und Beanspruchung federnder Ausgleichroehren," Zeitschrift des Vereines Deutscher Ingeniere, Vol. 54, No. 2, Jan 1910, pp. 43-49.

3. v.Karman, Th., "Ueber die Formaenderung duennwandiger Rohre, insbesondere federnder Ausgleichrohren," Zeitschrift des Vereines Deutscher Ingenieure, Vol. 55, No. 45, Nov 1911, pp. 1889-1895.

4. Lorenz, H., "Die Biegung krummer Rohre," Physik. Zeitschrift, XIII, 1912, pp. 768-774.

5. Timoshenko, S., "Bending Stresses in Curved Tubes of Rectangular Cross-Section," Transactions ASME, Vol. 45, 1923, pp. 135-140.

6. Sunatani, Chido, "The Theory of a Bourdon Tube Pressure Gauge and An Improvement in its Mechanism," Tohoku Imperial University, Japan, Vol. 4, No. 1, 1924-25, pp. 69-110.

7. Brazier, L. G., "On the Flexure of Thin Cylindrical Shells and other 'Thin' Sections," in Proceedings of Royal Society of London, Series A, Vol. 116, No. A27, Sep 1927, pp. 104-114.

8. Hovgaard, W., "The Elastic Deformation of Pipe Bends," Journal of Mathematics & Physics, VI, 1926-27, pp. 69-118, "Deformation of Plane Pipes," VII, 1927-28, pp. 198-238; "Further Research on Pipe Bends," VII, 1927-28, pp. 239-297.

9. Wahl, A. M., "Stresses and Reactions in Expansion Pipe Bends," Transactions ASME, Vol. 49-50, Part I, AER-FSP, 1927-28, pp. 241-262.

10. Mossman, R. W., and Robinson, R. G., "Bending Tests of Metal Monocoque Fuselage Construction," NACA Technical Note No. 357, Nov 1930.

11. Chwalla, E., "Elastostatische Probleme schlanker, duennwandiger Rohre mit gerader Achse," Sitzungsberichte Akademie der Wissenschaften, Mathematische Nat. Klasse, Wien, 140, 1931, pp. 163-198.

REFERENCES (Cont.)

12. Crocker, S., and McCutchan, A., "Frictional Resistance and Flexibility of Seamless-Tube Fittings Used in Pipe Welding," Transactions of ASME, Vol. 53, No. 14, FSP-53-17, Sep-Dec 1931, pp. 215-245.

13. Stange, K., "Der Spannungszustand einer Kreisringschale," Ingenieur Archiv, Vol. 2, 1931, pp. 47-91.

14. Cope, E. T., and Wert, E. A., "Load-Deflection Relations for Large, Corrugated, and Creased Pipe Bends," Transactions of ASME, Vol. 54, No. 16, FSP-54-12, Aug 1932, pp. 115-159.

15. Chwalla, E., "Reine Biegung schlanker duennwandiger Rohre mit gerader Achse," ZAMM, Vol. 13, No. 1, Feb 1933, pp. 48-53.

16. Lundquist, E. E., Strength Tests of Thin-Walled Duralumin Cylinders in Compression, NACA Report No. 473, 1933.

17. Lundquist, E. E., "Strength Tests of Thin-Walled Duralumin Cylinders in Pure Bending," NACA TN 479, Dec 1933.

18. Lundquist, E. E., Burke, W. F., "Strength Tests of Thin-walled Duralumin Cylinders of Elliptic Section," NACA TN 527, 1935.

19. Tueda, M., "Mathematical Theories of Bourdon Pressure Tubes and Bending of Curved Pipes," Mem. Coll. Engineering Kyoto Imperial University, Vol. 8, 1934, pp. 102-115; Vol. 9, 1936, pp. 132-152.

20. Heck, O. S., "Stability of Orthotropic Elliptic Cylinders in Pure Bending," NACA TN 834, 1937, pp. 1-33.

21. Osgood, W., "The Crinkling Strength and the Bending Strength of Round Aircraft Tubing," NACA TR 632, 1938.

22. Dean, W. R., "The Distorition of a Curved Tube due to Internal Pressure," Philosophical Magazine, No. 189, Vol. XXVIII, Seventh Series, Oct 1939, pp. 452-464.

23. Schubert, G., "Ueber Effekte zweiter Ordnung bei Biegung und Torsion duennwandiger Rohre elliptischer Querschnitts," Ingenieur Archiv, Vol. 12, 1941, pp. 53-63.

24. Lundquist, E. E., "Strength Tests on Thin-Walled Duralumin Cylinders," NACA TN 427, Aug 1932.

25. Lundquist, E. E., and Stowell, E. Z., "Strength Tests of Thin-Walled Elliptic Duralumin Cylinders in Pure Bending and in Combined Pure Bending and Torsion," NACA TN 861, Jun 1942.

26. Moore R. L., Marshall, H., "Beam and Torsion Tests of Aluminum Alloy 615-T Tubing," NACA TN 867, 1942.

REFERENCES (Cont.)

27. Karl, H., "Biegung gekruemmter, duennwandiger Rohre," ZAMM, Vol. 23, 1943, pp. 331-345.

28. Vingness, I., "Elastic Properties of Curved Tubes," Transactions ASME, Vol. 65, No. 2, Feb 1943, pp. 105-120.

29. Pardue, T. E., Symonds P. S., Vigness, I., "Characteristics of Short Radius Tube Bends," NRL First Partial Report 0-2317, 1944.

30. Beskin, L., "Bending of Curved Thin Tubes," J. Appl. Mech., 1945, pp. A-1 through A-7.

31. Salzmann, F., "Die Nachqiebiqkeit von Wellrohrexpansionen," Schweizerisches Bauzeitung, No. 11, Vol. 127, 1946, pp. 127-130.

32. Symond, P. S., and Pardue, T. E., "Characteristics of Short Radius Tube Bends," Second Partial Report, NRL Report 0-2761, 1946.

33. Wolf, A., "An Elementary Theory of the Bourdon Gage," Journal of Applied Mechanics, Vol. 68, Sep 1946, pp. A-207 through A-210. Discussion in Journal of Applied Mechanics, No. 2, Vol. 4, Jun 1947, pp. A-165 and A-166.

34. Reissner, E., "On Bending of Curved Thin-Walled Tubes," in Proceedings of National Academy of Sciences, Vol. 35, 1949, pp. 204-208.

35. Huber, M. T., "The Bending of the Curved Tube of Elliptic Section," in Proceedings of the Seventh Congress of Applied Mechanics, Vol. 1, 1949, pp. 322-328.

36. Clark, R. A., and Reissner, E., "Bending of Curved Tubes," Advances in Applied Mechanics, II, 1950, pp. 93-122.

37. Clark, R. A., Gilroy, T. I., and Reissner, E., "Stresses and Deformations of Toroidal Shells of Elliptical Cross Section with Applications to Problems of Bending of Curved Tubes and of the Bourdon Gage," J. Appl. Mech., Vol. 19, No. 1, Mar 1952, pp. 37-48. Discussion in Vol. 19, No. 4, 1952, pp. 565-566.

38. Gross, N., and Ford, H., "The Flexibility of a Short-Radius Pipe-Bend," in Proceedings of the Institution of Mechanical Engineers, 1B, 1952-53, pp. 480-491. (Discussion on pp. 492-497).

39. Gross, N., "Experiments on Short-Radius Bends," in Proceedings of Institution of Mechanical Engineers, 1B, 1952-53, pp. 465-479.

40. Moore, R. L., Clark, J. W., "Torsion, Compression, and Bending Tests of Tubular Sections Machined from 75S-T6 Rolled Round Rod," NACA RM 52125, 1952, pp. 1-33.

REFERENCES (Cont.)

41. Pardue, T. E., and Vingness, I., "Characteristics of Pipe Bends Under Applied Moments," Summary Report, NRL 4253, 1953, pp. 1-20.

42. Anderson, R. A., Pride, R. A., Johnson, A. E. Jr., "Some Information on the Strength of Thick-skin wings with Multiweb and Multipost Stabilization," NACA RM L53F16, 1953, pp. 1-19.

43. Fralich, R. W., Mayers, J., Reissner, E., "Behavior in Pure Bending of a Long Monocoque Beam of Circular-Arc Cross Section," NACA TN 2875, 1953.

44. Wuest, W., "Einige Anwendungen der Theorie der Zylinderschale," ZAMM, Vol. 34, No. 12, Dec 1954, pp. 444-454.

45. Vissat, P. L., and Del Buono, A. J., "In-plate Bending Properties of Welding Elbows," Transactions ASME, Vol. 77, 1955, pp. 161-175.

46. Kafka, P. G. and Dunn, M. B., "Stiffness of Curved Circular Tubes with Internal Pressure," J. Appl. Mech., Jun 1956, pp. 247-254.

47. Peterson, J. P., "Bending Tests of Ring-Stiffened Circular Cylinders," NACA TN 3735, Jul 1956, pp. 1-14.

48. Ades, C. S., "Bending Strength of Tubing in the Plastic Range," Journal of Aeronautical Sciences, Vol. 24, Aug 1957, pp. 605-610.

49. Turner, C. E., and Ford, H., "Examination of the Theories for Calculating Stresses in Pipe Bends Subjected to In-Plane Bending," in Proceedings of the Institution of Mechanical Engineers, Vol. 171, 1957, pp. 513-525.

50. Rodbaugh, E. C., and George, H. H., "Effect of Internal Pressure on Flexibility and Stress-Intensification Factors of Curved Pipe or Welding Elbows," Transactions of American Society of Mechanical Engineers, Vol. 79, 1957, pp. 939-948.

51. Wood, J. D., "The Flexure of a Uniformly Pressurized, Circular, Cylindrical Shell," J. Appl. Mech., Dec 1958, pp. 453-458.

52. Suer, H. S, Harris, L. A., Skene, W. T., and Benjamin, R. J., "The Bending Stability of Thin-Walled Unstiffened Circular Cylinders Including the Effects of Internal Pressure," Journal of the Aeronautical Sciences, Vol. 25, No. 5, May 1958, pp. 281-287.

53. Reissner, E., "Rotationally Symmetric Problems in the Theory of Thin Elastic Shells," in Proceedings of 3rd U.S. National Congress of Applied Mechanics, Brown University, 1958, pp. 51-69.

54. Chernin, V. S., "On the System of Differential Equations of Equilibrium of Shells of Revolution under Bending Loads," PMM, Vol. 23, 1959, pp. 372-382.

55. Reissner, E., "On Finite Bending of Pressurized Tubes," J. Appl. Mech., Sep 1959, pp. 386-392.

REFERENCES (Cont.)

56. Turner, C. E., "Study of the Symmetrical Elastic Loading of Some Shells of Revolution with Special Reference to Toroidal Elements," Journal of Mechanical Engineering Science, Vol. 1, 1959, pp. 113-129.

57. Knowles, J. K., and Reisner, E., "On Stress-Strain Relations and Strain-Energy Expressions in the Theory of Thin Elastic Shells," Journal of Applied Mechanics, Mar 1960, pp. 104-106.

58. Dow, M. B., and Peterson, J. P., "Bending and Compression Tests of Pressurized Ring-Stiffened Cylinders," NASA Technical Note D-360, Apr 1960, pp. 1-27.

59. Seide, P., and Weingarten, V. I., "On the Buckling of Circular Cylindrical Shells Under Pure Bending," J. Appl. Mech., Mar 1961, pp. 112-116.

60. Reissner, E., "On Finite Pure Bending of Cylindrical Tubes," Oesterreichisches Ingenieur Archiv, Vol. 15, 1961, pp. 165-172.

61. Zender, G. W., "The Bending Strength of Pressurized Cylinders," Journal of the Aerospace Sciences, Vol. 29, Mar 1962, pp. 362-363.

62. Weingarten, V. I., "Effects of Internal Pressure on the Buckling of Circular-Cylindrical Shells Under Bending," Journal of the Aerospace Sciences, Jul 1962, pp. 804-807.

63. Akselrad, E. L., "Equations of Deformation for Shells of Revolution and for the Bending of Thin-Walled Tubes Subjected to Large Elastic Displacements," American Rocket Society, Vol. 32, Jul 1962, pp. 1147-1151.

64. Yao, J. C., "Large-Deflection Analysis of Buckling of a Cylinder under Bending," J. Appl. Mech., Dec 1962, pp. 708-714.

65. Reissner, E., and Weinitschke, H. J., "Finite Pure Bending of Circular Cylindrical Tubes," Quarterly of Applied Mathematics, Vol. XX, No. 4, Jan 1963, pp. 305-319. (Correction in Vol. XXIII, No. 4, 1965, p. 368).

66. Courtie, M. G., and Maunder, L., "Bend-Buckling of Pressurized Cylindrical Shells," in Proceedings of the Institution of Mechanical Engineers, Vol. 178, Part 3J, 1963-64, pp. 130-139.

67. Wittrick, W. H., "Non-linear Discontinuity Stresses in Shells of Revolution Under Internal Pressure," International Journal of Engineering Science, Vol. 2, 1964, pp. 155-177.

68. Thurston, G. A., "Newton's Method Applied to Problems in Nonlinear Mechanics," J. Appl. Mech., Vol. 32, Jun 1965, pp. 383-388.

REFERENCES (Cont.)

69. Schilling, C. G., "Buckling Strength of Circular Tubes," Journal of the Structural Division ASCE, Vol. 91, Oct 1965, pp. 325-348.

70. Akselrad, E. L., "Refinement of the Upper Critical Loading of Pipe Bending Taking Account of Geometrical Nonlinearity," Izvestiya Akademii Nauk SSSR, Mekhanika i Mash., Vol. 4, 1965, pp. 133-139 (in Russian).

71. Dow, D. A., "Buckling and Postbuckling Tests of Ring-Stiffened Circular Loaded by Uniform External Pressure," NASA TN D-3111 (N66-11255), Nov 1965, pp. 1-21.

72. Caldwell, J. B., "Ultimate Longitudinal Strength," Transactions of Royal Institution of Naval Architects, Vol. 107, 1965, pp. 411-430.

73. Johns, D. J., "On the Linear Buckling of Circular Cylindrical Shells Under Asymmetric Axial Compressive Stress Distributions," J. of the Royal Aeronautical Society, Vol. 70, 1966, pp. 1095-1097.

74. Aksel'rad, E. L., "Periodic Solutions of an Axially Symmetric Problem in the Theory of Shells," Mechanics of Solids, No. 2, 1966.

75. Jones, N., "On the Design of Pipe-Bends," Nuclear Engineering and Design, Vol. 4, 1966, pp. 399-405.

76. Aksel'rad, E. L., "Stability of a Curved Pipe of Circular Cross-Section Under External Pressure," Mechanics of Solids, No. 2, 1967, pp. 117-120 (Translation of Mekhanika Tverdogo Tela).

77. Lakshmikantham, C., and Gerard, G., "On the Bending Elastic Stability of Isotropic Cylinders," Journal of the Royal Aeronautical Society, Vol. 71, Feb 1967, pp. 136-138.

78. Aksel'rad, E. L., "Various Definitions of Curvature-Change Parameters for Shells and their Relation to the Strain-Compatibility Equations," Mechanics of Solids, Vol. 2, 1967, pp. 68-69.

79. Aksel'rad, E. L., "Stability of a Curved Pipe of Circular Cross-Section Under External Pressure," Mechanics of Solids, Vol. 2, 1967, pp. 117-120.

80. Jones, N., "In-Plane Bending of a Short-Radius Curved Pipe Bend," Journal of Engineering for Industry, May 1967, pp. 271-277.

81. Smith, R. T., "Theoretical Analysis of the Stresses in Pipe Bends Subjected to Out-Of-Plane Bending," Journal of Mechanical Engineering Science, Vol. 9, 1967, pp. 115-123.

82. Marcal, P. V., "Elastic-Plastic Behavior of Pipe Bends With In-Plane Bending," Journal of Strain Analysis, Vol. 2, 1967, pp. 84-90.

REFERENCES (Cont.)

83. Smith, R. T., and Ford, H., "Experiments on Pipe Lines and Pipe Bends Subjected to Three-Dimensional Loads," Journal of Mechanical Engineering Science, Vol. 9, No. 2, 1967, pp. 124-137.

84. Afendik, L. G., "Bending of Thin-Walled Tubes with Considerable Curvature Beyond the Elastic Limit," Prikladnaia Mekhanika, Kiev, Naukova Dumka, Vol. IV, 1968 (in Russian). (English Translation in Soviet Applied Mechanics by Plenum Press, pp. 27-30.)

85. Cheng, D. H., Thailer, H. J., "In-Plane Bending of Curved Circular Tubes," Journal of Engineering for Industry, Nov 1968, pp. 666-670.

86 Buckling of Thin-Walled Circular Cylinders, NASA SP-8007, Revised in Aug 1968, NASA Space Vehicle Design Criteria (Structures), pp. 7 and 19 for bending.

87. Ariaratnam, S. T., and Dubry, R. N., "Instability in an Elastic Plastic Cylindrical Shell Under Axial Compression," Journal of Applied Mechanics, Mar 1969, pp. 47-50.

88. Tenerelli, and Horton, W. H., "An Experimental Study of Local Buckling of Ring-Stiffened Cylinders Subject to Axial Compression," Israel Journal of Technology, Vol. 7, No. 1-2, 1969, pp. 181-194.

89. Afendik, L. G., "The Stability of a Circular Cylindrical Shell in Bending Beyond the Elastic Limit," Prikladnaia Mekhanika, Kiev, Naukova Dumka, Vol. VI, 1970, pp. 39-44 (in Russian). (English Translation in Soviet Applied Mechanics by Plenum Press, pp. 951-955.)

90. Weinitschke, H. J., "Die Stabilitaet elliptischer Zylinderschalen bei reiner Biegung," Zeitschrift fuer Angewandte Mathematik und Mechanik, Vol. 50, 1970, pp. 411-422.

91. Wilhoit, J. C. Jr., and Merwin, J. E., "The Effects of Axial Tension on Moment Carrying Capacity of Line Pipe Stressed Beyond the Elastic Limit," OTC Paper No. 1355, 3rd OTC Conference, 1971, pp. 1-293 - 1-296.

92. Perrone, N., Kao, R., "A General Nonlinear Relaxation Iteration Technique for Solving Nonlinear Problems in Mechanics," J. Appl. Mech., 1971, pp. 371-376.

93. Jirsa, J. O., Lee, F. H., Wilhoit, J. C. Jr., and Merwin, J. E., "Ovaling of Pipelines under Pure Bending," OTC paper No. 1569, Fourth OTC Conference, 1972, pp. I-573 - I-578.

94. Blomfield, J. A., Turner, C. E., "Theory of Thin Elastic Shells Applied to Pipe Bends Subjected to Bending and Internal Pressure," Journal of Strain Analysis, Vol. 7, No. 4, 1972, pp. 285-293.

REFERENCES (Cont.)

95. Dodge, W. G., and Moore, S. E., "Stress Indices and Flexibility Factors for Moment Loadings on Elbows and Curved Pipe," Welding Research Bulletin No. 179, 1972, pp. 1-20.

96. Dodge, W. G., Moore, S. E., ELBOW: A Fortran Program for the Calculation of Stresses, Stress Indices, and Flexibility Factors for Elbows and Curved Pipes, ORNL-TM-4098, 1973.

97. Koroleva, E. M., "Stability of Cylindrical Shells of Oval Cross Section in the Bending State of Stress," PMM, Vol. 37, 1973, pp. 901-904 (dates refer to translation).

98. Bowkamp, J. G., Stephen, R. M., "Large Diameter Pipe Under Combined Loading," Transportation Eng. J. ASCE, Vol. 99, No. 3, 1973, pp. 521-536.

99. Mello, R. M., Griffin, D. S., "Plastic Collapse Loads for Pipe Elbows Using Inelastic Analysis," J. Pressure Vessel Technology, ASME, 1974, pp. 177-183.

100. Almorth, B. O., and Starnes, J. H. Jr., "The Computer in Shell Stability Analysis," presented at the 1973 ASCE National Structural Engineering Meeting, San Francisco, California, 9-13 Apr 1973. Also in ASCE J. Eng. Mech., Vol. 101, EM6, Dec 1975, pp. 873-888.

101. Kempner, J., and Chen, Y. N., "Buckling and Initial Postbuckling of Oval Cylindrical Shells under Combined Axial Compression and Bending," Transactions of New York Academy of Sciences, Vol. 36, No. 2, 1974, pp. 171-191.

102. Schroeder, J., Srinivasaiah, K. R., and Graham, P., "Analysis of Test Data on Branch-Pipe Connections Exposed to Internal Pressure and/or External Couples," WRC Bulletin No. 200, Nov 1974, pp. 1-26.

103. Na, T. Y., and Turski, C. E., "Solution of the Nonlinear Differential Equations for Finite Bending of a Thin-Walled Tube by Parameter Differentiation," Aeronautical Quarterly, Vol. XXV, No. 1, Feb 1974, pp. 14-18.

104. Sherman, D. R., and Glass, A. M., "Ultimate Bending Capacity of Circular Tubes," OTC paper No. 2119, in Proceedings of Sixth OTC Conference, 1974, pp. 901-910.

105. Aksel'rad, E. L., and Kvasnikov, B. N., "Semi-Zero-Moment Theory of Curvilinear Bar-Shells," Mechanics of Solids, Vol. 2, 1974, pp. 125-133.

106. Wilhoit, J. C. Jr., and Merwin, J. E., "Critical Plastic Buckling Parameters for Tubing in Bending Under Axial Tension," in Proceedings of 5th Offshore Technology Conference, OTC 1974, Vol. 2, pp. 11-465.

107. Calladine, C. R., "Limit Analysis of Curved Tubes," Journal of Mechanical Engineering Science, Vol. 16, No. 2, 1974, pp. 85-87.

REFERENCES (Cont.)

108. Stephens, W. B., Starnes, J. H. Jr., and Almorth, B. O., "Collapse of Long Cylindrical Shells Under Combined Bending and Pressure Loads," AIAA Journal, Vol. 13, No. 1, Jan 1975, pp. 20-25.

109. Storakers, B., "On Buckling of Axisymmetric Thin Elastic-Plastic Shells," Intr. J. Solids and Structures, Vol. 11, 1975, pp. 1329-1346.

110. Johns, J. G., Mesloh, R. E., Winegarter, R., and Sorenson, J. E., "Inelastic Buckling of Pipelines under Combined Loads," OTC paper No. 2209, in Proceedings of Seventh OTC Conference, 1975, pp. 635-646.

111. Chen, Y. N., and Kempner, J., "Buckling of Oval Cylindrical Shells under Compression and Asymmetric Bending," AIAA Journal, Vol. 14, No. 9, Sep 1976, pp. 1235-1240.

112. Grinenko, N. I., and Khishchenko, Y. M., "Experimental Study of Stability of Reinforced Cylindrical Shells Under Pure Bending," Soviet Applied Mechanics, Vol. 12, May 1976, pp. 468-472.

113. Sherman, D. R., "Tests of Circular Steel Tubes in Bending," ASCE J. Strl. Div., Nov 1976, pp. 2181-2195.

114. Fabian, O., "Collapse of Cylindrical, Elastic Tubes under Combined Bending, Pressure and Axial Loads," Intl. J. Solids & Structures, Vol. 13, 1977, pp. 1257-1270.

115. Remseth, S. N., Holthe, K., Bergan, P. G., and Holand, I., "Tube Buckling Analysis by the Finite Element Method," in Proceedings of Finite Elements in Nonlinear Mechanics, International Conf., Geilo, Norway, Tapir, Aug 1977, pp. 671-694.

116. Weller, J., and Singer, J., "Experimental Studies on the Buckling Under Axial Compression of Integrally Stringer-Stiffened Circular Cylindrical Shells," Journal of Applied Mechanics, Dec 1977, pp. 721-730.

117. Sobel, L. H., "In-Plane Bending of Elbows," J. Computers and Structures, Vol. 7, No. 6, 1977, pp. 701-715.

118. Thurston, G. A., "Critical Bending Moment of Circular Cylindrical Tubes," J. Appl. Mech., 1977, pp. 173-175.

119. Gudramovich V. S., Gaiduchenko, A. P., Demeshko, M. F., Konovalenkov, V. S., "Plastic Buckling of Cylindrical Shells in the Case of Complex Loading Paths," Prikladnaia Mekhanika, Kiev, Naukova Dumka, 1977, Translation in Soviet Applied Mechanics, Plenum Press, 1980, pp. 19-24.

120. Harding, J. E., "The Elasto-Plastic Analysis of Imperfect Cylinders," in Proceedings of Institution of Civil Engineers, Part 2, Vol. 65, Dec 1978, pp. 875-892.

REFERENCES (Cont.)

121. Axelrad, E. L., "Flexible Shell-Theory and Buckling of Toroidal Shells and Tubes," Ingenieur Archiv, Vol. 47, 1978, pp. 95-104.

122. Reddy, B. D., and Calladine, C. R., "Classical Buckling of a Thin-Walled Tube Subjected to Bending Moment and Internal Pressure," Intl. J. Mech. Science, Vol. 20, 1978, pp. 641-650.

123. Korol, R. M., "Inelastic Buckling of Circular Tubes," ASCE J. Eng. Mech. Div., (EM4) Aug 1978, pp. 939-950.

124. Spence, J., and Toh, S. L., "Collapse of Thin Orthotropic Elliptical Cylindrical Shells under Combined Bending and Pressure Loads," J. Appl. Mech., Vol. 46, Jun 1979, pp. 363-371.

125. Reddy, B. D., "Plastic Buckling of a Cylindrical Shell in Pure Bending," Intl. J. Mech. Sciences, Vol. 21, 1979, pp. 671-679.

126. Tugcu, P., and Schroeder, J., "Plastic Deformation and Stability of Pipes exposed to External Couples," Intl. J. Solids and Structures, Vol. 15, 1979, pp. 643-658.

127. Khalig, A. A., and Schilling, C. G., "Plastic Buckling Strength of Seamless Steel Tubes under Bending Loads," U.S. Steel Bulletin, Feb 1979.

128. Reddy, B. D., "An Experimental Study of the Plastic Buckling of Circular Cylinders in Pure Bending," Intl. J. Solids and Structures, Vol. 15, 1979, pp. 669-683.

129. Boyle, J. T., Spence, J., "A Simple Analysis for Oval Presesurized Pipe Bends Under External Bending," in Proceedings of Intl. Conf. on Pressure Vessel Technology, London, paper C87/80, 1980, pp. 201-207.

130. Axelrad, E. L., "Flexible Shells," IUTAM Proceedings 15th Congress, University of Toronto, Aug 1980, pp. 45-56.

131. Gellin, S., "The Plastic Buckling of Long Cylindrical Shells under Pure Bending," Intl. J. Solids and Structures, Vol. 16, 1980, pp. 397-407.

132. Boyle, J. T., "The Finite Bending of Curved Pipes," Intl. J. Solids and Structures, Vol. 17, 1981, pp. 515-529.

133. Harding, J. E., "Ring-Stiffened Cylinders Under Axial and External Pressure Loading," in Proceedings of Institution of Civil Engineers, Part 2, Vol. 71, Sep 1981, pp. 863-878.

134. Emmerling, F. A., "Nichtlineare Biegung eines schach gekruemmten Rohres," ZAMM, Vol. 61, 1981, pp. T86 - T89.

135. Fabian, O., "Elastic-Plastic Collapse of Long Tubes Under Combined Bending and Pressure Load," Ocean Engineering, Vol. 8, No. 3, 1981, pp. 295-330.

REFERENCES (Cont.)

136. Bushnell, D., "Elastic-Plastic Bending and Buckling of Pipes and Elbows," J. of Computers and Structures, Vol. 13, 1981, pp. 241-248.

137. Reissner, E., "On Finite Pure Bending of Curved Tubes," Intl. J. Solids and Structures, Vol. 17, No. 9A, 1981, pp. 839-844.

138. Lang, H. A., "Pure Bending of Elliptic Ring Sector," Journal of Applied Mechanics, Vol. 49, Jun 1982, pp. 456-458.

139. Emmerling, F. A., "Nichtlineare Biegung und Beulen von Zylindern und krummen Rohren," Ingenieur Archiv, Vol. 52, 1982, pp. 1-16.

140. Kyriakides, S., and Shaw, P. K., "Response and Stability of Elastoplastic Circular Pipes under Combined Bending and External Pressure," Intl. J. Solids and Structures, Vol. 18, No. 11, 1982, pp. 957-973.

141. Kitching, R., Hussain, D., and Jones, N., "Limit Loads for Cylindrical Shells Subjected to Local Longitudinal Bending Moments," Intl. J. Mech. Sciences, Vol. 24, No. 11, 1982, pp. 673-690.

142. Obraztsov, I. F., Vol'mir, A. S., "Toroidal Shells, Stability, and Catastrophes," Sov. Phys. Dokl., Vol. 27, No. 10, 1982; English Translation in American Institute of Physics, 1983.

143. Bannister, K., "Large Deformation Analysis of a Cylindrical Shell Under Pure Bending and Pressurization," Ph.D. Thesis, Penn. State University May 1983.

144. Villhard, V. C., Bang, C., and Paluzotto, A. N., "Instability of Short Stiffened Composite Cylindrical Shells Under Bending with Prebuckling Displacements," J. Computers and Structures, Vol. 16, No. 6, 1983, pp. 773-775.

145. Kecman, D., "Bending Collapse of Rectangular & Square Section Tubes," Intl. J. Mech. Sciences, Vol. 25, No. 9, 1983, pp. 623-636.

146. Suqimoto, H. and Chen, W. F., "Inelastic Post Buckling Behavior of Tubular Members," Preprint SC-5, ASCE, Structures Congress Houston, Texas, 17-19 Oct 1983, pp. 1-14.

147. Chen, W. F., Suqimoto, H., "Moment-Curvature-Axial Compression-Pressure Relationship of Structural Tubes," Preprint SC-6, Structures Congress, Houston, ASCE, Oct 1983, pp. 1-14.

148. Benson, R. C., "Nonlinear Bending and Collapse of Long, Thin, Open Section Beams and Corrugated Panels," Journal of Applied Mechanics, Vol. 51, Mar 1984, pp. 141-145.

149. Rimrott, F., Draisey, S. H., "Critical Bending Moment of Double-Slit Tubing," J. of Spacecraft, Vol. 21, No. 3, 1984, pp. 316-318.

REFERENCES (Cont.)

150. Wu, J., Gould, Ph. L., "Pure Bending of Thin-Walled Beams," J. of Eng. Mechs. ASCE, Vol. 110, No. 7, 1984, pp. 1076-1085.

151. Fluegge, W., "Die Stabilitaet der Kreiszylinderschale," Ingenieur Archiv, Vol. 3, 1932, pp. 463-506.

152. Hibbitt, Karlsson and Sorensen, ABAQUS User's Manual, Version 4, Jul 1982, "ABAQUS Example Problems," Oct 1982.

153. Love, A. E., A Treatise on the Mathematical Theory of Elasticity, Fourth Edition, Dover Publications, Chapter V, Arts 87-89, 1944, pp. 129-132.

154. Washizu, K., Variational Methods in Elasticity and Plasticity, Third Edition, Pergamon Press, 1982, p. 8.

155. Wempner, G., "Mechanics of Solids with Applications to Thin Bodies," Sijthoff & Noordhoff, 1981, p. 62.

NOMENCLATURE

$\underline{a}_1, \underline{a}_2, \underline{a}_3$	= Local vectors along the local Y, Z, and X axes. Local z-axis is parallel to global y. Initially, local y is not parallel, but is coplanar with global x and in the same direction. Initially, local X is coplanar with global z and points in the same direction (Figure 2).
E	= Young's Modulus
F_0	= Axial force based on yield stress
k_{CR}	= Critical curvature at bifurcation (see Table 2)
h	= Shell thickness
I	= Moment of inertia of undeformed section (Table 2)
k	= Subscript in nodal values u_k, u_{k+1}, u_{k+2} (Eq. (24)). Mean curvature defined as the sum of absolute value of direct axial strains at the top and bottom of the cylinder divided by the undeformed diameter of the shell.
L	= Total length of cylindrical shell (Figure 1). In Equation (25), L is total arc length of end section ABC (Figure 2) prior to deformation.
ℓ_i	= Length of side of element i on arc where end rotation is applied (undeformed side ABC on Figure 2)
M_{BR}	= Critical bending moment by Brazier (Table 2)
M_{CR}	= Critical bending moment of bifurcation (Table 2)
M, M_{EXT}	= External bending moment calculated in the form of a reaction in this analysis
M_0	= Plastic moment or ultimate moment based on yield stress (Table 2)
N	= Total number of equal elements on undeformed arc ABC (Figure 2)

NOMENCLATURE (Cont.)

$\underline{r}$	= Final position vector on arc A'B'C' (Figure 2, after deformation)
r_o	= Initial position vector of any point on periphery of shell (arc ABC on Figure 2) at which the end rotation will be applied
$\underline{r}_o^b$	= Initial position vector of auxiliary node
R	= Mean shell radius
$\underline{u}$	= In the "APPLIED LOADING" section, $\underline{u}$ is the vector displacement after deformation; it is not to be confused with u
$\underline{u}^b$	= In the context of analysis given in "APPLIED LOADING," vector displacement of auxiliary node after deformation; it is not to be confused with u
u_x, u_y, u_z	= Vertical, transverse and longitudinal translations (along global X, Y, Z axes). Also referred to as u, v, and w.
(u)	= Vertical displacement at any point ξ on an element side
u_k, u_{k+1}, u_{k+2}	= Nodal values of displacement $u(\xi)$ at end node k, midside node k+1, end node k+2.
u_s	= Nodal value at s (point on arc where end rotation is being applied)
u	= Translation along global x-axis
v	= Translation along global y-axis
w	= Translation along global z-axis
	= Angle from vertical global x-axis up to end of arc to be analyzed
ν	= Poisson's ratio
ξ	= Local normalized variable in interval (0, 1) employed in describing vertical displacement distribution $u(\xi)$.
σ_{CR}	= Critical stress at bifurcation (Table 2)
σ_Y	= Yield stress of material
φ_o	= Initial inclination of cylindrical shell about y-axis. For straight tubes (present case) $\varphi_o = 0$
φ_x	= Rotation about global x-axis

NOMENCLATURE (Cont.)

φ_y	= Rotation about global y-axis
φ_y^b	= Prescribed end rotation about y-axis
φ_z	= Prescribed end rotation about z-axis

DISTRIBUTION

	Copies
Chief of Naval Technology	
Office of Naval Technology	
Attn: ASW-14	1
Dr. A. J. Faulstich (Code 023)	1
Navy Department	
Arlington, VA 22217-5000	
Commander	
Naval Sea Systems Command	
Attn: SEA-03B	1
SEA-05B (P. Palermo)	1
SEA-55B (J. B. O'Brian)	1
SEA-55Y1 (S. G. Arntson)	1
SEA-55Y2 (R. E. Provencher)	1
SEA-63R32 (D. Houser)	1
SEA-9G32	1
SEA-32R (C. Pohler)	1
PMS-402	1
PMS-406	1
PMS-407	1
Department of the Navy	
Washington, DC 20362	
Commander	
David W. Taylor Naval Ship Research and Development Center	
Attn: Code 17 (M. Krenzke)	1
Code 175 (J. Sykes)	1
Code 175.2 (B. Whang)	1
Code 175.2	1
Code 175.2 (T. Gilbert)	1
Code 175.3 (W. Conley)	1
Code 175.3 (P. Manny)	1
Code 184.4 (M. Hurwitz)	1
Code 172	1
Code 1620.3 (R. Jones)	1
Code 1720.6 (A. E. Dadley)	1
Code 1730.5 (J. C. Adamchak)	1
Bethesda, MD 20084	

	Copies
David W. Taylor Naval Ship Research and Development Center	
Attn: Code 177 (R. Fuss)	1
Code 177.1 (V. Bloodgood)	1
Code 177.1 (M. Riley)	1
Code 177.1 (R. Higginbotham)	1
Underwater Explosion Research Division	
Portsmouth, VA 23709	
Naval Coastal Systems Center	
Attn: Code 4210 (J. Rumbough)	1
Panama City, FL 32407	
Lockheed Palo Alto Laboratory	
Lockheed Missiles and Space Company Labs	
Attn: Dr. John DeRuntz	1
3251 Hanover Street	
Palo Alto, CA 94304	
Commander	
Naval Weapons Center	
Attn: Code 533 (Technical Library)	1
China Lake, CA 93555	
Commander	
Naval Ocean Systems Center	
Attn: Technical Library	1
San Diego, CA 92152	
Commanding Officer	
Naval Underwater Systems Center	
Attn: D. J. Lepore	1
Newport, RI 02840	

DISTRIBUTION (Cont.)

	Copies
Massachusetts Institute of Technology Attn: Prof. T. Wierzbicki Department of Ocean Engineering Cambridge, MA 02139	1
Massachusetts Institute of Technology Attn: Prof. T. H. Pian Prof. E. A. Witmer Department of Aeronautics and Astronautics Cambridge, MA 02139	 1 1
Massachusetts Institute of Technology Attn: Prof. K. J. Bathe Department of Mechanical Engineering Cambridge, MA 02139	1
Massachusetts Institute of Technology Attn: Prof. J. J. Connor Department of Civil Engineering Cambridge, MA 02139	1
Purdue University Attn: Prof. W. F. Chen School of Civil Engineering West Lafayette, IN 47907	1
Office of Naval Research Attn: Code 432 (A. Kushner) 800 North Quincy Street Arlington, VA 22217	1
Defense Nuclear Agency Attn: SPSS (C. McFarland) Washington, DC 20305	1
Defense Technical Information Center Cameron Station Alexandria, VA 22314	12

	Copies
Weidlinger Associates Weidlinger Consultant Attn: M. Bowen A. Misovich 110 East 58th Street New York, NY 10022	 1 2
Hibbitt, Karlson & Sorensen, Inc. Attn: Dr. B. Karlson Dr. P. Sorensen 35 South Angell Street Providence, RI 02906	 1 1
American Bureau of Shipping Attn: Mr. Stanley G. Stiansen, Vice President Dr. Y. K. Chen Dr. D. Liu 65 Broadway New York, NY 10006	 1 1 1
Stevens Institute of Technology, Castle Point Attn: Prof. David Nicholson Department of Mechanical Engineering Hoboken, NJ 07030	1
Library of Congress Attn: Gift and Exchange Division Washington, DC 20540	4
Westinghouse Electric Corporation Attn: Dr. Aspi K. Dhalla Advanced Energy Systems Division P. O. Box 158 Madison, PA 15663	1
Lockheed Palo Alto Research Laboratory Attn: Dr. David Bushnell Department 52-33, Building 205 3251 Hanover Street Palo Alto, CA 94304	1

DISTRIBUTION (Cont.)

	Copies
Internal Distribution:	
R10	1
R10 (D. Phillips)	1
R10 (M. Marshall)	1
R10 (H. Huang)	1
R102	2
R14	20
R14 (M. Moussouros)	20
R14 (K. Bannister)	1
R14 (K. Kiddy)	1
R14 (G. Harris)	1
R14 (S. Wilkerson)	1
R14 (F. Bandak)	1
R14 (D. Bendt)	1
R14 (J. Shaker)	1
E231	9
E232	3
E35	1
U01	1

END
DTIC
1-86